N° d'ordre : 389/2026-C/MT

REPUBLIQUE ALGERIENNE DEMOCRATIQUE ET POPULAIRE

Ministère de l'Enseignement Supérieur et de la Recherche Scientifique

Université des Sciences et de la Technologie Houari Boumediène

Faculté de Mathématiques

جامعة هواري بومدين للعلوم والتكنولوجيا
U S T H B

THESE DE DOCTORAT

Présentée pour l'obtention du **grade** de **DOCTEUR**

En : Mathématiques Appliquées

Spécialité : Modélisation, Econométrie et Statistique

Par : Imane REHOUMA

Sujet

Spatialisation des modèles de panels avec effet de seuil

Soutenue publiquement, le 09/12/2025 , devant le jury composé de :

M. BELBACHIR Hacéne	Professeur	à l'USTHB	Président
M. HAMDI Fayçal	Professeur	à l'USTHB	Directeur de thèse
M. BELARBI Yacine	Directeur de Recherche	au CREAD	Co-directeur de Thèse
Mme. EL SAADI Nadjia	Professeur	à l'ENSSEA	Examinatrice
M. SOUAM Saïd	Professeur	à l'Univ. Paris Nanterre	Examinateur

Spatialization of Panel Models with Threshold Effects

Imane REHOUMA
Department of Operational Research
Faculty of Mathematics,
University of Science and Technology Houari Boumediene,
U. S. T. H. B.

Abstract

This dissertation is dedicated to the nonlinear modeling of spatial panel data. We propose a new approach that accounts for nonlinearity, heterogeneity, and smooth regime changes, which are frequently observed in many empirical datasets. Specifically, we introduce the Panel Buffered Threshold Spatial Durbin (PBTSD) model. It is worth noting that traditional spatial models often assume linearity and homogeneity, which limits their ability to capture regime-specific behaviors. Furthermore, conventional threshold models rely on the assumption of abrupt transitions, which is often unrealistic. To address these limitations, the PBTSD model incorporates a buffer zone, allowing for gradual transitions between regimes and a better representation of variations in spatial spillover effects. The proposed model can be estimated using quasi-maximum likelihood (QML) or two-stage least squares (2SLS). These two estimation methods are compared through Monte Carlo simulations, and their finite-sample performance is evaluated. Empirical applications reveal that innovation-driven R&D dynamics vary across countries or regions due to regime-dependent and nonlinear spatial interactions. This study makes a methodological contribution by extending threshold modeling to spatial panel data, and an empirical contribution by providing new insights into the spatial mechanisms of innovation and R&D investment. As such, it offers useful elements for policymakers aiming to foster innovation and regional development.

Keywords: Spatial econometrics, Panel data, Threshold models, Buffered threshold, Spatial Durbin model, R&D expenditure, Innovation spillovers, Heterogeneous effects, Quasi-maximum likelihood estimation, Two-stage least squares (2SLS).

Résumé

Cette thèse est consacrée à la modélisation non linéaire des données de panel spatiales. Nous proposons une nouvelle approche permettant de prendre en compte la non-linéarité, l'hétérogénéité, ainsi que les changements de régime progressifs observés dans de nombreuses données empiriques. Plus précisément, nous introduisons le modèle Panel Buffered Threshold Spatial Durbin (PBTSD). Il est à noter que les modèles spatiaux traditionnels supposent souvent la linéarité et l'homogénéité, ce qui limite leur capacité à capturer les comportements spécifiques à chaque régime. Par ailleurs, les modèles à seuil classiques reposent sur l'hypothèse de transitions brusques, souvent peu réalistes. En réponse à ces limitations, le modèle PBTSD intègre une zone tampon (buffer), permettant des transitions graduelles entre les régimes et une meilleure prise en compte des variations dans les effets de spillover spatiaux. L'estimation du modèle proposé peut être réalisée à l'aide du quasi-maximum de vraisemblance (QML) ou de la méthode des moindres carrés en deux étapes (2SLS). Ces deux méthodes ont été comparées par le biais de simulations de Monte Carlo, et leur performance à taille finie a été évaluée. Les applications empiriques montrent que les dynamiques de R&D induites par l'innovation varient selon les pays ou les régions, en raison d'interactions spatiales non linéaires et dépendantes du régime. Cette étude apporte une contribution méthodologique en étendant la modélisation à seuil pour les panels spatiaux, et une contribution empirique en offrant un éclairage nouveau sur les mécanismes spatiaux de l'innovation et de l'investissement en R&D. Elle fournit ainsi des éléments utiles aux décideurs souhaitant promouvoir l'innovation et le développement régional.

Mots-clés: Économétrie spatiale, Données de panel, Modèles à seuil, Zone tampon (Buffered threshold), Modèle spatial Durbin, Dépenses en R&D, Effets de retombées de l'innovation, Effets hétérogènes, Estimation par quasi-vraisemblance, Moindres carrés en deux étapes (2SLS).

Acknowledgement

Above all, I thank **Almighty Allah** for providing me with the strength, courage, will, and patience to accomplish this modest work.

I would like to express my deepest gratitude to my supervisors, Professor **Fayçal HAMDI** and Research Director **Yacine BELARBI**, for their invaluable guidance, support, and patience throughout this work. Words cannot fully express my appreciation.

I also wish to extend my heartfelt thanks to the members of my thesis jury: Professor **Hacéne BELBACHIR**, Professor **Nadjia EL SAADI**, and Professor **Saïd SOUAM**, for their insightful comments, guidance, and the time they devoted to evaluating my work.

To my colleagues, friends, and everyone at the University of Science and Technology Houari Boumediene (USTHB), thank you for your support, collaboration, and for making even the most challenging days lighter with your kindness and humor.

My deepest gratitude goes to my family. To my parents, sisters, and brother, your understanding, and encouragement have been my foundation. Thank you for always believing in me, celebrating my achievements, and standing by me through every challenge.

Finally, to all who contributed to this journey, whether in significant or subtle ways, I extend my sincere thanks. Your support has been essential to this accomplishment, and I will always cherish it with gratitude.

I. REHOUMA.

Contents

List of Figures

List of Tables

List of abbreviations and notations

2SLS	Two-Stage Least Squares.
GNS	General Nesting Spatial model.
SAR	Spatial Autoregressive Model.
SDM	Spatial Durbin Model.
SEM	Spatial Error Model.
OLS	Ordinary Least Squares.
QML	Quasi- Maximum Likelihood.
TSAR	Threshold Spatial Autoregressive Model.
TSD	Threshold Spatial Durbin.
PTR	Panel Threshold Regression.
PTSD	Panel Threshold Spatial Durbin.
PBTSD	Panel Buffered Threshold Spatial Durbin.
IV	Instrumental Variables.
R&D	Research and Development.

General Introduction

Innovation, economic growth, and regional development have become central concerns in contemporary research across economics, geography, and policy analysis. It is widely acknowledged that regions, cities, or countries do not operate in isolation; rather, they interact and influence one another through trade, migration, knowledge diffusion, and technological spillovers. This interdependence implies that traditional econometric models, which assume independence among observational units, may provide biased or inefficient estimates and lead to misleading conclusions and policy recommendations (Anselin, 1988; LeSage & Pace, 2009). Recognizing the importance of spatial interactions, spatial econometrics has emerged to provide tools that explicitly account for spatial dependence and heterogeneity in empirical data. Tobler's First Law of Geography "everything is related to everything else, but near things are more related than distant things" (Tobler, 1970) encapsulates the essence of these spatial relationships.

Spatial econometric methods have evolved considerably since their inception. Early developments in spatial econometrics can be traced back to the pioneering works of Cliff and Ord (1973, 1981) and Anselin (1988), who formalized the treatment of spatial dependence in econometric models. These early contributions primarily focused on cross-sectional frameworks, where spatial dependence was introduced either in the dependent variable or in the disturbance term. Models such as the Spatial Autoregressive (SAR) model, the Spatial Error Model (SEM), and later the Spatial Durbin Model (SDM) provided the foundational tools for analyzing spatial spillover effects and interdependence across regions.

As empirical applications expanded, it became increasingly evident that many socioeconomic

and environmental phenomena evolve not only across space but also over time. This recognition led to the extension of spatial models into the panel data framework, combining the advantages of temporal and spatial information. Early contributions in this area include Elhorst (2003, 2010, 2014), who developed a comprehensive framework for estimating and interpreting spatial panel data models, distinguishing between static and dynamic specifications. These models enable researchers to capture unobserved heterogeneity, temporal dynamics, and spatial spillovers simultaneously, thereby offering a richer representation of real-world interactions.

More recent advances have further generalized these frameworks to include spatiotemporal dependence, heteroskedasticity, and endogeneity issues (see Lee and Yu, 2010; Elhorst, 2014; Baltagi, Fingleton and Pirotte, 2014). Collectively, these developments mark the transition from simple spatial cross-sectional analysis to a more integrated spatial–temporal econometric paradigm, now widely applied in regional science, environmental economics, and urban studies.

While classical spatial models capture linear spatial interactions, real-world processes often exhibit nonlinear dynamics, structural heterogeneity, and regime-specific behaviors. Threshold models provide a flexible framework to address these limitations by allowing relationships to vary depending on a threshold variable. The concept of threshold modeling was first introduced by Tong (1978), who introduced the Threshold Autoregressive (TAR) model in the context of nonlinear time series analysis. The TAR model allows the dynamic relationship between variables to shift across regimes determined by a threshold variable, thereby capturing structural changes and nonlinear adjustment processes. This model was later extended to regression and panel data settings, notably by Hansen (1999, 2000), who developed consistent estimation and inference procedures for threshold models using least squares and instrumental-variable approaches. These methodological advances made threshold models a powerful tool for modeling nonlinearity and regime-dependent relationships in economics and finance.

Building on this foundation, threshold models were gradually integrated into spatial econometrics to address the possibility that spatial interactions may vary across regimes. This evolution reflects the growing recognition that spatial dependence "how an observation is influenced by its neighbors" may itself be nonlinear or heterogeneous. In this context, Deng

(2018) proposed the Threshold Spatial Autoregressive (TSAR) model, representing one of the first formal attempts to combine threshold and spatial structures. In Deng's specification, only the spatial autoregressive parameter varies across regimes, while the slope coefficients of exogenous regressors remain constant. To deal with the endogeneity of the spatially lagged dependent variable, Deng employed a spatial two-stage least squares (S2SLS) estimator based on Kelejian and Prucha (1998) type instruments.

Extending Deng's contribution, Zhu et al (2020) developed the Threshold Spatial Durbin Model (TSDM), which generalizes the TSAR model by allowing all parameters including spatial, exogenous, and contextual effects to differ across regimes. This generalization captures richer forms of spatial heterogeneity and interaction effects. From an econometric standpoint, Zhu et al. proposed a Bayesian estimation framework using a Markov Chain Monte Carlo (MCMC) algorithm, which is more efficient and computationally tractable than classical two-stage procedures.

Building on the advances in cross-sectional threshold spatial models, recent developments have extended the threshold framework to panel data settings. This transition was largely inspired by Hansen's (1999) Panel Threshold Regression (PTR) model, which introduced regime-switching behavior into panel structures while controlling for individual fixed effects. Incorporating this mechanism into spatial econometrics has significantly enhanced the capacity to capture cross-sectional dependence, spatial heterogeneity, and nonlinear regime dynamics in data that evolve across both space and time.

In this line, Wei et al. (2021) proposed the Panel Threshold Spatial Durbin (PTSD) model, which unifies the spatial Durbin structure with Hansen's threshold mechanism. The PTSD model allows the parameters governing spatial dependence and local spillovers to change across regimes defined by a continuous threshold variable, while simultaneously controlling for unobserved individual effects. The transition mechanism adopted by Wei et al. (2021) follows the same principle as Hansen's (1999) approach, allowing spatial units to move between regimes as the threshold variable evolves over time. To address the endogeneity of spatial lags and account for individual fixed effects, the authors proposed a within-group spatial two-stage least squares (S2SLS) estimator.

It is well established that Hansen's formulation involves an abrupt transition between regimes

and implicitly assumes a clear distinction between the two groups of observations. This assumption can be problematic in certain practical situations (see, e.g., Gonzalez et al., 2005; Belarbi et al., 2021). When assuming a threshold effect in the data, there are cases where the regime shift does not occur at a single, well-defined threshold value. Specifically, if the threshold variable exceeds a certain upper value, r_U, the dependent variable is typically assumed to follow a particular dynamic. The transition to a different dynamic is confirmed only once the threshold variable falls below a lower value, r_L. The interval $[r_L; r_U]$ acts as a buffer zone, within which no new regime information is inferred, and the dynamics of the dependent variable are assumed to remain unchanged.

The concept of incorporating a buffer zone into threshold models first appeared in the time-series literature with the hysteretic autoregressive model of Li et al. (2015), who generalized the classical TAR model of Tong (1978) by allowing the regime to remain unchanged within a specific buffer region. This innovation avoids abrupt switching near the threshold and provides a smoother and more realistic transition mechanism.

Building on this idea, Belarbi et al. (2021) were the first to extend the buffered approach to panel data by proposing the Buffered Threshold Panel Data (BTPD) model. The BTPD model allows frequent and gradual regime transitions across heterogeneous units and can be viewed as an extension of Hansen's (1999) Panel Threshold Regression (PTR) model. Though still emerging, it offers a new lens to understand data nonlinearity. Indeed, Belarbi et al. (2021) examined the combined effects of oil dependence and institutional quality on economic growth, applying the BTPD to 19 oil rent-dependent countries over 1996–2017. Their findings reveal a nonlinear relationship between growth and oil rents, where institutional quality plays a central role. They identify three country groups according to institutional quality and show that, apart from a few countries with strong and stable institutions, most economies fall within a transitional buffer zone where the effect of oil dependence on growth remains uncertain. Results also indicate that institutional quality enhances growth when oil dependence is either low or high, but has a negative effect at intermediate levels, suggesting the possibility of an oil-dependence trap. Similarly, Hamdi et al. (2025) investigated the heterogeneous effects of economic complexity on economic growth and human development by applying the BTPD model to a balanced panel of 92 developed and developing countries observed over 15 years (2002–2016). Their results confirm the

presence of nonlinearity driven by a buffered transition between regimes. They identify three groups of countries based on their level of economic complexity and show that, while a small number of highly complex economies clearly benefit from sustained improvements in growth and human development, most developing countries remain trapped within the buffer zone.

Given the superior ability of BTPD modeling to explain nonlinear dynamics compared to the traditional PTR model, in this thesis we propose an extension that adds further flexibility within the context of spatial panel data. We introduce a new model, the Panel Buffered Threshold Spatial Durbin (PBTSD) model, by modifying the regime indicator process which governs transitions between regimes. This modification allows for smooth transitions and, as in BTPD modeling, incorporates a buffer zone into the spatial panel framework. Building on the Panel Threshold Spatial Durbin (PTSD) model developed by Wei et al.(2021), the PBTSD model aims to more effectively capture complex nonlinear dynamics and enhance our understanding of nonlinear patterns in spatial panel data.

The empirical motivation for this research stems from the critical role of innovation and R&D expenditure in driving economic growth. While the Knowledge Production Function (KPF) framework links R&D inputs to outputs such as innovation and productivity, cross-regional spillovers and development disparities complicate the relationship. Advanced economies often benefit more from innovation spillovers than less-developed regions, and international knowledge diffusion depends on trade, policy, and institutional quality (Rodríguez-Pose and Burlina, 2021). By applying the PBTSD model, this thesis investigates the nonlinear and heterogeneous spatial effects of R&D on innovation expenditure, capturing threshold-driven dynamics and spatial interdependencies across countries or regions.

In summary, this thesis makes methodological and empirical contributions. Methodologically, it extends threshold spatial panel models to include buffered transitions, providing a flexible framework to analyze nonlinear spatial dynamics. Empirically, it applies this framework to study the spatial effects of R&D on innovation, accounting for heterogeneity across regions and countries. The outline of the thesis is as follows:

In Chapter 1, we present several spatial econometric models and trace their evolution from cross-sectional to panel data frameworks. We also revisit the main concepts and tools used in spatial data modeling, such as spatial correlation, Moran's I statistic, and spatial weight

matrices, along with their interpretation. In addition, we address the issue of model estimation, highlighting the specific challenges posed by spatial dependence and heterogeneity. In Chapter 2, we develop the PTSD model and propose an alternative estimation method to the two-stage least squares (2SLS) approach introduced by Wei et al. (2021). Specifically, we introduce the quasi-maximum likelihood (QML) method and demonstrate, through a simulation study, that it outperforms the 2SLS method. In Chapter 3, we present our main contribution: the introduction of the PBTSD model and two associated estimation methods: 2SLS and QML. The 2SLS approach is an adaptation of the method proposed by Wei et al. (2021) for estimating the PTSD model, providing explicit estimators within the PBTSD framework. The QML method serves as an alternative, offering improved statistical efficiency, as demonstrated through Monte Carlo simulations. It is worth noting that the QML approach requires initial parameter values, for which the 2SLS estimates can serve as effective starting points. Additionally, we develop a linearity test. Since the distribution of this test is nonstandard, we propose a bootstrap procedure to simulate the likelihood ratio test distribution. In Chapter 4, we apply the model to analyze the spatial effects of R&D expenditure on innovation. Finally, in Chapter 5, we conclude the thesis by discussing policy implications and potential avenues for future research.

Chapter 1

Introduction to Spatial modeling

1.1 Introduction

In empirical research in economics, geography, epidemiology, and environmental sciences, data are often characterized by a spatial dimension. Regions, cities, or countries are not isolated entities; rather, they interact and influence one another through trade, migration, knowledge diffusion, or environmental spillovers. The assumption of independence among observational units, which underlies traditional econometric models, is therefore frequently unrealistic. Ignoring these spatial interactions can lead to biased or inefficient estimates, misleading inference, and poor policy recommendations (see, e.g Anselin, 1988; LeSage and Pace, 2009).

Spatial econometrics emerged as a response to these challenges, providing tools to explicitly account for the spatial dependence and heterogeneity inherent in many types of data. The central idea is that outcomes in one location may be systematically related to outcomes in neighboring locations a phenomenon concisely captured by Tobler's First Law of Geography (Tobler, 1970). To model such interdependence, spatial econometric techniques introduce spatial structures through a spatial weights matrix, which formalizes the notion of "neighborhood" and allows the measurement of spillover effects across units. The fundamental idea is that observations located close to each other geographically or through economic or

social networks tend to exhibit similar behaviors. This phenomenon, known as spatial autocorrelation, implies that values observed in one location are systematically related to values observed in nearby locations. In other words, the assumption of independence across units, central in classical econometrics, is violated when spatial interactions exist. Positive spatial autocorrelation means that high (or low) values tend to cluster together, while negative spatial autocorrelation reflects situations where high and low values alternate across space. Spatial autocorrelation can appear directly in the outcome of interest (e.g., crime rates or GDP per capita exhibiting spatial clusters) or indirectly through omitted spatially structured factors such as climate, institutions, infrastructure, or social diffusion mechanisms.

Over the past decades, the field has evolved significantly. Early applications primarily focused on cross-sectional spatial models, which extend classical regression frameworks by incorporating spatial dependence in either the dependent variable or the error terms. These specifications showed that ignoring spatial autocorrelation can lead to biased coefficients, incorrect inference, and an underestimation of spillover effects, ultimately resulting in misguided policy conclusions.

However, many empirical questions involve both spatial and temporal dimensions. For example, regional economic growth depends not only on its past performance but also on the trajectories of neighboring economies. Likewise, innovation diffusion, international trade shocks, environmental pollution, or the spread of diseases unfold gradually across space and time. Such dynamics cannot be captured by purely cross-sectional or purely temporal frameworks.

These limitations motivated the development of spatial panel models, which combine the richness of panel data controlling for unobserved heterogeneity and allowing for dynamic adjustments with the explicit treatment of spatial dependence (see, e.g., Elhorst, 2014). By leveraging variation across both space and time, spatial panel methods offer a powerful framework to identify how shocks propagate, how local policies generate indirect effects, and whether regions converge or diverge over time. Consequently, spatial panel models have become a central tool in empirical research across economics, regional science, public policy, epidemiology, and environmental studies.

The purpose of this chapter is to trace this methodological progression from classical cross-sectional analysis to spatial econometrics and finally to spatial panel models. The discussion

begins by highlighting the limitations of traditional econometric frameworks when applied to spatial data and the theoretical justifications for incorporating spatial effects. It then introduces the spatial weights matrix and illustrates the different ways spatial relationships can be defined. Subsequently, various types of spatial econometric models are presented, including the spatial autoregressive model, the spatial error model, and the spatial Durbin model. The chapter concludes with an overview of spatial panel models, which represent the most advanced tools in spatial econometrics for handling data that vary across both space and time.

Overall, this chapter builds on the fundamental contributions of the spatial econometrics literature. Its structure and methodological orientation are inspired by the seminal work of Anselin (1988), which established the theoretical foundations for modeling spatial dependence. The treatment of spatial spillovers and model specification follows the comprehensive exposition of LeSage and Pace (2009), while the discussion of spatial panel models draws on the detailed framework developed by Elhorst (2014). These references collectively provide the conceptual and empirical basis on which the analyses in this chapter are constructed.

1.2 From cross-sectional models to spatial models

1.2.1 Classical cross-sectional regression models

The starting point of most econometric analyses is the cross-sectional regression model:

$$y = X\beta + \varepsilon, \tag{1.2.1}$$

where y is the vector of observations for the dependent variable, X is the matrix of explanatory variables, β represents the coefficients to be estimated, and ε is the error term. Ordinary Least Squares (OLS) estimation of this model relies on a number of classical assumptions. First, it is assumed that the error term has zero conditional mean, which ensures that the regressors are exogenous and uncorrelated with the disturbances. Second, the variance of the errors is taken to be constant across all observations, a condition known as homoscedasticity. Finally, the observations are considered independent and identically distributed, which implies the absence of correlation among error terms across units. Under these conditions, the OLS estimator is unbiased, consistent, and efficient, and the conventional inference pro-

cedures remain valid.

These assumptions are generally reasonable when dealing with non-spatial cross-sectional data, such as the relationship between individual wages and education levels, or between household consumption and income, where each observational unit is presumed to be independent of the others. In such contexts, the cross-sectional regression model provides reliable insights and serves as a powerful tool for policy analysis and economic interpretation.

Nevertheless, the applicability of this framework becomes problematic when the data under study have an explicit spatial dimension. Examples include regional unemployment rates, housing prices across neighborhoods, or disease incidence across provinces. In these cases, the assumptions of error independence and parameter homogeneity are frequently violated, since units located in geographic proximity often influence one another and may be subject to context-specific dynamics. As a result, the traditional regression model, though elegant and analytically convenient, can prove inadequate for capturing the complexity of spatial processes.

1.2.2 Limitations with spatial data (dependence and heterogeneity)

When dealing with spatially referenced data, the validity of the classical regression framework is often challenged by two fundamental issues: spatial dependence and spatial heterogeneity. These features are inherent to geographical, economic, and social processes, and they undermine the assumptions that justify the use of regression model.

Spatial dependence, also referred to as spatial autocorrelation, arises when the value of a variable observed in one location is systematically correlated with values observed in neighboring locations. In such a context, observations are no longer independent, violating a core assumption of classical econometric models. Spatial dependence typically reflects the presence of spillover effects, diffusion processes, or contagion mechanisms that transmit impacts across adjacent units.

From a statistical perspective, spatial dependence manifests when similar values tend to cluster together in space (positive spatial autocorrelation) or when high and low values alternate between neighboring areas (negative spatial autocorrelation). Positive dependence

is the most common form and is observed, for example, when wealthy neighborhoods are surrounded by other wealthy neighborhoods, or when regions with high unemployment are located next to regions facing similar difficulties. Negative spatial dependence, though less frequent, may occur when a strong contrast separates units, such as a wealthy urban district bordering a disadvantaged informal settlement.

Numerous real-world phenomena illustrate spatial dependence. Housing prices in one neighborhood often respond to price changes in adjacent areas, as buyers consider nearby locations credible substitutes. A classic example comes from hedonic pricing models: suppose we observe property sales over one year using only structural characteristics of homes as explanatory variables. If a particular house is sold for a higher price than expected because a nearby school suddenly received a positive quality report, this information although omitted from the model may lead other sellers in the same school district to increase asking prices in the following months. As a result, neighboring property prices become correlated in space even after controlling for observable characteristics. In such a case, spatial dependence arises from omitted local amenities such as school quality, transportation accessibility, shopping centers, or parks, meaning that prices of nearby homes improve the predictive power of the model (see e.g Lesage and Pace, 2009)

Environmental pollution spreads across administrative borders due to wind and water flows, meaning pollution levels in one city partly depend on emissions from neighboring cities. The spread of infectious diseases offers another well-known illustration: regions strongly affected by an epidemic tend to transmit infections to surrounding regions through population mobility. Ignoring spatial dependence can lead to biased estimates and misleading inference, as relationships are incorrectly attributed to individual characteristics rather than spatial interactions.

Spatial heterogeneity, on the other hand, refers to the fact that relationships between variables may not be stable or homogeneous across space. In practice, the strength, and sometimes even the sign, of a relationship may vary across regions due to differences in economic structures, cultural backgrounds, institutional frameworks, or natural conditions. For example, the determinants of agricultural productivity may depend heavily on climatic factors in one region, while institutional or infrastructural variables may play a more prominent role in another. Similarly, the impact of education on income may be stronger in urban

areas with diversified labor markets than in rural or peripheral regions where employment opportunities are scarce. Such heterogeneity violates the assumption that regression coefficients are constant across observations. If it is ignored, estimated coefficients represent averages that conceal local variations, leading to misleading generalizations and potentially flawed policy recommendations. For instance, a national policy designed on the basis of a homogeneous model may fail to account for regional disparities, thereby exacerbating rather than reducing inequalities.

Taken together, spatial dependence and spatial heterogeneity highlight the inadequacy of classical regression techniques for spatial data analysis. Dependence implies that observational units cannot be treated as isolated entities, while heterogeneity challenges the notion of a single, invariant relationship across space. Both features undermine the i.i.d. assumption, the efficiency of OLS, and the validity of conventional statistical inference. These limitations have motivated the development of spatial econometric models, which explicitly account for interdependence among units and allow for the modeling of spatially varying processes.

1.2.3 Transition to the Spatial Framework

The limitations of classical regression models have motivated a shift toward frameworks that explicitly account for spatial interactions. Traditional econometric methods rely on the assumption that observations are independent, yet this rarely holds when data are geographically structured. In many real-world settings, outcomes observed in one location are systematically influenced by surrounding areas, meaning that ignoring spatial linkages can lead to biased estimates and misleading inference. Spatial econometrics overcomes this issue by incorporating a spatial weights matrix, which formalizes the connections between units and quantifies the strength of their interaction. On this basis, spatial models allow interdependence to appear in the dependent variable, the explanatory variables, or the error term, offering a more realistic and robust analytical framework for spatially connected data.

1.3 Spatial autocorrelation

Spatial autocorrelation refers to the correlation of a variable with itself through space, i.e. the degree to which the value of a variable observed in one geographic location is similar (or

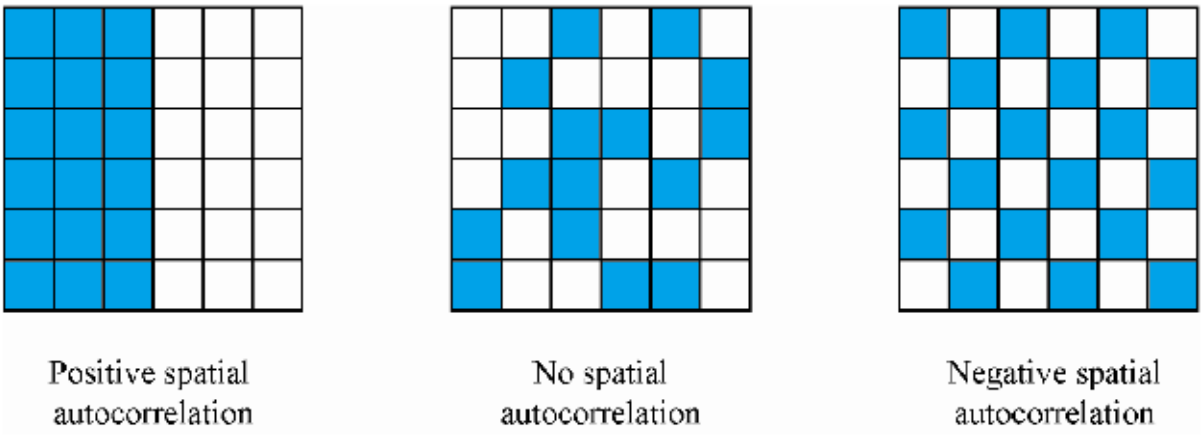

Figure 1.3.1. Type of spatial autocorrelation

dissimilar) to values observed in nearby locations.

This underlying principle suggests that spatial processes often produce non-random structure in geographic data: values do not occur randomly in space but tend to cluster or disperse, depending on the underlying processes.

When spatial autocorrelation is positive, observations with similar values tend to be located near one another, resulting in spatial clusters where high–high or low–low patterns dominate. This configuration indicates that neighboring units share similar characteristics, and the spatial distribution is far from random. In contrast, negative spatial autocorrelation arises when dissimilar values are positioned next to each other, producing a systematic alternation of high and low values across space, often described as a checkerboard-type arrangement. Finally, zero spatial autocorrelation reflects spatial randomness, meaning that the spatial arrangement of values shows no discernible structure and that knowing the value of one location provides no information about the values observed in nearby units. In this case, the observed pattern is consistent with what would be expected under random spatial allocation, see Figure(1.3.1) .

Although spatial autocorrelation reflects the tendency of nearby units to exhibit related values, this pattern is an inherent property of the data rather than something generated by the model. To study or quantify this dependence, it is necessary to define how spatial units interact with one another. This role is fulfilled by the spatial weight matrix, which formally encodes the neighborhood structure and the strength of spatial connections. By specifying

which units are considered neighbors and how strongly they are linked, the spatial weight matrix provides the foundation for detecting, measuring, and modelling spatial dependence. The next subsection describes how spatial weight matrices are constructed and their role in empirical spatial econometric analysis.

1.3.1 Spatial weights matrix

A key distinction between traditional time-series econometrics and spatial econometrics lies in how dependence is modeled. While time-series analysis captures temporal dependence using lagged observations (such as $t-1$), spatial econometrics focuses on dependence across locations. To represent these cross-sectional interactions, spatial econometrics introduces the spatial weights matrix.

A spatial weight matrix (often denoted W) is a square matrix that formally encodes how spatial units interact with each other. Its purpose is to specify which units are neighbors and how strongly their values are related. The matrix is typically an $n \times n$ square matrix, where n denotes the number of spatial entities (regions, cities, households, etc.). The $(i,j) - th$ element, $w_{i,j}$, of W reflects the degree of interaction or "closeness" between unit i and unit j.

By convention, the diagonal elements are set to zero ($w_{ij} = 0$) to exclude self-interaction. The values of w_{ij} can be binary (indicating whether two units are neighbors) or continuous (reflecting distance or intensity of interaction). To ensure comparability across units, it is common to row-standardize W, so that the weights of each row sum to one.

The spatial weights matrix plays a central role in spatial models because it generates spatial lags, such as WY (spatially lagged dependent variable) or WX (spatially lagged explanatory variables). These lags capture the idea that outcomes in one location are influenced by outcomes or characteristics of neighboring locations.

1.3.2 Common types of spatial weights

The specification of W is not unique and depends on the empirical context. Several common approaches are used in practice:

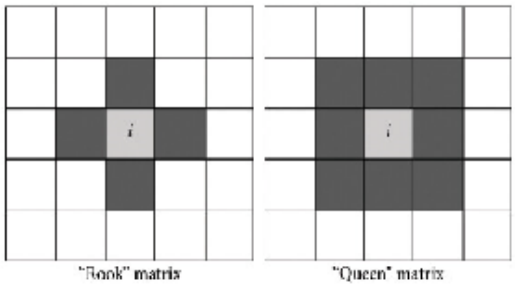

Figure 1.3.2. Spatial adjency

- **Contiguity-based weights** define spatial relationships based on whether regions share a common boundary or point of contact. It is defined as:

$$w_{i,j} = \begin{cases} 1 & \text{if spatial unit } i \text{ is contiguous (neighbor) with unit } j, \\ 0 & \text{Otherwise.} \end{cases} \tag{1.3.1}$$

  Within this approach, rook contiguity considers two regions as neighbors only when they share a common border, while queen contiguity expands the definition of neighborhood to include regions that share either a border or a vertex (a single point or a corner where regions meet). Such specifications are frequently applied in the context of administrative units, for example provinces or municipalities, where official boundaries serve as natural indicators of spatial interaction (see Figure(1.3.2)).

- **Distance-based** spatial weights are constructed based on the physical distance $d_{i,j}$ between two spatial units i and j. The general idea is that the closer two units are, the stronger their relationship. Two main approaches are commonly used:

  – Inverse-Distance (or Distance Decay): The weight between two units decreases as the distance $d_{i,j}$ increases. The general formula is $w_{i,j} = \frac{1}{d_{i,j}^{\alpha}}$, where $d_{i,j}$ is Euclidean or geodesic distance between i and j, α distance decay parameter (commonly 1 or 2).

  – Threshold Distance (Cutoff Distance): Two units are considered neighbors only if their distance is less than a threshold d_0 otherwise, the weight is zero:

$$w_{i,j} = \begin{cases} 1 & \text{if } d_{i,j} \leq d_0 \\ 0 & \text{otherwise} \end{cases}$$

- **K-nearest neighbors (KNN)** weights establish connections by linking each spatial unit to a fixed number of its closest neighbors. Unlike threshold distance measures, this method ensures that every unit has the same number of neighbors, regardless of absolute geographic distance. KNN specifications are especially useful when the distribution of observations is irregular, since they avoid situations in which some units would otherwise have very few neighbors while others might have too many.

- **Economic or functional weights** define spatial dependence not in terms of geography, but through patterns of social, cultural, or economic interaction. In this case, neighborhood structures are determined by flows such as trade, commuting, migration, or shared cultural ties. By moving beyond physical space, these weights capture functional interdependencies and allow spatial models to reflect networks of interaction that are economic or social in nature.

1.3.3 Interpretation and implications

The choice of spatial weights matrix has profound implications for empirical analysis. Different specifications may lead to different conclusions about the presence and magnitude of spatial effects (see, e.g, Anselin, 2002). As such, the specification of W should be guided by theoretical reasoning about the nature of interactions in the data, rather than chosen arbitrarily.

In practice, researchers often experiment with alternative specifications of W and test the robustness of their results. Because W encodes assumptions about the structure of interdependence, it is not merely a technical detail but a substantive modeling decision.

1.3.4 Measures of spatial autocorrelation: Moran's I

Spatial data often exhibit autocorrelation, meaning that observations in nearby locations are more similar (or dissimilar) than would be expected if they were independent. Detecting this

phenomenon is essential, because ignoring spatial dependence may bias statistical inference and lead to misspecified models.

The most widely used global measure of spatial autocorrelation is Moran's I, introduced by Moran (1950). It provides a single summary statistic indicating whether a variable of interest is spatially clustered, spatially dispersed, or randomly distributed. Unlike purely visual methods (such as choropleth maps), Moran's I offers a formal statistical test.

The Global Moran's I takes the form:

$$I = \frac{n \sum_{i=1}^{n} \sum_{j=1}^{n} w_{ij} \left(Y_i - \bar{Y}\right) \left(Y_j - \bar{Y}\right)}{\left(\sum_{i=1}^{n} \sum_{j=1}^{n} w_{ij}\right) \sum_{i=1}^{n} \left(Y_i - \bar{Y}\right)^2}, \tag{1.3.2}$$

where n is the number of regions, Y_i is the observed value of the variable of interest in region i , and $\bar{Y}$ is the mean of all values. w_{ij} are spatial weights that denote the spatial proximity between regions i and j, with $w_{ii} = 0$ and $i, j = 1, \ldots, n$. The definition of the spatial weights depends on the variable of study and the specific setting.

We can test the presence of spatial autocorrelation using the Moran's I, which quantifies how similar each region is with its neighbors and averages all these assessments. Under the null hypothesis of no spatial autocorrelation, observations Y_i are independent and identically distributed, and I is asymptotically normally distributed with mean and variance equal to

$$E\left[I\right] = \frac{-1}{n-1}, \tag{1.3.3}$$

and

$$Var\left[I\right] = \frac{n^2 \left(n-1\right) S_1 - n \left(n-1\right) S_2 - 2 S_0^2}{\left(n+1\right) \left(n-1\right)^2 S_0^2}, \tag{1.3.4}$$

where

$$\begin{aligned} S_0 &= \sum_{i=1}^{n} \sum_{j=1}^{n} w_{ij}, \\ S_1 &= \frac{1}{2} \sum_{i=1}^{n} \sum_{j=1}^{n} \left(w_{ij} + w_{ji}\right)^2, \end{aligned}$$

and

$$S_2 = \sum_{k=1}^{n} \left(\sum_{i=1}^{n} w_{ik} + \sum_{j=1}^{n} w_{kj} \right).$$

Moran's I values usually range from -1 to 1. Moran's I values significantly above $E[I]$ indicate positive spatial autocorrelation or clustering. This occurs when neighboring regions tend to have similar values. Moran's I values significantly below $E[I]$ indicate negative spatial autocorrelation or dispersion. This happens when regions that are close to one another tend to have different values. Finally, Moran's I values around $E[I]$ indicate randomness, that is, absence of spatial pattern.

When the number of regions is sufficiently large, I has a normal distribution and we can assess whether any given pattern deviates significantly from a random pattern by comparing the z-score

$$z = \frac{I - E[I]}{\sqrt{Var[I]}}, \tag{1.3.5}$$

to the standard normal distribution. An alternative approach to judge significance is Monte Carlo randomization. This method creates random patterns by reassigning the observed values among the areas and calculates the Moran's I for each of the patterns, providing a randomization distribution for the Moran's I. If the observed value of Moran's I lies in the tails of this distribution, the assumption of independence among observations is rejected. Thus, we can test spatial autocorrelation by following these steps:

1. State the null and alternative hypotheses:

   $H_0 : I = E[I]$ (no spatial autocorrelation),

   $H_1 : I \neq E[I]$ (spatial autocorrelation).

2. Choose the significance level α we are willing to tolerate, which represents the maximum value for the probability of incorrectly rejecting the null hypothesis when it is true (usually $\alpha = 0.05$).

3. Calculate the test statistic z (1.3.5).

4. Find the p-value for the observed data by comparing the z-score to the standard normal distribution or via Monte Carlo randomization. The p-value is the probability of obtaining a test statistic as extreme as or more extreme than the one observed test statistic in the direction of the alternative hypothesis, assuming the null hypothesis is true.

5. Make one of these two decisions and state a conclusion:

   If $p-value < \alpha$, we reject the null hypothesis. We conclude that data provide evidence for the alternative hypothesis.

   If $p-value \geq \alpha$, we fail to reject the null hypothesis. The data do not provide evidence for the alternative hypothesis.

1.4 Specification of spatial models

The detection of spatial dependence provides the motivation to extend classical regression models in order to capture the underlying interaction processes. Depending on how spatial dependence enters the data-generating process, different specifications can be formulated. The most widely used are the Spatial Autoregressive model, the Spatial Error Model, and the Spatial Durbin Model. More general forms such as the Spatial Autoregressive Combined model and the Spatial Lag of X model provide additional flexibility. These models differ not only in their mathematical structure, but also in their economic interpretation, the channels of interaction they emphasize, and the econometric issues they raise (see, e.g, Anselin, 1988; Elhorst, 2014).

1.4.1 The spatial autoregressive model

The starting point is the Spatial Autoregressive (SAR) model, which incorporates a spatial lag of the dependent variable as an explanatory factor:

$$y = \lambda W y + X\alpha + \varepsilon, \text{ with } \quad \varepsilon \sim N\left(0, \sigma^2 I\right). \tag{1.4.1}$$

Here, y denote the $N \times 1$ vector of dependent variable, X the $N \times K$ matrix of explanatory variables, W the spatial weights matrix, and λ the spatial autoregressive parameter.

The presence of Wy introduces an endogenous interaction effects. This term captures the idea that the outcome in one location depends directly on the outcomes in neighboring locations as defined by the weights matrix W. To see this more clearly, the SAR can be rewritten in reduced form by rearranging terms:

$$(I - \lambda W)\, y = X\alpha + \varepsilon,$$

or equivalently,

$$y = (I - \lambda W)^{-1} X\alpha + (I - \lambda W)^{-1} \varepsilon, \tag{1.4.2}$$

Provided that $(I - \lambda W)^{-1}$ exists. The key object here is the spatial multiplier matrix $(I - \lambda W)^{-1}$.

This inverse expands as a Neumann series when $|\lambda| \leq 1$:

$$(I - \lambda W)^{-1} = I + \lambda W + \lambda^2 W^2 + \lambda^3 W^3 + \cdots$$

This expansion reveals how shocks propagate through the system. A direct effect on a unit not only affects that unit (through I), but transmits to its immediate neighbors (λW) to neighbors of neighbors $\left(\lambda^2 W^2\right)$, and so forth. In othor words, the SAR model implies a cascade of feedback effects across space: a local shock ripples through the network of spatial interactions and eventually feeds back to the original unit (see, e.g, Anselin, 1988, pp. 57–61).

Illustration

Suppose $\lambda > 0$ and W is a simple contiguity matrix. An increase in the explanatory variable X in region i raises y_i. Through the term $\lambda W y$, this increase spills over to neighboring regions j connected to i. Those neighbors' outcomes, in turn, feed back into region i via higher-order powers of W. The magnitude of these effects declines with distance (in terms of network connectivity) and with successive powers of λ. This mechanism explains why the SAR model is suited to phenomena that diffuse spatially and are mutually reinforcing.

Applications

This property makes the SAR particularly appropriate in contexts where outcomes are jointly determined across space. In housing markets, the price of one property is influenced by the prices of surrounding properties, which themselves adjust in response, leading to recursive

interactions. In regional growth analysis, the economic performance of one region depends on the growth trajectories of its neighbors, generating regional convergence or divergence patterns. In the diffusion of innovations, the adoption decision of one unit increases the likelihood that neighboring units adopt, producing spatial contagion.

Econometric Implications

Because of this simultaneity, the regressor Wy is endogenous: it is correlated with the error term ε. Estimation by ordinary least squares is therefore biased and inconsistent (Anselin, 1988, pp. 57–61). Consistent estimation requires maximum likelihood methods, which account for the spatial multiplier and the Jacobian of the transformation, or instrumental variable approaches using spatial lags of exogenous covariates as instruments.

1.4.2 The spatial error model

An alternative formulation is the Spatial Error Model (SEM), which assumes that spatial dependence arises not in the dependent variable itself, but in the error structure:

$$y = X\beta + u, \quad u = \rho W u + \varepsilon \quad \text{with} \quad \varepsilon \sim N\left(0, \sigma^2 I\right), \tag{1.4.3}$$

In this model, the unobserved component u follows a spatial autoregressive process, with ρ measuring the strength of spatial correlation, and ε is an independant and identically distributed disturbance vector. In this formulation, the observed outcome depends on explanatory variables as in the classical regression model, but the unobserved component follows a spatial autoregressive process.

Sources of Spatial Error Dependence

The SEM is particularly appropriate when unobserved or omitted factors that influence the dependent variable are themselves spatially correlated. Such correlation may arise for a number of reasons. First, it may be due to omitted variables that follow geographic patterns, such as climate conditions, cultural traits, or historical legacies that affect several neighboring regions simultaneously. Second, spatial error correlation may emerge from unmeasured shocks that cluster across space, such as a regional economic downturn or a natural disaster that affects multiple units at once. Third, errors in measurement can also display spatial correlation when data are aggregated over contiguous areas or when survey collection

procedures introduce spatial clustering. In all of these cases, the correlation is not in the observed regressors or in the dependent variable itself, but rather in the unobserved residual component of the model (see, e.g, Anselin, 1988, pp. 23–24).

Practical Interpretation

Spatial econometric literature often distinguishes between models that capture substantive spatial dependence and those that primarily address statistical concerns. While the SAR model reflects a situation in which outcomes are jointly determined across space, the SEM focuses instead on spatial correlation present in the unobserved components that influence those outcomes (see e.g, Anselin, 1988, p. 24). In this respect, the SEM functions as a corrective device for violations of the classical regression assumptions rather than as a framework offering a behavioral explanation of spatial interaction. Nevertheless, such a correction is indispensable in applied research, as disregarding spatial error dependence can lead to flawed inference, even if the coefficient estimates themselves remain unbiased.

Applications of the SEM are widespread in empirical studies where local influences are difficult to observe but are likely to be spatially clustered. For instance, in regional productivity analysis, unmeasured institutional quality or cultural factors may be spatially correlated across neighboring regions. In housing market studies, unobserved neighborhood amenities or environmental conditions may drive correlated residuals across adjacent locations. In epidemiology, unrecorded behavioral or environmental risk factors may lead to spatial clustering of residuals in disease incidence models. In all such cases, the SEM provides a way to restore efficiency and validity in econometric estimation by explicitly modeling the spatial structure of the disturbances.

1.4.3 The Spatial Durbin Model

The Spatial Durbin Model (SDM) constitutes one of the most general and flexible specifications in spatial econometrics. It extends the SAR model by not only including a spatially lagged dependent variable but also incorporating spatially lagged explanatory variables. Its functional form can be expressed as:

$$y = \lambda W y + X\alpha + WX\beta + \varepsilon \ , \ \ \varepsilon \sim N\left(0, \sigma^2 I\right), \tag{1.4.4}$$

where y is the dependent variable, X the matrix of explanatory variables, Wy the spatial

lag of the dependent variable, and WX the matrix of spatial lags of the explanatory variables. The coefficient λ captures endogenous interaction effects, while the parameter vector β reeflects the influence of neighboring units' covariates on local outcomes.

The SDM therefore nests both the SAR and the SEM as special cases. When $\beta = 0$, the model reduces to the SAR specification, in which dependence occurs only in the dependent variable. When $\lambda = 0$ but $\beta \neq 0$, the model becomes a spatially extended regression model often referred to as the Spatial Lag of X (SLX) model. Furthermore, under certain parametric restrictions, the SDM can be shown to be equivalent to a SEM specification. This nesting property makes the SDM an extremely versatile model, capable of representing a broad range of spatial processes (see, e.g, Anselin, 1988, pp. 59–61).

The interpretation of the SDM hinges on distinguishing between different types of spatial effects. The inclusion of the lagged dependent variable, as in the SAR, generates endogenous interaction effects, whereby the outcome of one unit depends directly on the outcomes of its neighbors. In addition, the presence of spatially lagged explanatory variables WX captures exogenous interaction effects. These effects arise when the characteristics of neighboring units such as their income, education levels, infrastructure, or policy choices exert an influence on local outcomes. The combination of both terms allows the SDM to model situations where outcomes depend not only on neighboring outcomes but also on neighboring covariates.

From a reduced-form perspective, the SDM can be written as:

$$y = (I - \lambda W)^{-1} (X\alpha + WX\beta + \varepsilon), \tag{1.4.5}$$

As in the SAR model, provided that $(I - \lambda W)^{-1}$ exists, the presence of the spatial multiplier $(I - \lambda W)^{-1}$ implies that shocks in one unit propagate throughout the spatial system via a series of feedback effects. In the SDM, however, the propagation mechanism is richer since the model also includes spatially lagged explanatory variables. Consequently, a change in an explanatory variable in one unit generates not only a direct effect on that unit but also indirect effects transmitted through its neighbors' outcomes. These effects may further circulate across higher-order neighbors, reinforcing the feedback process (see, e.g, Elhorst, 2014, pp. 19–22).

One of the most important implications of the SDM is that the marginal effects of explanatory variables cannot be interpreted as simple regression coefficients, as in the classical linear

model. Instead, the total impact of a change in a covariate must be decomposed into direct effects, which measure the average impact on the unit experiencing the change, and indirect or spillover effects, which measure the impact of neighboring units. The sum of these two components constitutes the total effect. Estimation of these effects relies on the spatial multiplier and requires matrix algebra to compute the traces of successive powers of the weights matrix (LeSage and Pace, 2009). This decomposition has become a standard practice in empirical applications of the SDM and represents one of its main contributions to applied spatial econometrics.

The SDM has several attractive features for empirical research. Its flexibility allows it to capture both endogenous and exogenous interaction effects, making it suitable for a wide range of applications where spillovers are theoretically plausible. For example, in regional economics, the growth of one region may depend both on its own initial conditions and on the economic characteristics of neighboring regions, such as their capital stocks or levels of human capital. In housing markets, property values may be influenced not only by neighboring house prices (endogenous dependence) but also by neighborhood attributes such as school quality or crime rates (exogenous dependence). In environmental studies, pollution levels may depend simultaneously on emissions in nearby locations and on their socioeconomic characteristics.

In summary, the SDM represents the most general of the basic spatial econometric specifications, combining endogenous and exogenous interaction effects in a unified framework. By accommodating both direct and indirect effects of explanatory variables and nesting more restrictive models, it provides a powerful and flexible tool for empirical research on spatial processes.

1.4.4 The General Nesting Spatial Model

The models discussed so far are the SAR, SEM, and SDM each capture distinct dimensions of spatial dependence. Yet in practice, spatial processes are rarely confined to a single channel of interaction. Local outcomes may be simultaneously influenced by the outcomes of neighboring regions, by the characteristics of those regions, and by unobserved shocks that are themselves spatially correlated. To accommodate this complexity, spatial econometrics has developed more encompassing specifications that unify these channels of dependence.

The most general of these is the GNS model, sometimes referred to as the general spatial model (see, e.g, Anselin, 1988; Elhorst, 2014).

The GNS model can be expressed as:

$$y = \lambda Wy + X\alpha + WX\beta + u \text{ and } \; u = \rho Wu + \varepsilon, \tag{1.4.6}$$

with $\varepsilon \sim N\left(0, \sigma^2 I\right)$. This formulation combines all three sources of spatial interaction within a single framework. The term λWy reflects endogenous dependence, capturing the idea that outcomes in one region directly depend on outcomes in neighboring regions. The term $WX\beta$ introduces exogenous dependence, where the characteristics of neighboring regions influence local outcomes. Finally, the error process $u = \rho Wu + \varepsilon$ accounts for nuisance dependence, arising when omitted variables, unmeasured shocks, or measurement errors are spatially correlated.

A key advantage of the GNS specification is that it encompasses the more restricted models as special cases. Setting $\beta = 0$ and $\rho = 0$ reduces the model to the SAR. If instead $\lambda = 0$ and $\beta = 0$ the model collapses to the SEM. Setting only $\rho = 0$ yields the SDM. In this sense, the GNS functions as an overarching theoretical structure from which the classical spatial models can be derived by imposing restrictions (see, e.g, Anselin, 1988, pp. 59–61; Elhorst, 2014, pp. 19–22).

Conceptually, the GNS highlights the multidimensional nature of spatial dependence. Real-world processes often involve feedback between outcomes, external influences from neighboring covariates, and correlated unobserved shocks, all operating at once. The GNS model provides a way of recognizing this complexity and ensuring that empirical analysis does not prematurely impose a narrow definition of spatial dependence.

In applied research, the GNS model is particularly useful as a starting point for model specification. By encompassing the SAR, SEM, and SDM within a single framework, it allows researchers to begin with the most general form of spatial dependence and subsequently explore whether more parsimonious structures provide an adequate description of the data. While issues of estimation and model selection will be discussed in the following section, it is important to emphasize here that the GNS serves as the theoretical unifying model in spatial econometrics, capturing the full range of possible interactions across space.

1.4.5 Estimation of Spatial Econometric Models

Estimation in spatial econometrics raises challenges that go well beyond those encountered in classical regression analysis. In the conventional linear regression framework, ordinary least squares (OLS) estimators are unbiased, consistent, and efficient under the classical assumptions of exogeneity and independence of the error terms. However, in spatial models, these assumptions rarely hold. Two distinct but often interrelated problems appear. The first arises when spatial lags of the dependent variable are introduced, as in the SAR or GNS models. In such cases, simultaneity emerges because the outcome in a given region depends on outcomes in neighboring regions, which themselves depend on the first region. This feedback mechanism makes the spatial lag endogenous, since it is inevitably correlated with the error term, leading OLS to produce biased and inconsistent estimates. The second difficulty appears in SEM, where the disturbances are spatially correlated. In this case, even if the regressors are exogenous, shocks in one region spill over to others, violating the independence assumption. Here OLS estimates remain unbiased but are inefficient, and the usual standard errors cannot be relied upon for valid inference. The most general specification that captures these two difficulties simultaneously is GNS model defined by(1.4.6), which combines endogenous interaction effects, exogenous interaction effects, and spatial error dependence.

1.4.6 Maximum likelihood

The first and most widely used estimation approach in spatial econometrics is maximum likelihood (ML). The idea underlying ML is straightforward: if we assume the error term is normally distributed, then the entire model implies a multivariate normal distribution for the dependent variable. The likelihood function measures how probable the observed data are given a set of parameter values, and estimation consists in finding the parameter values that maximize this probability. In spatial models, the presence of feedback effects across units means that the covariance structure of the dependent variable is no longer spherical. The reduced form of the model involves the inverses $(I - \lambda W)^{-1}$ and $(I - \rho W)^{-1}$, which capture the fact that shocks in one region propagate through the entire system. These inverses give rise to Jacobian terms such as $\ln|I - \rho W|$ and $\ln|I - \lambda W|$ in the log-likelihood, ensuring that the density function integrates to one.

For the GNS model, the log-likelihood can be written as

$$l\left(\lambda,\rho,\alpha,\beta,\sigma^2\right)=\ln|I-\rho W|+\ln|I-\lambda W|-\frac{n}{2}\ln\left(2\pi\sigma^2\right)-\frac{1}{2}\varepsilon'\varepsilon, \tag{1.4.7}$$

with residuals defined as

$$\varepsilon=(I-\rho W)(I-\lambda W)y-(I-\rho W)(X\alpha+WX\beta),$$

Although this expression looks complicated, its structure is quite systematic. It consists of the Jacobian terms associated with the spatial lag and error components, a constant term, and a quadratic form in the transformed residuals. In practice, estimation is simplified by concentrating out the regression coefficients and the variance parameter, which reduces the problem to the numerical optimization of the likelihood with respect to the spatial parameters ρ and λ. Once these are obtained, the other coefficients can be estimated in a second step.

The main computational difficulty is the evaluation of the log-determinants $\ln|I-\rho W|$ and $\ln|I-\lambda W|$. For small systems, these can be obtained exactly using eigenvalue decompositions. For larger datasets, approximation methods such as Chebyshev polynomials, Monte Carlo simulation, or sparse matrix techniques are employed. Despite these challenges, ML remains the benchmark estimation method because it yields estimators that are consistent and asymptotically efficient under Gaussian assumptions, and it provides a natural framework for hypothesis testing and model comparison. Likelihood ratio tests, Wald tests, and Lagrange Multiplier tests are all derived from the likelihood function and allow researchers to discriminate between competing spatial specifications. Information criteria such as the Akaike Information Criterion (AIC) or the Bayesian Information Criterion (BIC) are likewise based on the maximized likelihood and are commonly used to compare SAR, SEM, SDM, and GNS models.

A major advantage of presenting estimation from the GNS perspective is that restricted versions of the likelihood directly yield the estimators for simpler models. If both β and ρ are set equal to zero, the GNS reduces to the SAR model, where the only Jacobian term is $\ln|I-\lambda W|$. If λ and β are set to zero, the model becomes the SEM, in which dependence is confined to the error term and the likelihood includes only $\ln|I-\rho W|$. If ρ is set to zero while λ and β remain, the model becomes the SDM, essentially a SAR augmented with spatial lags of the regressors. Thus, the ML estimator provides a unifying framework within which all standard spatial models can be estimated as special cases.

1.5 Spatial Panel Models

Spatial panel models extend the analytical power of econometric models by combining spatial dependence with panel data structures. Traditional cross-sectional spatial models capture interactions among units at a single point in time (see, e.g, Anselin, 1988), while non-spatial panel models exploit temporal variation and control for unobserved heterogeneity (see, e.g, Baltagi, 2013). Spatial panels integrate both dimensions, making it possible to account for spatial interactions that evolve over time and to correct for individual heterogeneity that might otherwise bias estimates. This dual consideration has made spatial panel models increasingly relevant in empirical research across economics, regional science, environmental studies, and public health (see, e.g, Elhorst, 2014).

1.5.1 Motivation for Spatial Panels

The motivation for spatial panels lies in the limitations of purely spatial cross-sectional or non-spatial panel approaches. On one hand, cross-sectional spatial econometric models identify spatial spillovers but ignore how these evolve dynamically. On the other hand, classical panel data methods allow researchers to control for time-invariant unobserved heterogeneity but assume independence across units, which is rarely realistic in regional or network data (Elhorst, 2010; Lee and Yu, 2010).

Spatial panels provide several advantages:

- **Control for heterogeneity**: unobserved region-specific effects (fixed or random) can be included to avoid omitted variable bias.
- **Increased efficiency**: exploiting both spatial and temporal variation reduces standard errors and improves inference (see, e.g, Hsiao, 2014).
- **Dynamic spillovers**: they capture how shocks or policies diffuse both across space and over time, an essential feature in policy evaluation, environmental modeling, and epidemiology.

As Elhorst (2014) emphasizes, these models offer richer policy insights since they identify both direct effects (within a unit) and indirect effects (spatial spillovers), making them

particularly attractive for applied research.

1.5.2 Spatial Panel Models with Fixed Effects

In the previous section, we introduced the SDM in a cross-sectional framework. As one of the most general specifications in spatial econometrics, the SDM simultaneously incorporates endogenous interaction effects, through the spatial lag of the dependent variable WY, and exogenous interaction effects, through the spatial lags of the explanatory variables WX. This dual structure makes the SDM particularly appropriate for settings where outcomes in a given unit are influenced not only by the outcomes but also by the characteristics of neighboring units.

This specification can be extended to the panel data framework, which combines the spatial dimension with repeated observations over time. The availability of panel data allows researchers to control for unobserved heterogeneity across spatial units, typically through fixed effects, thereby reducing omitted-variable bias and improving the consistency of the estimates (see, e.g, Elhorst, 2014).

The fixed-effects SDM in a panel setting can be expressed as:

$$y_{i,t} = \mu_i + \lambda \sum_{j=1}^{n} w_{ij} y_{j,t} + x_{i,t}\alpha + \sum_{j=1}^{n} w_{ij} x_{j,t}\beta + \varepsilon_{i,t} \tag{1.5.1}$$

where $y_{i,t}$ denotes the dependent variable for unit i at time t, while $x_{i,t} = \left(x_{i,t}^{(1)}, x_{i,t}^{(2)}, \ldots, x_{i,t}^{(k)}\right)$ represents the associated vector of explanatory variables. The terms $\sum_{j=1}^{n} w_{ij} y_{j,t}$ and $\sum_{j=1}^{n} w_{ij} x_{j,t}$ represent the spatial lags of the dependent and explanatory variables, respectively. The parameter λ measuring endogenous interaction effects via the spatial lag of the dependent variable, and the parameter vector β reflecting exogenous interaction effects through spatial lags of the explanatory variables. The term μ_i represents the individual fixed effects, which account for unobserved and time-invariant characteristics specific to each unit, such as geography, history, or institutional context. Finally, $\varepsilon_{i,t}$ is the idiosyncratic error term, which captures random disturbances not explained by the model.

For notational convenience, the model (1.5.1) can be written in vector form:

$$Y_t = \mu + \lambda W Y_t + X_t\alpha + WX_t\beta + \varepsilon_t,$$

where $Y_t = (y_{1,t}, y_{2,t}, \ldots, y_{n,t})'$, $X_t = (x_{1,t}, x_{2,t}, \ldots, x_{n,t})$,

$$\mu = \begin{pmatrix} \mu_1 \\ \mu_2 \\ \vdots \\ \mu_n \end{pmatrix} \text{ and } W = \begin{pmatrix} 0 & w_{1,2} & \cdots & w_{1,n} \\ w_{2,1} & 0 & \ddots & \vdots \\ \vdots & \ddots & \ddots & w_{1,n-1} \\ w_{n,1} & w_{n,2} & \cdots & 0 \end{pmatrix}.$$

1.5.3 Estimation of Spatial Panel Models

When moving from cross-sectional to panel data, the estimation of spatial econometric models must account not only for spatial dependence but also for unobserved heterogeneity across units and over time. The fixed effects specification is particularly important in this context, as it allows to control for unit-specific and time-specific factors that are constant but unobserved, thereby avoiding omitted-variable bias. In spatial panel models, the same challenges encountered in cross-sectional estimation such as the endogeneity of the spatial lag and the spatial correlation of errors persist, but they must now be handled jointly with the elimination of individual and time effects. The fixed effects approach provides a robust framework for this purpose, since maximum likelihood estimation can be adapted to incorporate both spatial interaction terms and the transformation needed to remove unobserved heterogeneity. Thus, the estimation of spatial fixed effects panel models extends the cross-sectional methods while offering richer and more reliable inference on the role of spatial spillovers in a dynamic and heterogeneous environment.

The transition from cross-sectional to panel data in spatial econometrics enriches the analysis by introducing a temporal dimension, but it also raises additional estimation challenges. In panel settings, units are observed repeatedly over time, which implies that unobserved heterogeneity must be taken into account to avoid biased inference. Fixed effects specifications provide a natural solution by controlling for unit-specific and time-specific unobserved characteristics that remain constant over the period of observation.

The estimation of spatial panel models generally relies on the ML approach, which has become the standard method in the econometrics of spatial dependence (see, e.g, Anselin,

1988; Elhorst, 2014; Lee and Yu, 2010). The ML estimator exploits the full distributional assumptions of the model, typically assuming that the error terms $\varepsilon_{i,t}$ are iid with zero mean and constant variance σ^2. By maximizing the likelihood function, one obtains consistent and asymptotically efficient estimates of the parameters (λ, α, β), provided that the spatial weights matrix W is correctly specified.

A key challenge in panel settings is the presence of individual fixed effects μ_i which control for unobserved heterogeneity across spatial units. Direct inclusion of these effects in the likelihood function is computationally burdensome, especially when the number of units n is large. To address this, the model is typically estimated after applying the within transformation, also known as the demeaning procedure. Specifically, for each variable z_t, the transformation is:

$$\tilde{z}_t = z_t - \bar{z} \quad \text{,with} \quad \bar{z} = \frac{1}{T}\sum_{t=1}^{T} z_t, \tag{1.5.2}$$

where T denotes the number of time periods. This transformation eliminates the fixed effect μ thereby reducing the risk of omitted-variable bias and simplifying the estimation problem. After the within transformation, the likelihood function is constructed using the transformed variables $\tilde{Y}_t, \tilde{X}_t$, and their spatial lags.

The resulting log-likelihood function for the SDM can be written as:

$$l\left(\lambda, \alpha, \beta, \sigma^2\right) = T \ln |I_n - \rho W| - \frac{nT}{2} \ln\left(2\pi\sigma^2\right) - \frac{1}{2}\sum_{t=1}^{T} \tilde{\varepsilon}_t' \tilde{\varepsilon}_t, \tag{1.5.3}$$

where $\tilde{\varepsilon} = \tilde{y}_t - \lambda W \tilde{y}_t - \tilde{X}_t \alpha - W\tilde{X}_t \beta$. The term $\ln |I_n - \lambda W|$ reflects the Jacobian of the transformation, which corrects for the endogeneity induced by the spatial lag of the dependent variable. Maximizing this likelihood function with respect to the parameters yields the ML estimators. Numerical optimization techniques, such as Newton-Raphson or Expectation-Maximization algorithms, are generally required due to the nonlinear dependence on λ.This estimation procedure ensures that both the spatial dependence (through λ and β and unobserved heterogeneity (through the within transformation) are properly accounted for, providing reliable inference on the role of endogenous and exogenous spatial spillovers in panel data.

Chapter 2

Threshold Spatial Durbin model

2.1 Introduction

Spatial econometrics has undergone significant evolution over the past decades, progressing from cross-sectional spatial models to more sophisticated spatial–temporal frameworks. Early developments focused on capturing spatial dependence in cross-sectional data (see, e.g, Anselin, 1988; Cliff & Ord, 1981), which provided the foundation for models such as the Spatial Autoregressive SAR, SEM and SDM. As datasets with both spatial and temporal dimensions became increasingly available, researchers extended these frameworks into spatial panel and spatiotemporal models to better account for dynamic processes and long-term dependencies (see, e.g, Elhorst, 2003; Lee and Yu, 2010).

Each generation of models has been motivated by the need to provide an adequate representation of the underlying data-generating process. Classical spatial econometric models are essentially linear and assume homogeneity across units, which facilitates estimation but imposes strong restrictions on the relationships being modeled. In practice, however, real-world spatial phenomena often display nonlinear dynamics, structural heterogeneity, and complex interaction effects that cannot be fully captured within a purely linear framework (see, e.g, Elhorst, 2014; LeSage and Pace, 2009).

More recently, research has also turned to the issue of nonlinearity and heterogeneity in spa-

tial processes. Aquaro et al. (2015) were among the first to emphasize the role of regional heterogeneity in spatial econometric models. Building on this, the class of threshold models has received considerable interest in recent years. For example, Deng (2018) proposed the Threshold Spatial Autoregressive (TSAR) model, in which the spatial parameters vary across regimes defined by a threshold variable, while the coefficients of the exogenous regressors remain homogeneous across regimes. Zhu et al. (2020) extended this framework by introducing the Threshold Spatial Durbin (TSD) model, which allows heterogeneous slope coefficients not only for spatial lags but also for all exogenous variables. However, both the TSAR and TSD models are formulated in a cross-sectional context.

In parallel, significant progress has been made in developing threshold models for panel data. Hansen (1999, 2000) proposed the Panel Threshold Regression (PTR) model for non-dynamic panels, providing a flexible framework that allows different cross-sectional units to switch across regimes depending on the value of a threshold variable. This approach captures unobserved heterogeneity across units and highlights the nonlinear interactions between dependent and explanatory variables within a panel setting. Nevertheless, Hansen's framework does not address estimation and testing issues in the presence of spatial dependence.

To fill this gap, Wei et al. (2021) extended the threshold methodology to spatial panels by proposing the Panel Threshold Spatial Durbin (PTSD) model. This model generalizes the TSAR of Deng (2018) and the TSD of Zhu et al. (2020) to a panel-data framework, allowing both spatial dependence and threshold-driven heterogeneity to be modeled simultaneously.

A key challenge in estimating spatial threshold models is the well-known issue of endogeneity arising from spatial dependence (see, e.g, Kelejian and Prucha, 1998; Lee, 2007). As a result, the least squares estimation method used by Hansen (1999, 2000) in non-spatial panels cannot be directly applied. To address this, Deng (2018) and Wei et al. (2021) proposed using a two-stage least squares (2SLS) approach, while Zhu et al. (2020) suggested a Bayesian estimation strategy for the threshold spatial Durbin model. In line with these contributions, and in order to adapt threshold methods to the spatial panel framework, we propose a quasi-maximum likelihood (QML) approach for the estimation of the non-dynamic threshold spatial panel model.

In this chapter, we therefore present the threshold spatial panel model with fixed effects pro-

posed by Wei et al. (2021) and develop our estimation procedure using the quasi-maximum likelihood method. Furthermore, we provide a comparative discussion of alternative estimation strategies, in particular contrasting the QML approach with the 2SLS method, in order to highlight their respective advantages and limitations.

2.2 Panel threshold spatial Durbin models

We consider a non-dynamic threshold spatial panel data model with two regimes, where each regime follows a standard balanced spatial panel structure that explicitly accounts for spatial dependence.

The general specification of the model is given by:

$$y_{i,t} = \begin{cases} \mu_i + \lambda_1 \sum\limits_{j=1\ i\neq j}^{n} w_{ij}y_{j,t} + x_{i,t}\alpha_1 + \sum\limits_{j=1\ i\neq j}^{n} w_{ij}x_{j,t}\beta_1 + v_{i,t} & q_{i,t} \leq \gamma, \\ \mu_i + \lambda_2 \sum\limits_{j=1\ i\neq j}^{n} w_{ij}y_{j,t} + x_{i,t}\alpha_2 + \sum\limits_{j=1\ i\neq j}^{n} w_{ij}x_{j,t}\beta_2 + v_{i,t} & q_{i,t} > \gamma, \end{cases} \tag{2.2.1}$$

where the subscript i represent cross section $(i = 1, 2, \ldots, n)$ and t is the time periods $(t = 1, 2, \ldots, T)$.

The model (2.2.1) can be written as :

$$\begin{aligned} y_{i,t} &= \left(\lambda_1 \sum_{j=1\ i\neq j}^{n} w_{ij}y_{j,t} + x_{i,t}\alpha_1 + \sum_{j=1\ i\neq j}^{n} w_{ij}x_{j,t}\beta_1 \right) I_{q_{i,t}\leq\gamma} \\ &\quad + \left(\lambda_2 \sum_{j=1\ i\neq j}^{n} w_{ij}y_{j,t} + x_{i,t}\alpha_2 + \sum_{j=1\ i\neq j}^{n} w_{ij}x_{j,t}\beta_2 \right) I_{q_{i,t}>\gamma} + \mu_i + v_{i,t}, \end{aligned} \tag{2.2.2}$$

where $I_{(.)}$ is the indicator function.

Here, $y_{i,t}$ denote the scalar observation of the dependent variable for unit i at time t. The term $\sum\limits_{j=1\ i\neq j}^{n} w_{ij}y_{j,t}$ captures the endogenous interaction effect between $y_{i,t}$ and the dependent variable in neighboring units, where w_{ij} is the (i, j)-th element of the spatial weight matrix W, assumed to be constant. The scalars $\lambda_r\,(r = 1, 2)$ measure the strength of these endogenous spatial interactions across regimes. Similarly, the term $\sum\limits_{j=1\ i\neq j}^{n} w_{ij}x_{j,t}$ accounts for the

exogenous interaction effects, that is, the influence of neighboring covariates on unit i. The associated parameter vector $\beta_r\,(r=1,2)$ measures the marginal impact of these spatially lagged exogenous variables. The vector $x_{i,t}$ of dimension $1\times k$ contains the local exogenous regressors, linked with slope parameters $\alpha_i\,(i=1,2)$ that differ across regimes.

The disturbance term $v_{i,t}$ is assumed to be iid with zero mean and finite variance σ^2. The individual-specific fixed effect is denoted by μ_i. The regime-switching mechanism is introduced through the threshold variable $q_{i,t}$ and its associated threshold parameter γ, which jointly determine the allocation of observations across regimes.

To express the model in matrix form, define the diagonal indicator matrix:

$$d_{t,1}=\begin{pmatrix} I_{q_{1,t}\leq\gamma} & 0 & \dots & 0\\ 0 & I_{q_{2,t}\leq\gamma} & \ddots & \vdots\\ \vdots & \ddots & \ddots & 0\\ 0 & \dots & 0 & I_{q_{n,t}\leq\gamma}\end{pmatrix} \text{ and } d_{t,2}=I_n-d_{t,1},$$

Upon stacking the observations across all cross-sectional units, Equation (2.2.2) can be rewritten in a compact matrix form as:

$$Y_t=\mu+\lambda_1 d_{t,1}WY_t+d_{t,1}X_t\alpha_1+d_{t,1}WX_t\beta_1+\lambda_2 d_{t,2}WY_t+d_{t,2}X_t\alpha_2+d_{t,2}WX_t\beta_2+V_t \quad (2.2.3)$$

with $Y_t=(y_{1,t},y_{2,t},\dots,y_{n,t})'$, $X_t=(x_{1,t},x_{2,t},\dots,x_{n,t})'$, $V_t=(v_{1,t},v_{2,t},\dots,v_{n,t})'$,

$$\mu=(\mu_1,\mu_2,\dots,\mu_n)',\ \text{and } W=\begin{pmatrix} 0 & w_{1,2} & \cdots & w_{1,n}\\ w_{2,1} & 0 & \ddots & \vdots\\ \vdots & \ddots & \ddots & w_{1,n-1}\\ w_{n,1} & w_{n,2} & \cdots & 0\end{pmatrix}.$$

The reduced form of the (2.2.3) is given as:

$$\begin{aligned} Y_t &= \mu+\lambda_1 d_{t,1}WY_t+d_{t,1}X_t\alpha_1+d_{t,1}WX_t\beta_1\\ &\quad +\lambda_2 d_{t,2}WY_t+d_{t,2}X_t\alpha_2+d_{t,2}WX_t\beta_2+V_t,\\ (I_n-\lambda_1 d_{t,1}W-\lambda_2 d_{t,2}W)Y_t &= \mu+d_{t,1}X_t\alpha_1+d_{t,1}WX_t\beta_1+d_{t,2}X_t\alpha_2+d_{t,2}WX_t\beta_2+V_t, \end{aligned}$$

Defining

$$S_{\gamma,t}(\lambda)=I_n-\lambda_1 d_{t,1}W-\lambda_2 d_{t,2}W,$$

and assuming that $S_{\gamma,t}(\lambda)$ is non-singular, we obtain the compact reduced form:

$$Y_t=S_{\gamma,t}(\lambda)^{-1}\left(\mu+d_{t,1}X_t\alpha_1+d_{t,1}WX_t\beta_1+d_{t,2}X_t\alpha_2+d_{t,2}WX_t\beta_2+V_t\right). \quad (2.2.4)$$

2.3 Estimation approach

The threshold panel model introduced by Hansen (1999) relies on a least squares estimation procedure that provides consistent estimates of the parameters and the threshold value. However, this classical PTR framework does not account for spatial dependence. When the panel structure includes a spatially lagged dependent variable, estimation becomes more challenging (see Anselin et al., 2008). In particular, one of the major complications arises from the endogeneity of the spatial lag term $\sum_{j=1}^{n} w_{ij} y_{j,t}$ which violates the standard regression assumption $E\left(\sum_{j=1}^{n} w_{ij} y_{j,t} v_{i,t}\right) = 0$. Consequently, the least squares approach proposed by Hansen (1999) is no longer valid in this spatial setting.

A common solution, as suggested by Wei et al. (2021) for the TSDP model, is to employ instrumental variable (IV) estimation. This approach builds on the framework of Kelejian and Prucha (1998), who proposed using exogenous regressors and their spatial lags as instruments. In practice, Wei et al. (2021) recommend a 2SLS procedure, which yields consistent estimates of the spatial threshold model parameters. In this work, however, we propose an alternative estimation strategy based on the QML method. This approach is particularly attractive because it directly accounts for the joint distribution of the error terms and provides a likelihood-based framework for inference.

Let $\phi = (\lambda_1, \lambda_2, \beta_1, \beta_2, \alpha_1, \alpha_2)$ denote the vector of structural parameters and γ the unknown threshold parameter. For a given value of γ, the implicit reduced form of the model can be expressed as:

$$V_{\gamma,t}(\phi, \mu) = S_{\gamma,t}(\lambda) Y_t - \mu - d_{t,1} X_t \alpha_1 - d_{t,1} W X_t \beta_1 - d_{t,2} X_t \alpha_2 - d_{t,2} W X_t \beta_2.$$

Since the error vector $V_{\gamma,t}(\phi, \mu)$ is not observed directly, the likelihood function must be derived from the observed vector Y_t. This requires the Jacobian transformation from V_t to Y_t

$$J = \left| \frac{\partial V_t}{\partial Y_t} \right| = \left| S_{\gamma,t}(\lambda) \right|.$$

Based on a joint standard normal distribution for the error V_t, and using the jacobian ex-

pression, the likelihood fuction for joint vector of observation Y_t is obtained as:

$$\begin{aligned} L_{\gamma,t}\left(\phi,\mu,\sigma^2\right) &= \prod_{t=1}^{T} f_{\gamma,t}(Y_t,X_t,\phi,\mu)\times J \\ &= \prod_{t=1}^{T}\left(\frac{1}{\sqrt{2\pi}}\left|\sigma^2 I_n\right|^{-\frac{1}{2}}\right)^n \exp\left(-\frac{1}{2}V'_{\gamma,t}\left(\phi,\mu\right)\left(\sigma^2 I_n\right)^{-1}V_{\gamma,t}\left(\phi,\mu\right)\right)\times\left|S_{\gamma,t}\left(\lambda\right)\right| \\ &= \prod_{t=1}^{T}\left(\frac{1}{\sqrt{2\pi\sigma^2}}\right)^n \exp\left(-\frac{1}{2\sigma^2}V'_{\gamma,t}\left(\phi,\mu\right)V_{\gamma,t}\left(\phi,\mu\right)\right)\times\left|S_{\gamma,t}\left(\lambda\right)\right|. \end{aligned}$$

The log-likelihood function of (2.2.4), as if the disturbance were normally distributed is:

$$\begin{aligned} \ln L_{\gamma,t}\left(\phi,\mu,\sigma^2\right) &= \ln\left(\prod_{t=1}^{T}\left(\frac{1}{\sqrt{2\pi\sigma^2}}\right)^n \exp(-\frac{1}{2\sigma^2}V'_{\gamma,t}\left(\phi,\mu\right)V_{\gamma,t}\left(\phi,\mu\right)\times\left|S_{\gamma,t}\left(\lambda\right)\right|\right) \\ &= \sum_{t=1}^{T}\ln\left(\left(\frac{1}{\sqrt{2\pi\sigma^2}}\right)^n \exp(-\frac{1}{2\sigma^2}V'_{\gamma,t}\left(\phi,\mu\right)V_{\gamma,t}\left(\phi,\mu\right)\times\left|S_{\gamma,t}\left(\lambda\right)\right|\right) \\ &= \sum_{t=1}^{T}\left[\ln\left(\frac{1}{\sqrt{2\pi\sigma^2}}\right)^n - \frac{1}{2\sigma^2}V'_{\gamma,t}\left(\phi,\mu\right)V_{\gamma,t}\left(\phi,\mu\right)+\ln\left|S_{\gamma,t}\left(\lambda\right)\right|\right] \\ &= \sum_{t=1}^{T}\ln\left(\frac{1}{\sqrt{2\pi\sigma^2}}\right)^n - \frac{1}{2\sigma^2}\sum_{t=1}^{T}V'_{\gamma,t}\left(\phi,\mu\right)V_{\gamma,t}\left(\phi,\mu\right)+\sum_{t=1}^{T}\ln\left|S_{\gamma,t}\left(\lambda\right)\right| \end{aligned}$$

$$\ln L_{\gamma,t}\left(\phi,\mu,\sigma^2\right) = -\frac{nT}{2}\ln(2\pi\sigma^2)+\sum_{t=1}^{T}\ln\left|S_{\gamma,t}\left(\lambda\right)\right|-\frac{1}{2\sigma^2}\sum_{t=1}^{T}V'_{\gamma,t}\left(\phi,\mu\right)V_{\gamma,t}\left(\phi,\mu\right), \quad (2.3.1)$$

The partial derivatives of the log-likelihoood of μ is:

$$\frac{\partial \ln L_{\gamma,t}\left(\phi,\mu,\sigma^2\right)}{\partial\mu} = \frac{1}{\sigma^2}\sum_{t=1}^{T}\left(S_{\gamma,t}\left(\lambda\right)Y_t - d_{t,1}X_t\alpha_1 - d_{t,1}WX_t\beta_1 - d_{t,2}X_t\alpha_2 - d_{t,2}WX_t\beta_2 - \mu\right) = 0 \quad (2.3.2)$$

when solving (2.3.2) we obtains:

$$\hat{\mu} = \frac{1}{T}\sum_{t=1}^{T}\left(S_{\gamma,t}\left(\lambda\right)Y_t - d_{t,1}X_t\alpha_1 - d_{t,1}WX_t\beta_1 - d_{t,2}X_t\alpha_2 - d_{t,2}WX_t\beta_2\right). \quad (2.3.3)$$

Substituting the solution for μ into the log-likelihood function, and after rearranging terms,

the concentrated log-likelihood function is obtained:

$$\ln L_{\gamma,t}\left(\phi,\sigma^2\right) = -\frac{nT}{2}\ln(2\pi\sigma^2) + \sum_{t=1}^{T}\ln\left|S_{\gamma,t}\left(\lambda\right)\right| - \frac{1}{2\sigma^2}\sum_{t=1}^{T}\tilde{V}_t'\left(\gamma\right)\tilde{V}_t\left(\gamma\right), \tag{2.3.4}$$

where $\widetilde{V}_t\left(\gamma\right) = \overline{Y}_t + \widetilde{B}_t\left(\gamma\right)\lambda - \widetilde{A}_t\left(\gamma\right)\theta$, $\widetilde{B}_t\left(\gamma\right) = \left(\overline{Y}_{t,1}\left(W,\gamma\right), \overline{Y}_{t,2}\left(W,\gamma\right)\right)$, $\theta = (\alpha_1, \alpha_2, \beta_1, \beta_2)$

$$\widetilde{A}\left(r_L, r_U\right) = \left(\overline{X}_{t,1}\left(\mathbf{I}_n,\gamma\right), \overline{X}_{t,2}\left(\mathbf{I}_n,\gamma\right), \overline{X}_{t,1}\left(W,\gamma\right), \overline{X}_{t,2}\left(W,\gamma\right)\right).$$

and $\overline{Z}_{t,i}\left(A, r_L, r_U\right) = d_{t,i}AZ_t - \frac{1}{T}\sum_{t=1}^{T} d_{t,i}AZ_t$,

Note that the parameters depend on the unknown threshold γ. So to determine it we must repeate the process for all the possible threshold values included in an interval Π, which is defined so as to guarantee a minimum number of observations in each regime. Chan (1993) and Hansen (1999) recommended the estimation of γ by minimizing the concentrated sum of squared errors. So in this case we would maximize the loglikelihood function

$$\hat{\gamma} = \arg\max_{\gamma\in\Pi} \ln L_{\gamma,t}\left(\phi,\sigma^2\right).$$

2.4 Simulation study

To assess the finite-sample properties of the proposed estimation procedure, we conduct a Monte Carlo simulation study comparing the performance of the QML estimator with that of the 2SLS estimator. The data-generating process follows the specification given in Equation (2.2.3), with the parameter vector defined as:

$$\phi = (\lambda_1, \lambda_2, \beta_1, \beta_2, \alpha_1, \alpha_2).$$

The regressors X_t and the disturbance term V_t are generated independently from a standard normal distribution, ensuring exogeneity. The spatial weight matrix W is generated to have three neighbors ahead and three behind.

We consider several combinations of cross-sectional units and time periods in order to evaluate the robustness of the estimators under different sample sizes. Specifically, we set:

$$n \in \{25, 50\} \text{ and } T \in \{10, 20, 30\}.$$

For each configuration of (n, T) a sample of observations is generated, and both the QML and 2SLS estimators are computed. The primary focus of the comparison is on the bias of the estimators. To obtain reliable inference, the simulation experiment is replicated 1,000

times for each parameter configuration. This experimental design allows us to systematically evaluate how the two estimation approaches perform in small and moderate samples, as well as how their properties vary with the degree of spatial dependence and threshold nonlinearity.

Table 2.4.1 indicates that the bias of the estimates obtained through the QML method (M_{QML}) is generally smaller and more stable than that of the 2SLS estimator (M_{2SLS}). This pattern is consistent across all parameters and becomes more pronounced as both the number of individuals n and the time dimension T increase. For instance, when $n = 50$ and $T = 30$, the QML estimates of parameters such as γ, λ_1, and λ_2 are very close to their true values, whereas the 2SLS estimates display slightly higher deviations. In terms of standard errors, S_{2SLS} are systematically larger than S_{QML}, confirming the higher efficiency of the QML estimator. This difference is particularly marked for parameters α_1 and α_2, where the dispersion of the 2SLS estimates remains relatively high even as T increases. For example, at $n = 25$ and $T = 30$, the standard error for α_2 under 2SLS is nearly eight times that under QML. Overall, both estimators exhibit the expected convergence properties: as the sample size increases (in both n and T), the bias and variability of the estimates decrease. However, QML consistently provides more accurate and precise estimates than 2SLS, indicating superior finite-sample performance and stronger empirical consistency.

Table 2.4.1. Results of simulation study.

			T											
			10				20				30			
n		$True$	M_{QML}	S_{QML}	M_{2SLS}	S_{2SLS}	M_{QML}	S_{QML}	M_{2SLS}	S_{2SLS}	M_{QML}	S_{QML}	M_{2SLS}	S_{2SLS}
	γ	1	0.9975	0.0401	1.0003	0.0594	1.0006	0.0209	1.0018	0.0296	0.9990	0.0151	0.9996	0.0188
	λ_1	0.3	0.2909	0.0878	0.3315	0.4865	0.2942	0.0578	0.2808	0.4673	0.2988	0.0457	0.2989	0.4548
	λ_2	0.6	0.5886	0.0787	0.6114	0.4831	0.5902	0.0549	0.6283	0.4479	0.5972	0.0440	0.6085	0.4351
25	β_1	1	1.0052	0.1050	0.9886	0.2722	1.0049	0.0719	1.0144	0.2576	1.0010	0.0564	1.0048	0.2448
	β_2	2	2.0131	0.1134	1.9971	0.3224	2.0091	0.0756	1.9808	0.3017	2.0012	0.0602	1.9921	0.2954
	α_1	1	1.0266	0.4009	0.8752	1.8378	1.0253	0.2509	1.0795	1.7567	1.0059	0.2071	1.0082	1.7342
	α_2	2	2.0429	0.3812	1.9687	1.8952	2.0323	0.2544	1.8806	1.7713	2.0064	0.2071	1.9598	1.7511
	σ^2	1	0.9343	0.0446	1.0793	0.0606	0.9692	0.0313	1.0974	0.0438	0.9809	0.0263	1.1063	0.0355
	γ	1	0.9976	0.0200	0.9986	0.0238	0.9998	0.0130	1.0006	0.0162	0.9896	0.0108	1.0145	0.0156
	λ_1	0.3	0.2959	0.0611	0.3118	0.4714	0.2985	0.0408	0.3014	0.4837	0.3082	0.0385	0.2856	0.4572
	λ_2	0.6	0.5951	0.0566	0.6160	0.4511	0.5961	0.0378	0.6047	0.4616	0.5884	0.0329	0.6159	0.4351
50	β_1	1	1.0045	0.0726	0.9984	0.2424	1.0026	0.0495	1.0011	0.2498	1.0337	0.0333	1.0446	0.2398
	β_2	2	2.0018	0.0754	1.9880	0.2915	1.9983	0.0532	1.9926	0.3009	1.9989	0.0508	1.9514	0.2734
	α_1	1	1.0106	0.2632	0.9502	1.7783	1.0085	0.1819	1.0008	1.8224	1.0361	0.1551	1.0927	1.7188
	α_2	2	2.0262	0.2596	1.9450	1.7907	2.0094	0.1832	1.9723	1.8615	1.9652	0.1686	1.9604	1.7117
	σ^2	1	0.9411	0.0325	1.0883	0.0438	0.9730	0.0219	1.0998	0.0298	1.0220	0.0201	1.0425	0.0281

Chapter 3

Panel buffered threshold spatial Durbin model

3.1 Introduction

Important empirical studies have demonstrated that the linearity hypothesis is not always suitable for spatial panel data analysis. As an alternative, threshold modeling has emerged as a sophisticated way to explore how spatial correlation extends to and interacts over time. This approach provides a simplified formulation to reproduce nonlinear stylized facts caused by regime changes in the dynamic of the data-generating process, which is often the case in practice when panel data is obtained from an environment that is subject to change, such as natural phenomena, new economic regulations, or emergence of new technologies.

Aquaro et al. (2015) provided an interesting example of data that cannot be adequately modeled by a spatial model with constant coefficients. Their example, based on a study by Holly et al. (2010), examined the determinants of real house prices in a panel of 49 U.S. states over 29 years. The authors concluded that assuming uniform spillover effects across all 49 states is unrealistic and overly restrictive due to the vast size of the United States and the uneven distribution of economic activity. Other studies, including Wei et al. (2021), Meng and Yang (2022) and Zheng and Ye (2023) provide additional evidence of similar issues.

Traditionally, spatial literature has relied on linearity assumptions to address complex relationships. However, only a limited number of studies have highlighted the importance of nonlinearity, particularly threshold effects. Deng (2018) proposed a threshold spatial autoregressive model, which Zhu et al. (2020) later extended into a threshold spatial Durbin model. These models, however, were limited to cross-sectional data. Recently, Wei et al. (2021) developed the panel threshold spatial Durbin ($PTSD$) model, an advancement that extends both previous models and Hansen's (1999) model. This extension enhances the ability to capture cross-sectional dependence and spatial heterogeneity (nonlinearities), particularly when panel data is obtained from an environment subject to change.

It is worth noting that the transition mechanism defined by Wei et al. (2021) allowing spatial units in a panel to be in different regimes during a given period is the same as that defined by Hansen (1999). Zheng and Ye (2023) employed this mechanism to investigate the asymmetry of peer effects in green innovation across various regional systems. Their findings indicate that enterprises tend to imitate and draw inspiration from large-scale, high-governance-level peer enterprises when making green innovation decisions. By assuming a single threshold parameter, their model dictates that when a threshold variable, such as enterprise scale or governance level, falls below this fixed value, the observed behavior corresponds to one regime. Conversely, exceeding the fixed threshold prompts a shift to another regime, even if the change is minimal. This characteristic of sudden regime changes, as seen in Wei et al.'s framework, can be problematic in cases where transitions are more gradual. To address this limitation, we propose an alternative model based on the concept of hysteresis, developed for spatial panel data, which offers a smooth and flexible regime-switching mechanism. This development of a hysteresis or buffered approach can be a solution to the weakness of sudden jumps, as demonstrated in recent work by Belarbi et al. (2021) and Li et al. (2015). Building on this idea, we incorporate the concept of a buffer zone into Wei et al.'s framework to further examine, for instance, the asymmetry of peer effects across various regional systems. Instead of relying on a fixed threshold, we define an interval with lower and upper bounds, forming a buffer zone. When the threshold variable drops below the lower bound, behavior aligns with one regime, while exceeding the upper bound leads to a shift to the other regime. However, within the buffer zone, the system retains the behavior of its most recent state, enabling smoother and more flexible transitions between regimes. This novel modeling approach

not only highlights the nonlinear dynamics present in panel spatial data but also provides a nuanced understanding of how spillover effects vary across spatial units with distinct characteristics.

The rest of the chapter is structured as follows. In Section 2, we introduce a new model, the Panel Buffered Threshold Spatial Durbin ($PBTSD$) model. This model extends Wei et al.'s $PTSD$ model, aiming to capture the nonlinearity in spatial panel dynamics and provide a better explanation for spatial heterogeneity in panel data. In Section 3, we explain two direct approaches to tackle the estimation problem, utilizing the two-stage least squares ($2SLS$) method and the quasi-maximum likelihood (QML) method for implementation. In Section 4, we develop a likelihood ratio test to evaluate linearity against the $PBTSD$ model. Since the distribution of this test is nonstandard, we propose a bootstrap procedure to simulate the likelihood ratio test distribution. Finally, in Section 5, we present a simulation study to evaluate the performance of the proposed estimation and testing procedures, confirming their consistency and adequacy.

3.2 Panel Buffered Threshold Spatial Durbin model

To capture the dynamics of the heterogeneous spatial dependence, we consider the following balanced panel $\{y_{i,t}, q_{i,t}, x_{i,t} : 1 \leq i \leq n, 1 \leq t \leq T\}$, where i and t represent individual and temporal indices, respectively. The dependent variable $y_{i,t}$ and the threshold variable $q_{i,t}$ are real valued variables. $x_{i,t}$ is an m-vector of observable regressors.

The observed data are generated from a non-dynamic two-regime $PBTSD$ model with individual fixed effects if they satisfy the following regression model:

$$y_{i,t} = \left(\lambda_1 \sum_{j=1 \ i \neq j}^{n} w_{i,j} y_{j,t} + x_{i,t}\alpha_1 + \sum_{j=1 \ i \neq j}^{n} w_{i,j} x_{j,t} \beta_1 \right) \mathbf{R}_{i,t} \tag{3.2.1}$$

$$+ \left(\lambda_2 \sum_{j=1 \ i \neq j}^{n} w_{i,j} y_{j,t} + x_{i,t}\alpha_2 + \sum_{j=1 \ i \neq j}^{n} w_{i,j} x_{j,t} \beta_2 \right) (1 - \mathbf{R}_{i,t}) + \mu_i + v_{i,t}, \tag{3.2.2}$$

where μ_i is the fixed effect for individual i and $v_{i,t}$ is the error term, which is assumed to be independent and identically distributed (i.i.d.) across i and t with mean zero and positive finite variance σ^2. $w_{i,j}$ is the (i,j)-th element of the exogenous spatial weight

matrix W.Although multiple spatial weight matrices could, in principle, be specified, their interpretation is not straightforward; hence, a common exogenous matrix is used. λ_1 and λ_2 are scalar spatial parameters that capture the heterogeneous spatial interaction effect in spatial lag dependent variable, α_1 and α_2 reflect the threshold effect in exogenous regressors, and β_1 and β_2 capture the heterogeneous exogenous interaction effect. $R_{i,t}$ is the regime indicator defined as follows:

$$R_{i,t} = \begin{cases} 1 & \text{if } q_{i,t} \leq r_L, \\ R_{i,t-1} & \text{if } r_L < q_{i,t} \leq r_U, \\ 0 & \text{if } r_U < q_{i,t}. \end{cases} \tag{3.2.3}$$

where r_L and r_U ($r_L \leq r_U$) are the boundary parameters that make up the buffer zone. Here, the transition mechanism is modeled in the same way as for the Buffered Threshold Panel Data ($BTPD$) model proposed by Belarbi et al. (2021). Our aim with this new formulation is to address, on the one hand, non-linearity and spatial heterogeneity of the threshold variable effect on the dependent variable and to allow, on the other hand, more flexibility and smoothness in the jumps between regimes. Indeed, each regime is characterized by a different spatial parameter (λ_1 and λ_2), different slope coefficient vectors of $x_{i,t}$ and $\sum_{j=1\ i\neq j}^{n} w_{i,j}x_{j,t}$ (α_1 and β_1 or α_2 and β_2), and the transition between the two regimes is gradual, in contrast to Wei et al.'s formulation. This change in the transition mechanism is justified by the fact that, in practice, regime $R_{i,t}$ may not shift immediately, and there could be a buffer region in which the regime of $y_{i,t}$ depends on the regime of $y_{i,t-1}$ (see e.g., Belarbi et al., 2021).

It is clear that when $r_L = r_U = r$, the model (3.2.1)-(3.2.3) is reduced to the $PTSD$ model introduced by Wei et al. (2021). However, it is worth noting that the transition is abrupt in Wei et al. (2021). Specifically, the dependent variable can switch from one regime to another if the threshold variable $q_{i,t}$ status crosses up or down the threshold r. In other words, if $q_{i,t}$ drops below the threshold r, even slightly, dependent variable is described by the first regime with spatial parameter λ_1 and slope coefficient vectors α_1 and β_1. Conversely, when this variable exceeds r, dependent variable is described by the second regime with spatial parameter λ_2 and slope coefficient vectors α_2 and β_2. The regime indicator $R_{i,t}$ depends only on whether the $q_{i,t}$ value is smaller or larger than r. In our formulation, and thanks to the relaxation of the assumption of the reaction, the model becomes more realistic, and the regime indicator may depend on the past of the regime indicators infinitely far away. As in

Li et al. (2015), we have:

$$R_{i,t} = \mathbf{1}_{(q_{i,t} \leq r_L)} + \mathbf{1}_{(r_L < q_{i,t} \leq r_U)} R_{i,t-1}$$

which can be iteratively calculated in the almost sure sense as follows:

$$R_{i,t} = \mathbf{1}_{(q_{i,t} \leq r_L)} + \sum_{j=0}^{\infty} \prod_{m=0}^{j} \mathbf{1}_{(r_L < q_{i,t-m} \leq r_U)} \mathbf{1}_{(q_{i,t-j-1} \leq r_L)}.$$

The transition mechanism is clearly modeled in the same way as in the $BTPD$ model, where it depends on the threshold variable, a crucial parameter in the context of threshold and buffer modeling. The selection of the threshold variable is typically guided by theoretical insights, empirical analysis, and practical considerations. A robust and interpretable choice often requires combining economic intuition with statistical validation. In some cases, testing multiple potential threshold variables can help identify the one that performs best within the model. Ultimately, the choice of a threshold variable in practice depends on the study's context and the specific characteristics of the phenomenon being analyzed.

It is important to note that our model is a spatial Durbin panel model, which explicitly incorporates spatial lags of both the dependent and independent variables. This design allows for the estimation of direct effects (from $x_{i,t}$ to $y_{i,t}$) and indirect or spillover effects (from $x_{j,t}$, for $j \neq i$, to $y_{i,t}$). While $y_{j,t}$ may indeed be influenced by $x_{j,t}\beta_k$, the spatial lag structure treats $\sum_{j=1}^{n} w_{i,j} y_{j,t}$ as a regressor within a simultaneous equations system.

The model (3.2.1)-(3.2.3) can be expressed as follows

$$\begin{aligned} Y_t &= \lambda_1 d_{t,1}(r_L, r_U) W Y_t + \lambda_2 d_{t,2}(r_L, r_U) W Y_t + d_{t,1}(r_L, r_U) X_t \alpha_1 + d_{t,2}(r_L, r_U) X_t \alpha_2 \\ &\quad + d_{t,1}(r_L, r_U) W X_t \beta_1 + d_{t,2}(r_L, r_U) W X_t \beta_2 + \mu + V_t, \end{aligned} \tag{3.2.4}$$

where $Y_t = (y_{1,t}, y_{2,t}, ..., y_{n,t})'$, $V_t = (v_{1,t}, v_{2,t}, ..., v_{n,t})'$, $X_t = \left(x'_{1,t}, x'_{2,t}, ..., x'_{n,t}\right)'$, $\mu = (\mu_1, \mu_2, ..., \mu_n)'$, $d_{t,k}(r_L, r_U) = diag\left(\mathbf{1}_{(R_{1,t}=k)}, \mathbf{1}_{(R_{2,t}=k)}, \ldots, \mathbf{1}_{(R_{n,t}=k)}\right)$ for $k = 1, 2$. Let

$$\begin{aligned} S_t(r_L, r_U, \lambda) &= \mathbf{I}_n - \lambda_1 d_{t,1}(r_L, r_U) W - \lambda_2 d_{t,2}(r_L, r_U) W, \\ A_t(r_L, r_U) &= \left(d_{t,1}(r_L, r_U) X_t, d_{t,2}(r_L, r_U) X_t, d_{t,1}(r_L, r_U) W X_t, d_{t,2}(r_L, r_U) W X_t\right), \end{aligned}$$

$\lambda = (\lambda_1, \lambda_2)'$ and $\theta = (\alpha'_1, \alpha'_2, \beta'_1, \beta'_2)'$. Using these notations, equation (3.2.4) can be written in the following compact representation:

$$S_t(r_L, r_U, \lambda) Y_t = A_t(r_L, r_U) \theta + \mu + V_t. \tag{3.2.5}$$

Then, presuming $S_t(r_L, r_U, \lambda)$ is non-singular matrix, (3.2.5) can be rewritten as

$$Y_t = S_t^{-1}(r_L, r_U, \lambda) A_t(r_L, r_U)\theta + S_t^{-1}(r_L, r_U, \lambda)\mu + S_t^{-1}(r_L, r_U, \lambda) V_t.$$

Note that if W is row-normalized, a sufficient condition that ensures $S_t(r_L, r_U, \lambda)$ is invertible is $\max\{|\lambda_1|, |\lambda_2|\} < 1$ (see e.g. Horn and Johnson, 1985).

3.3 Estimation problem

Belarbi et al. (2021) proposed a least squares estimation approach to estimate the $BPTR$ model, which yields good results. However, the $BPTR$ model does not consider spatial structure. Estimating fixed effect panel data with a spatially lagged dependent variable can lead to complications in estimation (see e.g. Anselin et al., 2008). One of these complications is the endogeneity of $\sum_{j=1}^{n} w_{i,j} y_{j,t}$, which violates the standard assumption of the regression model that $\mathbb{E}\left(\left(\sum_{j=1}^{n} w_{i,j} y_{j,t}\right) v_{i,t}\right) = 0$. As a result, the approach proposed by Belarbi et al. (2021) cannot be used. Wei et al. (2021) proposed a spatial $2SLS$ estimation approach that can achieve explicit estimates for the $PTSD$ model. Their Monte Carlo results show that the $2SLS$ estimation procedure has good finite-sample properties. In this section, we describe two straightforward methods for our estimation problem. The first one is the $2SLS$ method, whereas the second one is that of the QML method.

As noted above in the definition of our model, the spatial weights matrix W is exogenous and not estimated as part of the model parameters; therefore, its estimation procedure is not discussed here.

3.3.1 Two-stage least squares method

The first step of the $2SLS$ estimation process involves eliminating individual fixed effects by subtracting specific individual means. While this step is common in linear modeling, it requires more careful consideration in the context of thresholds, especially in the $PBTSD$ model, where estimated individual effects are influenced by the buffer zone.

Therefore, it would be convenient to introduce centered n-vectors for any $t = 1, ..., T$, and

$k = 1, 2,$

$$\overline{Z}_{t,k}\left(A, r_L, r_U\right) = d_{t,k}\left(r_L, r_U\right) AZ_t - \frac{1}{T}\sum_{t=1}^{T} d_{t,k}\left(r_L, r_U\right) AZ_t,$$

defined for any n-vector Z_t, and any square matrix A of dimension n. Similarly, we will denote the centered vectors $\overline{Y}_{t,k}\left(A, r_L, r_U\right)$ and $\overline{X}_{t,k}\left(A, r_L, r_U\right)$, where $A = W$ or $\mathbf{I}_n$. Consequently, we can express the model (3.2.4) in the following form:

$$\begin{aligned}\overline{Y}_t = {} & \lambda_1 \overline{Y}_{t,1}\left(W, r_L, r_U\right) + \lambda_2 \overline{Y}_{t,2}\left(W, r_L, r_U\right) + \overline{X}_{t,1}\left(\mathbf{I}_n, r_L, r_U\right)\alpha_1 \\ & + \overline{X}_{t,2}\left(\mathbf{I}_n, r_L, r_U\right)\alpha_2 + \overline{X}_{t,1}\left(W, r_L, r_U\right)\beta_1 + \overline{X}_{t,2}\left(W, r_L, r_U\right)\beta_2 + \overline{V}_t, \end{aligned} \tag{3.3.1}$$

where $\overline{Y}_t = Y_t - \frac{1}{T}\sum_{t=1}^{T} Y_t$.

To address endogeneity arising from WY_t, we can employ instruments as recommended by Kelejian and Prucha (1998). These instruments can be constructed using the exogenous variables in our $PBTSD$ model. To achieve this, we express (3.3.1) in the following equivalent representation:

$$\mathbf{Y} = \mathbf{X}\left(W, r_L, r_U\right)\vartheta + \mathbf{V},$$

where $\vartheta = \left(\lambda', \theta'\right)'$, $\mathbf{V} = \left(\overline{V}_1', \overline{V}_2, ..., \overline{V}_n'\right)$,

$$\mathbf{X}\left(W, , r_L, r_U\right) = \left(\mathcal{Y}\left(W, r_L, r_U\right), \mathcal{X}\left(W, r_L, r_U\right)\right),$$

$$\mathcal{Y}\left(W, r_L, r_U\right) = \begin{pmatrix} \overline{Y}_{1,1}\left(W, r_L, r_U\right) & \overline{Y}_{1,2}\left(W, r_L, r_U\right) \\ \overline{Y}_{2,1}\left(W, r_L, r_U\right) & \overline{Y}_{2,2}\left(W, r_L, r_U\right) \\ \vdots & \vdots \\ \overline{Y}_{T,1}\left(W, r_L, r_U\right) & \overline{Y}_{T,2}\left(W, r_L, r_U\right) \end{pmatrix},$$

and

$$\begin{aligned} & \mathcal{X}\left(W, r_L, r_U\right) \\ = {} & \begin{pmatrix} \overline{X}_{1,1}\left(\mathbf{I}_n, r_L, r_U\right) & \overline{X}_{1,2}\left(\mathbf{I}_n, r_L, r_U\right) & \overline{X}_{1,1}\left(W, r_L, r_U\right) & \overline{X}_{1,2}\left(W, r_L, r_U\right) \\ \overline{X}_{2,1}\left(\mathbf{I}_n, r_L, r_U\right) & \overline{X}_{2,2}\left(\mathbf{I}_n, r_L, r_U\right) & \overline{X}_{2,1}\left(W, r_L, r_U\right) & \overline{X}_{2,2}\left(W, r_L, r_U\right) \\ \vdots & \vdots & \vdots & \vdots \\ \overline{X}_{T,1}\left(\mathbf{I}_n, r_L, r_U\right) & \overline{X}_{T,2}\left(\mathbf{I}_n, r_L, r_U\right) & \overline{X}_{T,1}\left(W, r_L, r_U\right) & \overline{X}_{T,2}\left(W, r_L, r_U\right) \end{pmatrix}. \end{aligned}$$

Similar to the approach employed by Kelejian and Prucha (1998) and Wei et al. (2021), we utilize the exogenous variables $\mathcal{X}\left(W, r_L, r_U\right)$ and their spatial lags as instruments to address

endogeneity. Therefore, the $2SLS$ estimator for ϑ is:

$$\widehat{\vartheta}(r_L, r_U) = \left(\mathbf{X}'(W, r_L, r_U)\,\mathbf{Z}(W, r_L, r_U)\,\mathbf{X}(W, r_L, r_U)\right)^{-1}\mathbf{X}'(W, r_L, r_U)\,\mathbf{Z}(W, r_L, r_U)\,\mathbf{Y},$$

where

$$\mathbf{Z}(W, r_L, r_U) = \mathcal{H}(W, r_L, r_U)\left(\mathcal{H}'(W, r_L, r_U)\,\mathcal{H}(W, r_L, r_U)\right)^{-1}\mathcal{H}'(W, r_L, r_U)$$

and $\mathcal{H}(W, r_L, r_U)$ is the instrumental variable matrix, which can be composed of $\mathcal{X}(W, r_L, r_U)$, $(\mathbf{I}_T \otimes W)\,\mathcal{X}(W, r_L, r_U)$, $(\mathbf{I}_T \otimes W)^2\,\mathcal{X}(W, r_L, r_U)$, etc.

We then can obtain the residual vector as follows $\widehat{V}(r_L, r_U) = \mathbf{Y} - \mathbf{X}(W, r_L, r_U)\,\widehat{\vartheta}(r_L, r_U)$. This enables the calculation of the sum of the squared errors $\mathbf{S}(r_L, r_U) = \widehat{V}'(r_L, r_U)\,\widehat{V}(r_L, r_U)$. We can thus estimate the residual variance as follows:

$$\widehat{\sigma}^2(r_L, r_U) = \frac{1}{nT - n}\mathbf{S}(r_L, r_U).$$

It is important to note that estimating ϑ requires knowledge of the buffer zone (r_L, r_U), which must itself be estimated. The buffer zones can be estimated using empirical percentiles of the observed values of the threshold variable (see, e.g., Hansen, 1999; Belarbi et al., 2021). Specifically, we construct candidate threshold pairs from the empirical quantiles of the observed values of $q_{i,t}$. A grid search is then performed over all such candidate pairs. We select the optimal 2-vector (r_L, r_U) as the solution to $(\widehat{r}_L, \widehat{r}_U) = \arg\min_{(r_L, r_U)\in\Gamma}\mathbf{S}(r_L, r_U)$, where Γ denotes the set of candidate buffer zones, comprising all ordered 2-vectors formed from the a-th to the b-th empirical quantiles $(a < b)$ of the observed values of the threshold variable. An appropriate choice might be either $a = 0.25$, $b = 0.75$ or $a = 0.1$, $b = 0.9$. However, it is important to ensure that each regime contains a sufficient number of observations.

3.3.2 Quasi-maximum likelihood method

Let $\delta = (\lambda', \theta', \sigma^2)'$ be the parameters vector which belongs to a parameter space of the form $\Delta \subset]-1, 1[\times]-1, 1[\times \mathbb{R}^4 \times]0, +\infty[$. The log-quasi-likelihood function of (3.2.1)-(3.2.3)

assuming normally distributed disturbances is:

$$\log L(\delta,\mu) = -\tfrac{nT}{2}\log(2\pi\sigma^2) - \tfrac{1}{2\sigma^2}\sum_{t=1}^{T} V_t'(r_L,r_U,\lambda,\theta,\mu)\, V_t(r_L,r_U,\lambda,\theta,\mu) + \sum_{t=1}^{T}\log|S_t(r_L,r_U,\lambda)|,$$

where $V_t(r_L,r_U,\lambda,\theta,\mu) = S_t(r_L,r_U,\lambda)\,Y_t - A_t(r_L,r_U)\,\theta - \mu$. We can estimate μ directly and obtain the estimator of δ via a log-quasi-likelihood with μ concentrated out:

$$\log\mathcal{L}(\delta) = -\tfrac{nT}{2}\log(2\pi\sigma^2) - \tfrac{1}{2\sigma^2}\sum_{t=1}^{T} \widetilde{V}_t'(r_L,r_U,\lambda,\theta)\,\widetilde{V}_t(r_L,r_U,\lambda,\theta) + \sum_{t=1}^{T}\log|S_t(r_L,r_U,\lambda)|,$$

where $\widetilde{V}_t(r_L,r_U,\lambda,\theta) = \overline{Y}_t + \widetilde{B}_t(r_L,r_U)\,\lambda - \widetilde{A}_t(r_L,r_U)\,\theta$,

with $\widetilde{B}_t(r_L,r_U) = \left(\overline{Y}_{t,1}(W,r_L,r_U), \overline{Y}_{t,2}(W,r_L,r_U)\right)$ and

$$\widetilde{A}(r_L,r_U) = \left(\overline{X}_{t,1}(\mathbf{I}_n,r_L,r_U), \overline{X}_{t,2}(\mathbf{I}_n,r_L,r_U), \overline{X}_{t,1}(W,r_L,r_U), \overline{X}_{t,2}(W,r_L,r_U)\right).$$

Hence, the QML estimator of δ is defined as any measurable solution $\widehat{\delta}$ of

$$\widehat{\delta}(r_L,r_U) = \arg\max_{\delta\in\Delta}\log\mathcal{L}(\delta).$$

It's crucial to emphasize that estimating δ entails the determination of buffer zones (r_L, r_U), which must also be estimated, similar to the case of $2SLS$ method. Hence, we can estimate these buffer zones by utilizing empirical percentiles. More precisely, we select the 2-vector solution (r_L, r_U) that maximizes the log-likelihood function $\log\mathcal{L}\left(\widehat{\delta}(r_L,r_U)\right)$ within the set Γ.

3.4 Test of linearity

As in Hansen (1999) and Belarbi et al. (2021), we suggest a two-step methodology to apply $PBTSD$ modeling in our framework: a specification or testing linearity step and an estimation step. In the specification step, we test for linearity (homogeneity) against the two-regime $PBTSD$. This can be done, as in Hansen (1999), by using a likelihood ratio (LR) test. The null hypothesis (no buffered threshold effects) and the alternative hypothesis (the existence of buffered threshold effects) are given by:

$$H_0 : \vartheta_1 = \vartheta_2 \text{ and } H_1 : \vartheta_1 \neq \vartheta_2,$$

where $\vartheta_i = (\lambda_i, \alpha_i', \beta_i')'$, for $i = 1, 2$.

However, the testing problem is non-standard since the $PBTSD$ model contains unidentified nuisance parameters under H_0 (Davies, 1987). To address this issue, we can use a bootstrap procedure, similar to that used in Hansen (1999) for the PTR model and adapted in Belarbi et al. (2021) for the $BTPD$ case, to simulate the corresponding distribution of the LR test statistic. Let $\mathbf{S}_0$ and $\mathbf{S}(\widehat{r}_L, \widehat{r}_U)$ be the residual sums of squared errors obtained from (3.2.1)-(3.2.3) without and with buffered threshold effects, respectively. Then, the corresponding LR statistic is defined as follows:

$$F = (\mathbf{S}_0 - \mathbf{S}(\widehat{r}_L, \widehat{r}_U)) / \widehat{\sigma}^2(\widehat{r}_L, \widehat{r}_U),$$

where $\widehat{\sigma}^2(\widehat{r}_L, \widehat{r}_U)$ is the residual variance of the 2-regime $PBTSD$ estimation. The p-value can be approximated using the bootstrap procedure outlined in the following algorithm. The null hypothesis is rejected if the p-value is smaller than the desired critical value.

Algorithm

1. The regressors $x_{i,t}$, the spatial weight W and the threshold variable $q_{i,t}$ are considered as given, and their values remain fixed during the bootstrap simulations.

2. Collect the residual $\widehat{v}_{i,t}$ obtained under H_0 and group them by individual $\widehat{V}_i = (\widehat{v}_{i,1}, \widehat{v}_{i,2}, \ldots, \widehat{v}_{i,T})'$. Treat the sample $\left(\widehat{V}_1', \widehat{V}_2', \ldots, \widehat{V}_n'\right)'$ as the empirical distribution to be used for the bootstrapping.

3. Draw (with replacement) a sample of size n from the empirical distribution and use these errors to create a bootstrap sample under H_0.

4. Using the bootstrap sample, estimate the model under the null hypothesis and the alternative one and calculate the bootstrap value of F.

5. Repeat steps 3 and 4 a large number of times and calculate the percentage of draws for which the simulated statistic exceeds the observed statistic F. This percentage represents the p-value of F under H_0.

3.5 Simulation study

In order to assess the quality of our two proposed estimation procedures, we conduct a simulation study in this section. We simulate samples from three data generating processes given by (3.2.1)-(3.2.3) with parameters $\lambda = (0.3, 0.6)'$ and $\theta = (1, 0.2, 0.5, 1)'$ and buffer zone $(r_L, r_U) = (-0.25, 0.75)$. We generate the regressors $X_{i,t}$ and the threshold variable $q_{i,t}$ from independent standard normal distributions while the residuals $v_{i,t}$ are generated from three different distributions, namely, the standard normal distribution, Student distribution with 5 degrees of freedom, and centred exponential distribution with rate parameter 1. The choice of 5 degrees of freedom for the Student-t distribution is motivated by the need to model moderately heavy-tailed behaviour: it allows for excess kurtosis and occasional extreme observations compared to the normal distribution, while still ensuring the existence of finite variance.The spatial weight matrix W is generated to have three neighbors ahead and three behind.

The simulations are replicated 1000 times, and we choose the number of individuals n and the time period T from the combinations of $T = 10, 20, 30$, and $n = 25, 50$. For each replicate, we compute both the $2SLS$ and QML estimations.

Tables 3.5.2, 3.5.3 and 3.5.4 report the true values (True) of the parameters for each of the considered $PBTSD$ data-generating processes, as well as the means (M2SLS for 2SLS method and MQML for QML method) and corresponding empirical standard errors (SE_{2SLS} for $2SLS$ method and SE_{QML} for QML method) of their estimates over the 1000 replications.

The primary focus of this Monte Carlo study is on sample bias and standard error. The results provide preliminary evidence regarding the finite sample properties of the $2SLS$ and QML estimators in the $PBTSD$ framework. Tables 3.5.2–3.5.4 indicate that the bias of estimates obtained through the QML method is smaller and more reasonable than the bias of estimates from the $2SLS$ method. This bias decreases with increasing sample size, either in terms of individuals or time periods, a trend observed for both methods. Regarding standard errors, it is clear that those of $2SLS$ are larger than those of QML in all cases. For example, when the residuals follow a Student distribution and $(n, T) = (50, 10)$, the SE_{2SLS} for the parameter α_2 (as well as for λ_1 and λ_2) is approximately 1964% (and 981% and 989%, respectively) larger than the corresponding SE_{QML}. However, this issue is less pronounced

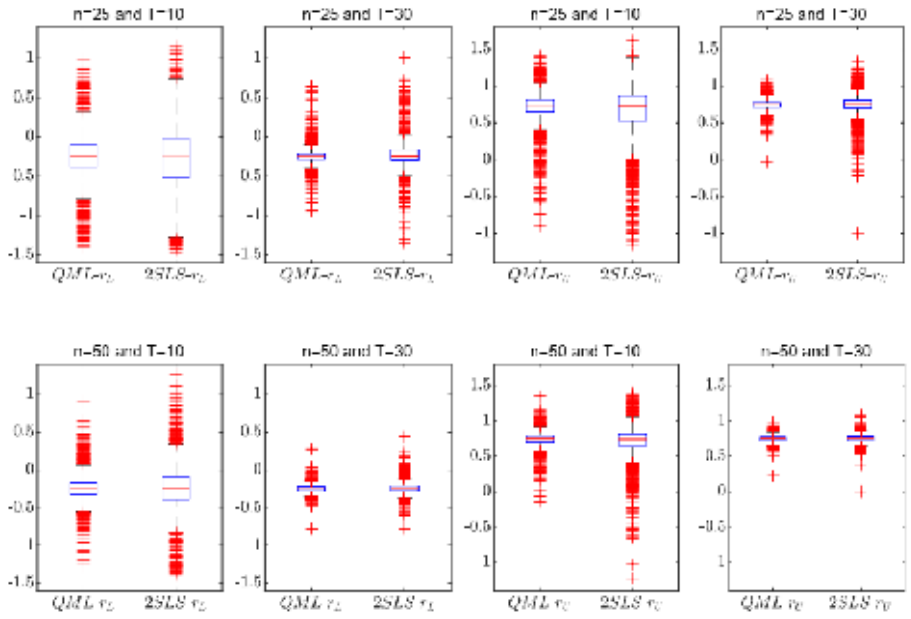

Figure 3.5.1. Boxplots of the estimated buffer zone for a two-regime PBTSD model, with $v_{i,t} \sim \mathcal{N}(0,1)$ *and* $q_{i,t} \sim \mathcal{N}(0,1)$.

for the other parameters compared to α_2, λ_1 and λ_2. Nonetheless, as the sample size increases, standard errors tend toward zero for both methods. This indicates that both methods exhibit empirical consistency, with the QML method outperforming 2SLS by yielding more reliable results. Figures 3.5.1-3.5.6 provide boxplots of the parameter estimate values, illustrating this superior performance. Since the 2SLS method provides explicit estimators, unlike the QML method, these estimators can be used as initial values in the optimization procedure to obtain QML estimates.

We now examine the empirical distribution of the two proposed estimators for the model parameters. Figures 3.5.7 - 3.5.12 present sample histograms of the estimated parameters under three configurations of the $PBTSD$ model, differentiated by the distribution of the residuals $v_{i,t}$: The Jarque-Bera (JB) test results (also shown in Figures 3.5.7 - 3.5.12) reveal that when the spatial panel's cross-sectional and temporal dimensions are small, the empirical distribution significantly deviates from normality for both the 2SLS and QML methods. Specifically, the corresponding JB statistics exceed 9.21, leading us to reject the normality hypothesis at the 1% significance level. However, when the number of individuals and the time period increase to 50 and 30, respectively, the QML method shows convergence toward

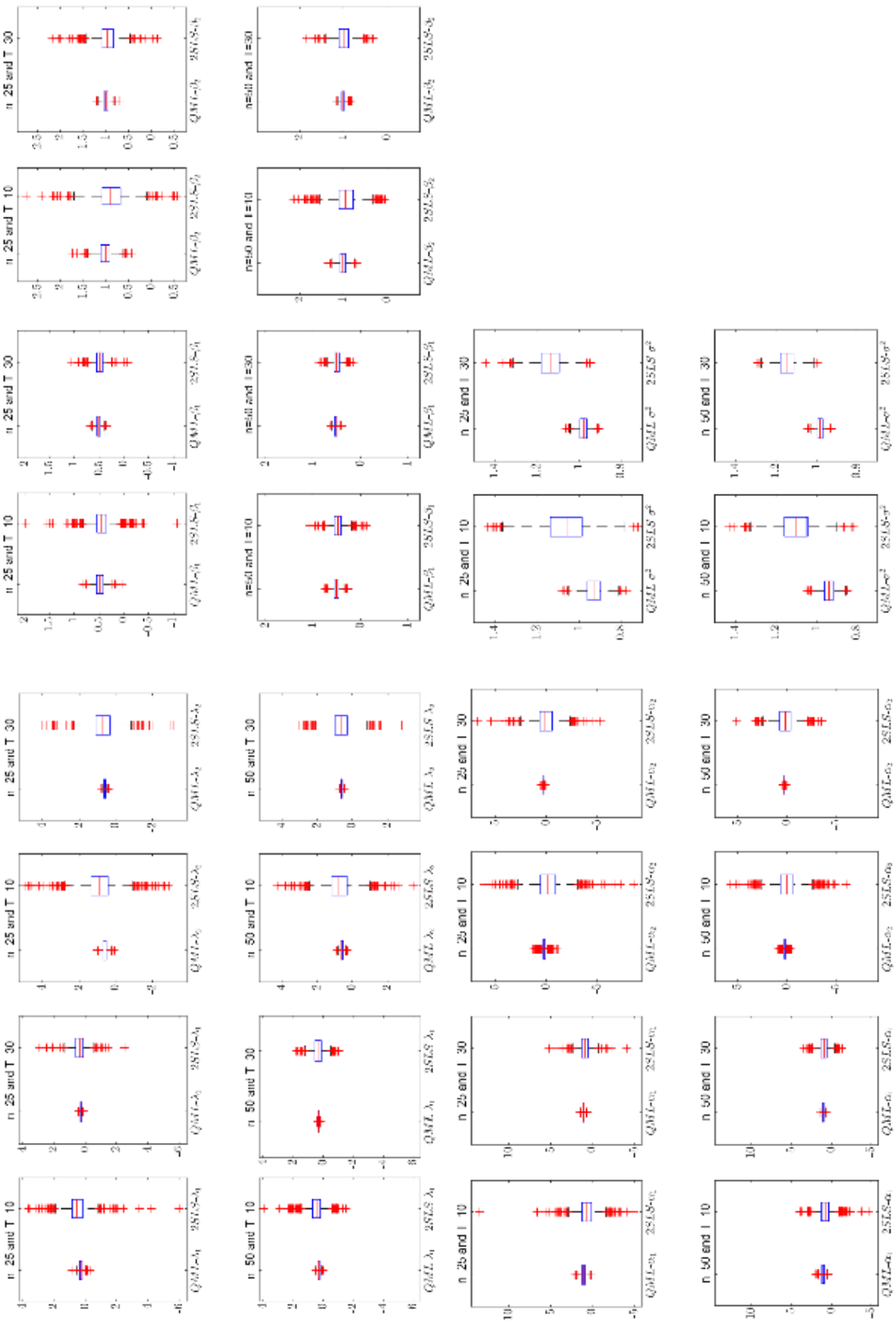

Figure 3.5.2. Boxplots of the estimated non-threshold parameters for a two-regime PBTSD model, with $v_{i,t} \sim \mathcal{N}(0,1)$, $X_{i,t} \sim \mathcal{N}(0,1)$, *and* $q_{i,t} \sim \mathcal{N}(0,1)$.

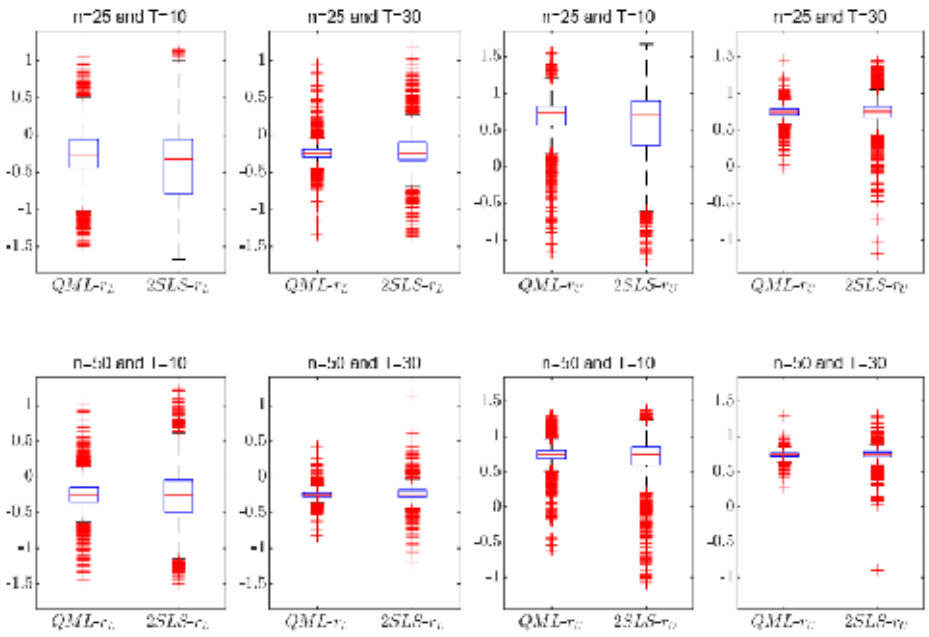

Figure 3.5.3. Boxplots of the estimated non-threshold parameters for a two-regime PBTSD model, with $v_{i,t} \sim t(5)$, $X_{i,t} \sim \mathcal{N}(0,1)$, *and* $q_{i,t} \sim \mathcal{N}(0,1)$.

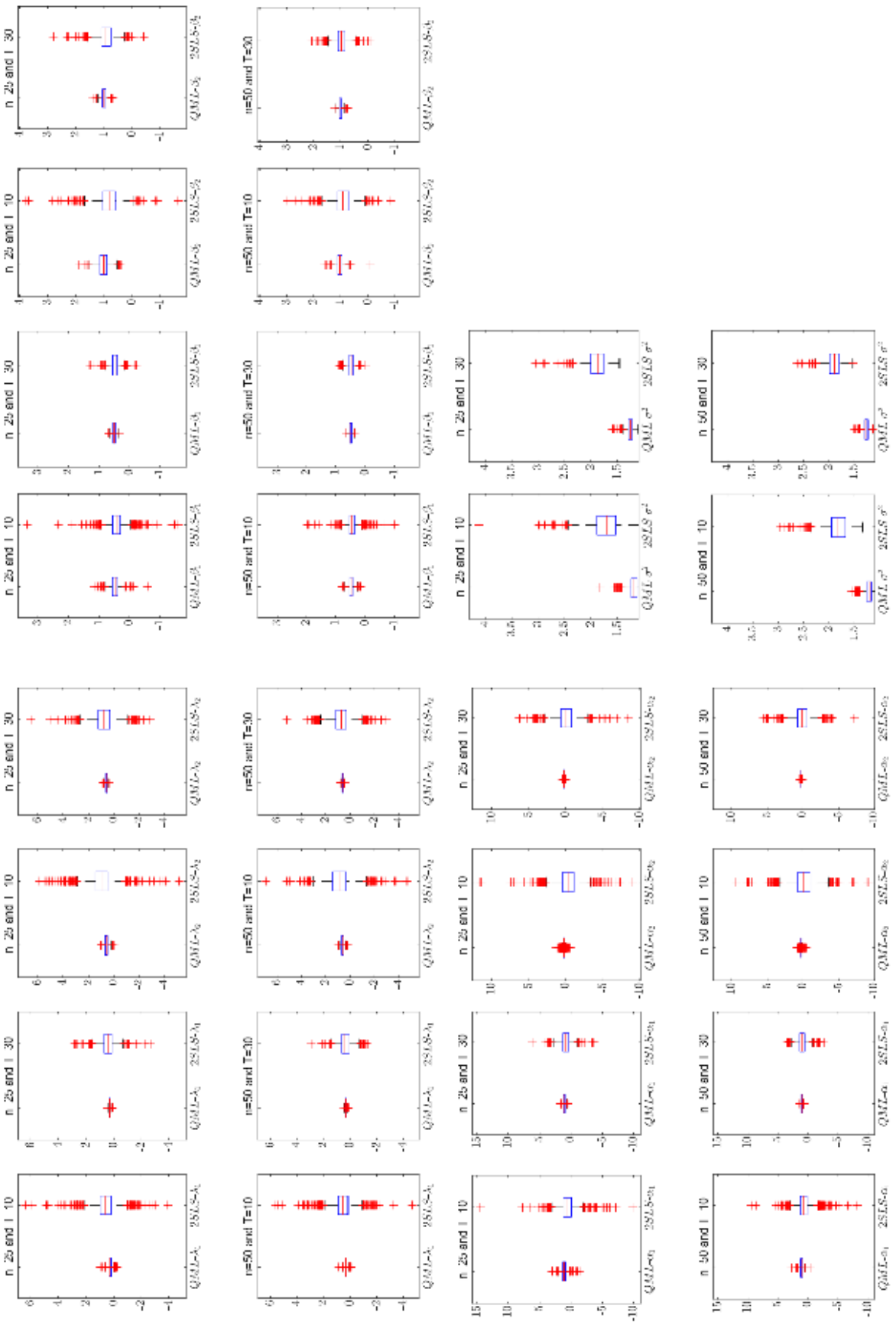

Figure 3.5.4. Boxplots of the estimated non-threshold parameters for a two-regime PBTSD model, with $v_{i,t} \sim t(5)$, $X_{i,t} \sim \mathcal{N}(0,1)$, *and* $q_{i,t} \sim \mathcal{N}(0,1)$.

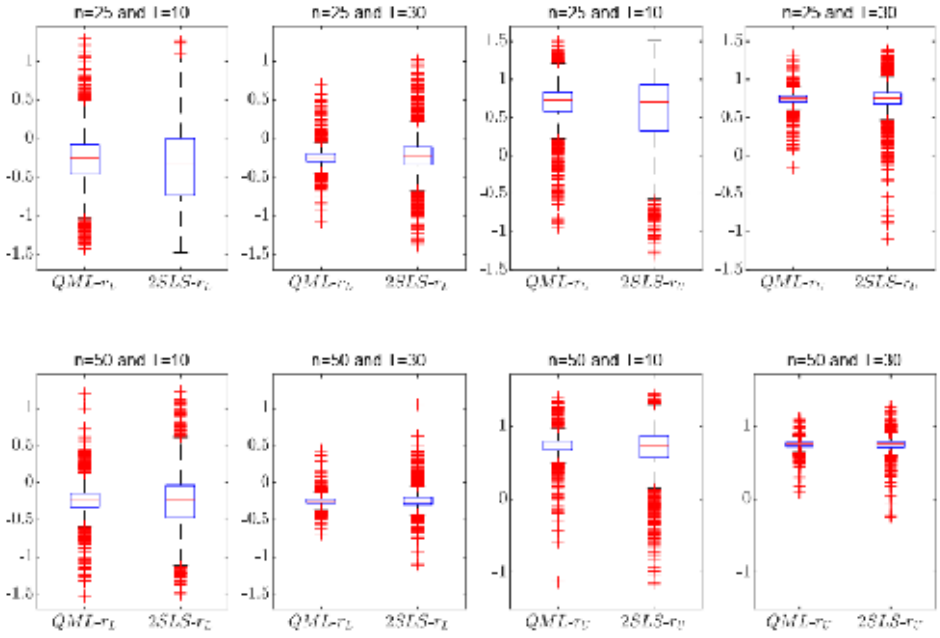

Figure 3.5.5. Boxplots of the estimated buffer zone for a two-regime PBTSD model, with $v_{i,t} \sim$ *centered* $\mathcal{E}(1)$, $X_{i,t} \sim \mathcal{N}(0,1)$, *and* $q_{i,t} \sim \mathcal{N}(0,1)$.. .

asymptotic normality for the non-threshold parameters (λ_1, λ_2, β_1, β_1 and α_1). In these cases, the JB test does not reject the normality of the empirical distribution for the non-threshold parameters at the 1% significance level. For the parameter α_2, larger sample sizes may be required for the empirical distribution to converge to normality.

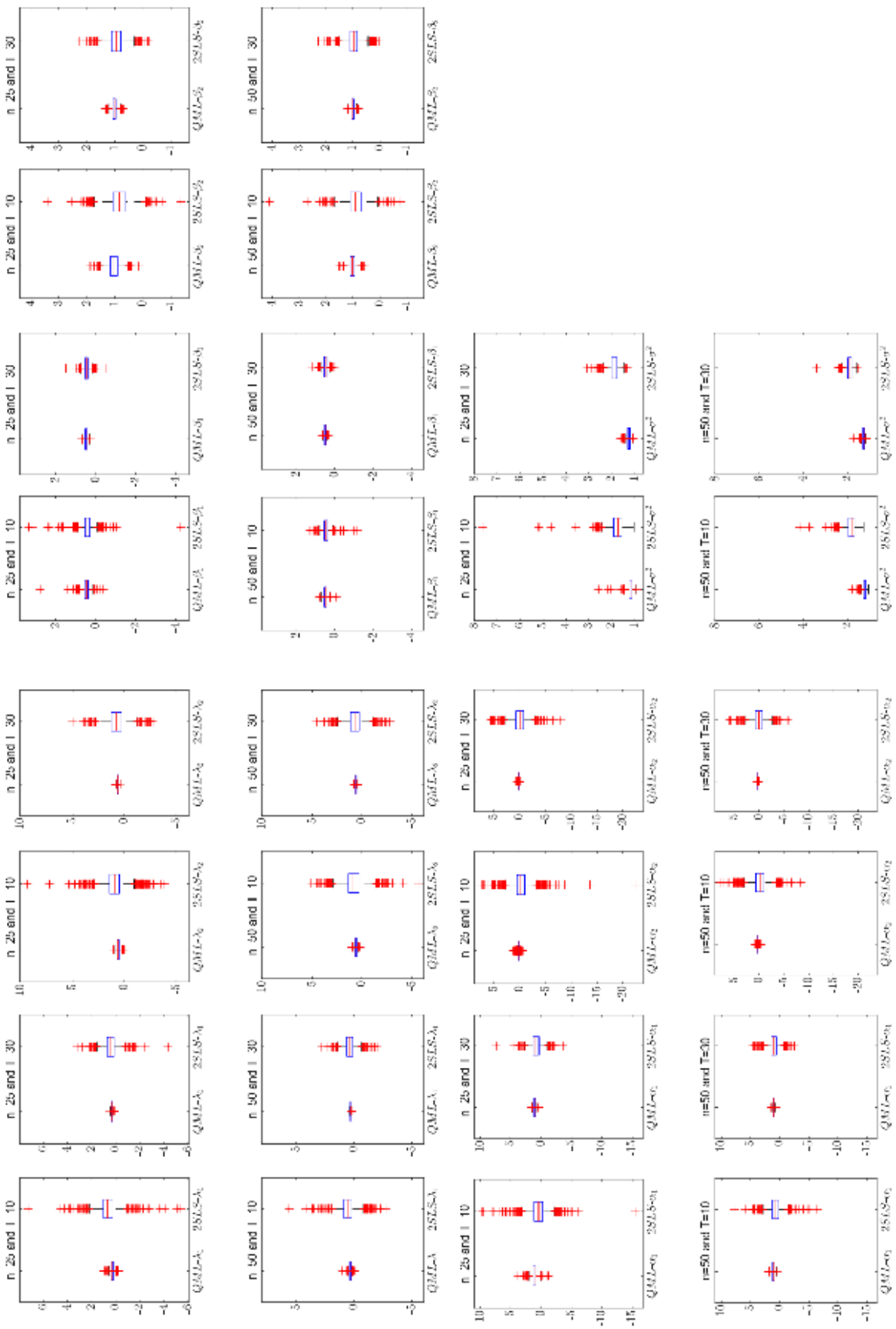

Figure 3.5.6. Boxplots of the estimated non-threshold parameters for a two-regime PBTSD model, with $v_{i,t} \sim$ centered $\mathcal{E}(1)$, $X_{i,t} \sim \mathcal{N}(0,1)$, and $q_{i,t} \sim \mathcal{N}(0,1)$.

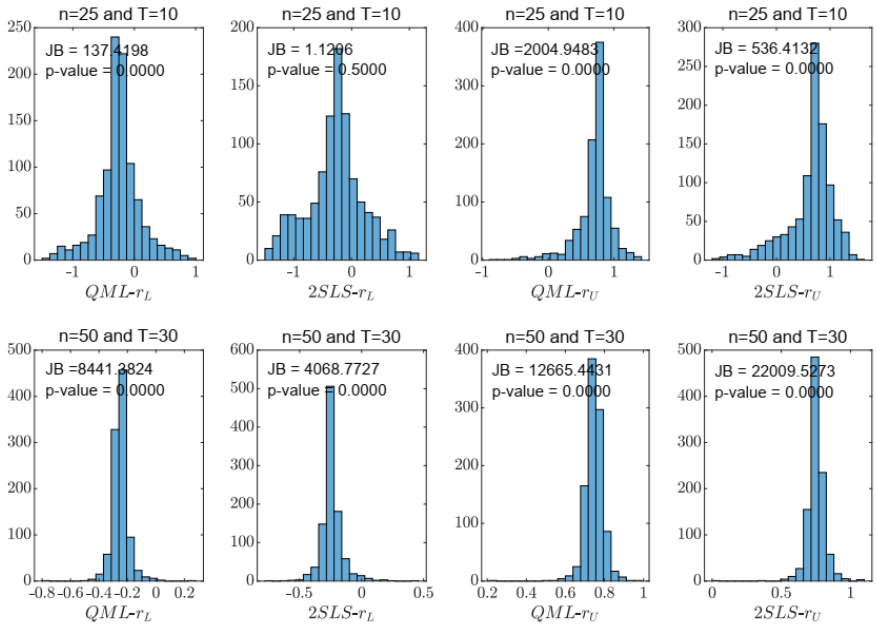

Figure 3.5.7. Histograms of the estimated buffer zone for a two-regime PBTSD model, with $v_{i,t} \sim \mathcal{N}(0,1)$, $X_{i,t} \sim \mathcal{N}(0,1)$, *and* $q_{i,t} \sim \mathcal{N}(0,1)$.

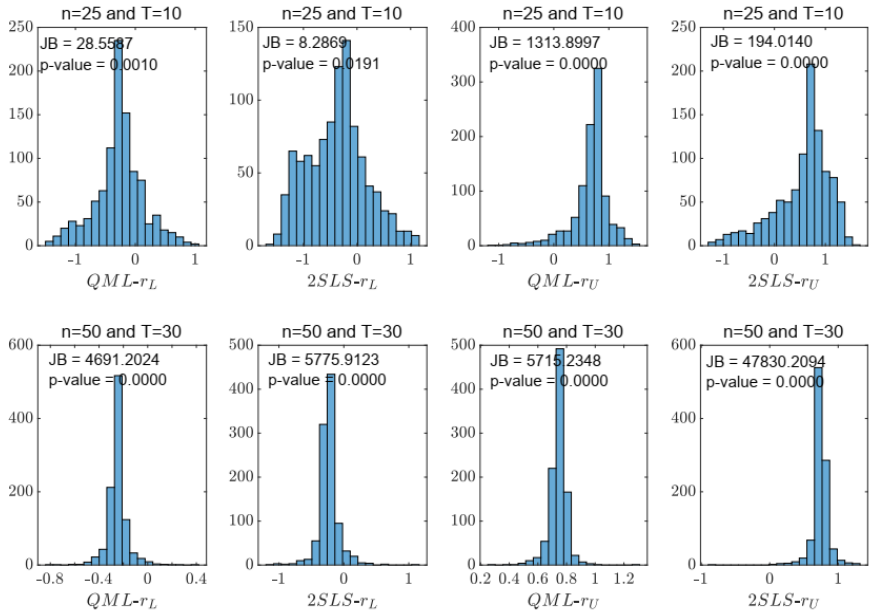

Figure 3.5.8. Histograms of the estimated buffer zone for a two-regime PBTSD model, with $v_{i,t} \sim t(5)$, $X_{i,t} \sim \mathcal{N}(0,1)$, *and* $q_{i,t} \sim \mathcal{N}(0,1)$.

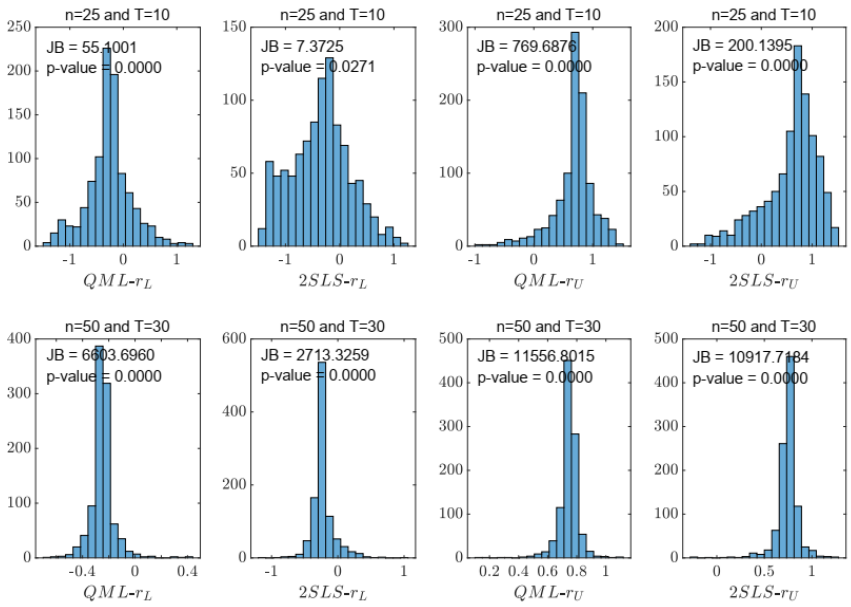

Figure 3.5.9. Histograms of the estimated buffer zone for a two-regime PBTSD model, with $v_{i,t} \sim$ centered $\mathcal{E}(1)$, $X_{i,t} \sim \mathcal{N}(0,1)$, and $q_{i,t} \sim \mathcal{N}(0,1)$.

Table 3.5.1. Rejection frequencies from the bootstrap-based test for linearity.

True model and H_0	H_1	n	α	$T = 10$	$T = 20$	$T = 30$
Empirical size						
Linear	Two-regime PBTSD	25	0.01	15	13	13
			0.05	59	52	53
			0.10	112	109	102
		50	0.01	16	14	9
			0.05	55	51	47
			0.10	110	105	96
Empirical power	Linear	25	0.01	878	1000	1000
Two-regime PBTSD			0.05	916	1000	1000
			0.10	950	1000	1000
		50	0.01	1000	1000	1000
			0.05	1000	1000	1000
			0.10	1000	1000	1000

It is worth noting that, for the $2SLS$ method, the normality hypothesis is still rejected at the 1% significance level for all parameters, even when $n = 50$ and $T = 30$: Furthermore, an important observation from this simulation study is that the estimated boundary parameters

defining the buffer zone are non-normal for both the QML and $2SLS$ methods, regardless of the sample sizes considered. We conclude by examining the finite sample performance of our proposed procedure for testing linearity within the $PBTSD$ model. To this end, we consider two data-generating processes: the first evaluates the test's size, while the second assesses its power. The number of replications is set to 1000. In each replication, the spatial model is estimated and analyzed using the proposed bootstrap-based linearity test, which is performed with 500 bootstrap replications.

Table 3.5.1 presents the rejection frequencies at nominal levels of 1%, 5%, and 10%. The results indicate that the rejection frequencies closely align with the nominal sizes. Additionally, the test's power improves as the cross-sectional and temporal dimensions of the spatial panel increase. In summary, our adaptation of the bootstrap-based test proposed by Belarbi et al. (2021) performs effectively in assessing linearity within our spatial framework.

Table 3.5.2. Results of a simulation study for a two-regime PBTSD model, with $v_{i,t} \sim \mathcal{N}(0,1)$, $X_{i,t} \sim \mathcal{N}(0,1)$, *and* $q_{i,t} \sim \mathcal{N}(0,1)$.

			T											
			10				20				30			
n		$True$	M_{Qml}	S_{Qml}	M_{2SLS}	S_{2SLS}	M_{Qml}	S_{Qml}	M_{2SLS}	S_{2SLS}	M_{Qml}	S_{Qml}	M_{2SLS}	S_{2SLS}
	r_L	-0.25	-0.2490	0.3455	-0.2728	0.4896	-0.2390	0.1852	-0.2343	0.3026	-0.2393	0.1298	-0.2240	0.2290
	r_U	0.75	0.6987	0.2636	0.6366	0.4266	0.7383	0.1259	0.7317	0.2295	0.7439	0.0779	0.7439	0.1726
	λ_1	0.3	0.2786	0.1141	0.5148	0.7212	0.2894	0.0683	0.4209	0.4843	0.2949	0.0454	0.3758	0.4222
	λ_2	0.6	0.5860	0.1412	0.8734	0.9284	0.5920	0.0898	0.7282	0.7438	0.5900	0.0576	0.6933	0.7074
25	α_1	0.5	0.4831	0.0985	0.4447	0.2039	0.4949	0.0617	0.4729	0.1345	0.5118	0.0490	0.4915	0.1072
	α_2	1	1.0217	0.1513	0.8995	0.3359	1.0134	0.0909	0.9635	0.2439	1.0048	0.0718	0.9694	0.2251
	β_1	1	1.0340	0.2960	0.6512	1.1371	1.0181	0.1769	0.8081	0.8029	1.0296	0.1330	0.8735	0.6776
	β_2	0.2	0.2112	0.2677	-0.1939	1.4621	0.2133	0.1869	0.0119	1.1453	0.2428	0.0351	0.0617	1.0806
	σ^2	1	0.9304	0.0451	1.0633	0.1123	0.9673	0.0318	1.1220	0.0812	0.9791	0.0256	1.1384	0.0680
	r_L	-0.25	-0.2322	0.2109	-0.2379	0.3661	-0.2423	0.0905	-0.2356	0.1520	-0.2507	0.0601	-0.2408	0.0861
	r_U	0.75	0.7363	0.1198	0.7041	0.2744	0.7504	0.0638	0.7496	0.1122	0.7476	0.0471	0.7513	0.0633
	λ_1	0.3	0.2869	0.0751	0.4502	0.5115	0.2978	0.0512	0.3285	0.4062	0.2968	0.0309	0.3431	0.3634
	λ_2	0.6	0.5974	0.0936	0.7515	0.8207	0.5994	0.0609	0.7160	0.6847	0.5917	0.0423	0.6330	0.6380
50	α_1	0.5	0.5012	0.0688	0.4705	0.1259	0.5028	0.0405	0.4989	0.0965	0.5118	0.0339	0.4965	0.0855
	α_2	1	1.0074	0.0922	0.9433	0.2597	1.0007	0.0599	0.9646	0.2000	1.0049	0.0486	0.9880	0.1805
	β_1	1	1.0254	0.1835	0.7656	0.8082	1.0000	0.1289	0.9473	0.6391	1.0284	0.0940	0.9315	0.5756
	β_2	0.2	0.2094	0.1717	-0.0265	1.2398	0.1957	0.1382	0.0175	1.0479	0.2413	0.0291	0.1483	0.9753
	σ^2	1	0.9389	0.0315	1.1028	0.0842	0.9723	0.0228	1.1416	0.0597	0.9826	0.0185	1.1433	0.0494

Table 3.5.3. Results of a simulation study for a two-regime PBTSD model, with $v_{i,t} \sim t(5)$, $X_{i,t} \sim \mathcal{N}(0,1)$, and $q_{i,t} \sim \mathcal{N}(0,1)$.

			T											
			10				20				30			
n		$True$	M_{Qml}	S_{Qml}	M_{2SLS}	S_{2SLS}	M_{Qml}	S_{Qml}	M_{2SLS}	S_{2SLS}	M_{Qml}	S_{Qml}	M_{2SLS}	S_{2SLS}
	r_L	-0.25	-0.2710	0.4038	-0.3793	0.5441	-0.2309	0.2768	-0.2502	0.4279	-0.2318	0.1835	-0.2078	0.3204
	r_U	0.75	0.6657	0.3363	0.5562	0.5383	0.7258	0.1888	0.7072	0.3450	0.7370	0.1174	0.7206	0.2594
	λ_1	0.3	0.2735	0.1302	0.6065	0.8543	0.2902	0.0757	0.4830	0.6514	0.2963	0.0551	0.4190	0.5086
	λ_2	0.6	0.5866	0.1574	0.9616	1.0536	0.5948	0.0980	0.7849	0.9973	0.5977	0.0712	0.7803	0.8816
25	α_1	0.5	0.4728	0.1409	0.4224	0.2946	0.4962	0.0815	0.4636	0.1696	0.5034	0.0617	0.4811	0.1311
	α_2	1	1.0292	0.1962	0.8533	0.4098	1.0184	0.1192	0.9284	0.3367	1.0048	0.0924	0.9367	0.2958
	β_1	1	1.0736	0.3724	0.5381	1.4184	1.0384	0.2120	0.7107	1.0546	1.0171	0.1635	0.8035	0.8190
	β_2	0.2	0.2425	0.1367	-0.3022	1.6757	0.2280	0.0810	-0.0806	1.5150	0.2220	0.0549	-0.0715	1.3554
	σ^2	1	1.1930	0.0943	1.7323	0.2881	1.2419	0.0682	1.8403	0.2218	1.2644	0.0588	1.8956	0.1842
	r_L	-0.25	-0.2500	0.2796	-0.2619	0.4532	-0.2329	0.1544	-0.2178	0.2765	-0.2482	0.0858	-0.2313	0.1589
	r_U	0.75	0.7256	0.2058	0.6738	0.3859	0.7450	0.0975	0.7476	0.1957	0.7425	0.0627	0.7413	0.1265
	λ_1	0.3	0.2883	0.0813	0.5301	0.7975	0.2995	0.0482	0.3877	0.5064	0.2998	0.0417	0.3531	0.4620
	λ_2	0.6	0.5883	0.1072	0.8340	1.0605	0.5987	0.0688	0.7537	0.8351	0.5960	0.0496	0.6885	0.8066
50	α_1	0.5	0.4914	0.0860	0.4555	0.2046	0.5014	0.0544	0.4857	0.1206	0.5017	0.0442	0.4920	0.1086
	α_2	1	1.0211	0.1308	0.9146	0.3516	1.0002	0.0812	0.9520	0.2665	0.9972	0.0610	0.9675	0.2361
	β_1	1	1.0309	0.2420	0.6346	1.2774	1.0056	0.1435	0.8560	0.8163	1.0028	0.1173	0.9093	0.7289
	β_2	0.2	0.2354	0.0840	-0.1571	1.6500	0.2260	0.0480	-0.0307	1.2865	0.2279	0.0369	0.0671	1.2323
	σ^2	1	1.2133	0.0693	1.8295	0.2180	1.2543	0.0542	1.8909	0.1755	1.2668	0.0458	1.9008	0.1429

Table 3.5.4. Results of a simulation study for a two-regime PBTSD model, with $v_{i,t} \sim$ centered $\mathcal{E}(1)$, $X_{i,t} \sim \mathcal{N}(0,1)$, and $q_{i,t} \sim \mathcal{N}(0,1)$.

			T											
			10				20				30			
n		$True$	M_{Qml}	S_{Qml}	M_{2SLS}	S_{2SLS}	M_{Qml}	S_{Qml}	M_{2SLS}	S_{2SLS}	M_{Qml}	S_{Qml}	M_{2SLS}	S_{2SLS}
	r_L	-0.25	-0.2648	0.4163	-0.3550	0.5448	-0.2398	0.2629	-0.2407	0.4240	-0.2392	0.1580	-0.2189	0.3303
	r_U	0.75	0.6817	0.3418	0.5779	0.5351	0.7242	0.1968	0.6667	0.3616	0.7401	0.1155	0.7300	0.2547
	λ_1	0.3	0.2827	0.1289	0.6331	0.8971	0.2903	0.0734	0.5127	0.6925	0.2976	0.0561	0.4145	0.5364
	λ_2	0.6	0.5929	0.1553	0.9346	1.1011	0.5984	0.1011	0.8034	0.9934	0.5939	0.0729	0.7730	0.8761
25	α_1	0.5	0.4785	0.1605	0.4313	0.3412	0.4943	0.0843	0.4584	0.1939	0.5000	0.0642	0.4765	0.1337
	α_2	1	1.0276	0.2079	0.8567	0.4174	1.0180	0.1263	0.9235	0.3567	1.0144	0.0922	0.9458	0.2870
	β_1	1	1.0489	0.3983	0.4500	1.5459	1.0219	0.2123	0.6653	1.1206	1.0064	0.1587	0.7988	0.8494
	β_2	0.2	0.2367	0.1406	-0.2638	1.8613	0.2267	0.0847	-0.0938	1.6430	0.2245	0.0603	-0.0685	1.3663
	σ^2	1	1.1993	0.1099	1.7568	0.3657	1.2490	0.0717	1.8661	0.2316	1.2628	0.0620	1.8914	0.1965
	r_L	-0.25	-0.2406	0.2841	-0.2451	0.4562	-0.2461	0.1332	-0.2419	0.2607	-0.2477	0.0909	-0.2229	0.1669
	r_U	0.75	0.7190	0.2101	0.6734	0.3795	0.7456	0.0845	0.7381	0.2069	0.7446	0.0708	0.7448	0.1168
	λ_1	0.3	0.2901	0.0792	0.5300	0.7127	0.2981	0.0502	0.4068	0.5213	0.3016	0.0399	0.3477	0.4859
	λ_2	0.6	0.5921	0.1046	0.8430	1.0753	0.5920	0.0675	0.6986	0.8527	0.5965	0.0529	0.7022	0.8359
50	α_1	0.5	0.4912	0.0879	0.4542	0.1863	0.5027	0.0547	0.4800	0.1200	0.5030	0.0454	0.4937	0.1115
	α_2	1	1.0146	0.1294	0.9088	0.3679	1.0052	0.0779	0.9646	0.2638	1.0001	0.0622	0.9678	0.2420
	β_1	1	1.0301	0.2297	0.6425	1.1094	1.0112	0.1405	0.8311	0.8206	1.0052	0.1159	0.9159	0.7542
	β_2	0.2	0.2316	0.0886	-0.1587	1.6416	0.2279	0.0496	0.0432	1.3141	0.2248	0.0378	0.0433	1.2715
	σ^2	1	1.2142	0.0754	1.8368	0.2456	1.2521	0.0513	1.8795	0.1604	1.2674	0.0458	1.9056	0.1463

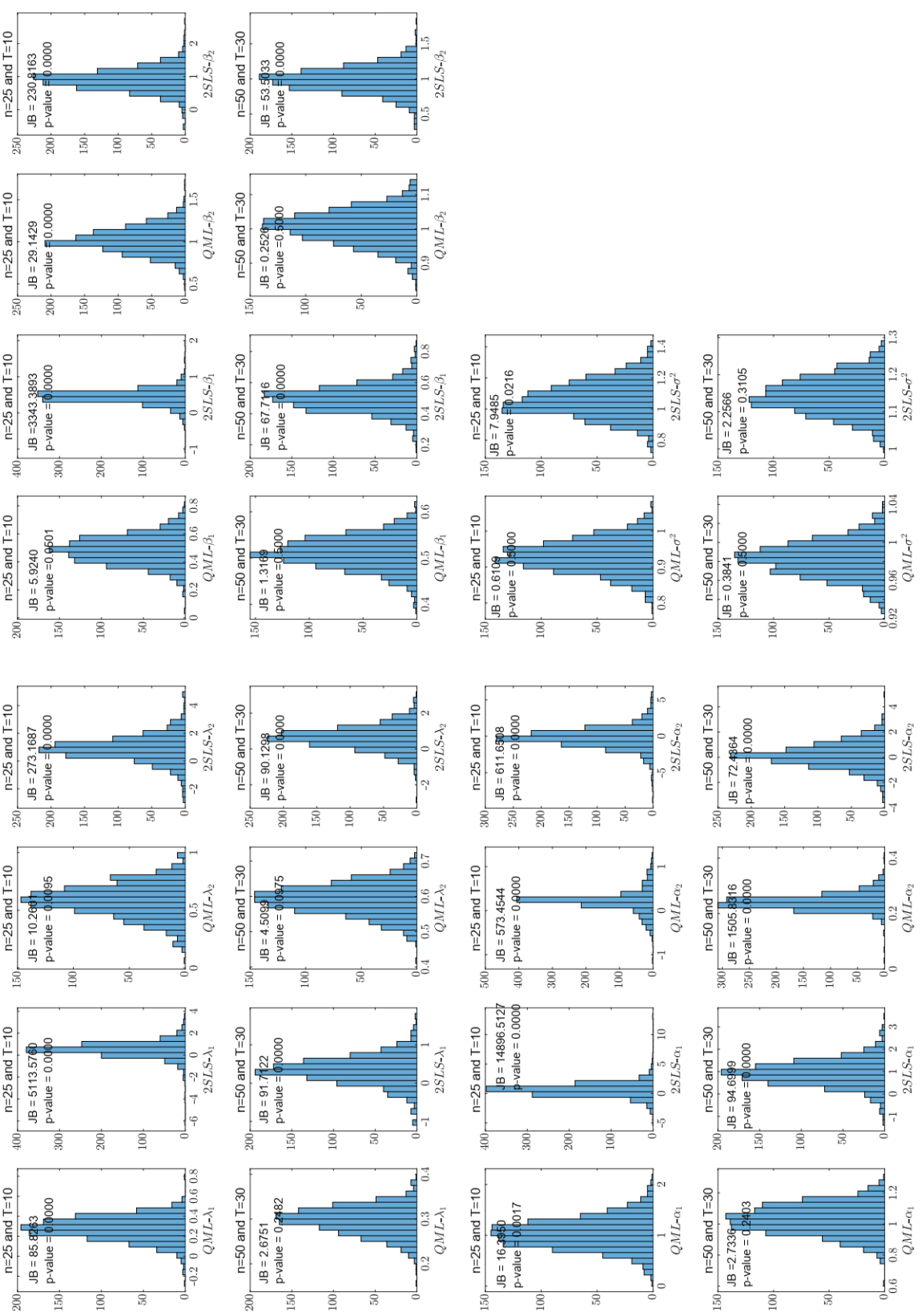

Figure 3.5.10. Histograms of the estimated non-threshold parameters for a two-regime PBTSD model, with $v_{i,t} \sim \mathcal{N}(0,1)$, $X_{i,t} \sim \mathcal{N}(0,1)$, *and* $q_{i,t} \sim \mathcal{N}(0,1)$. .

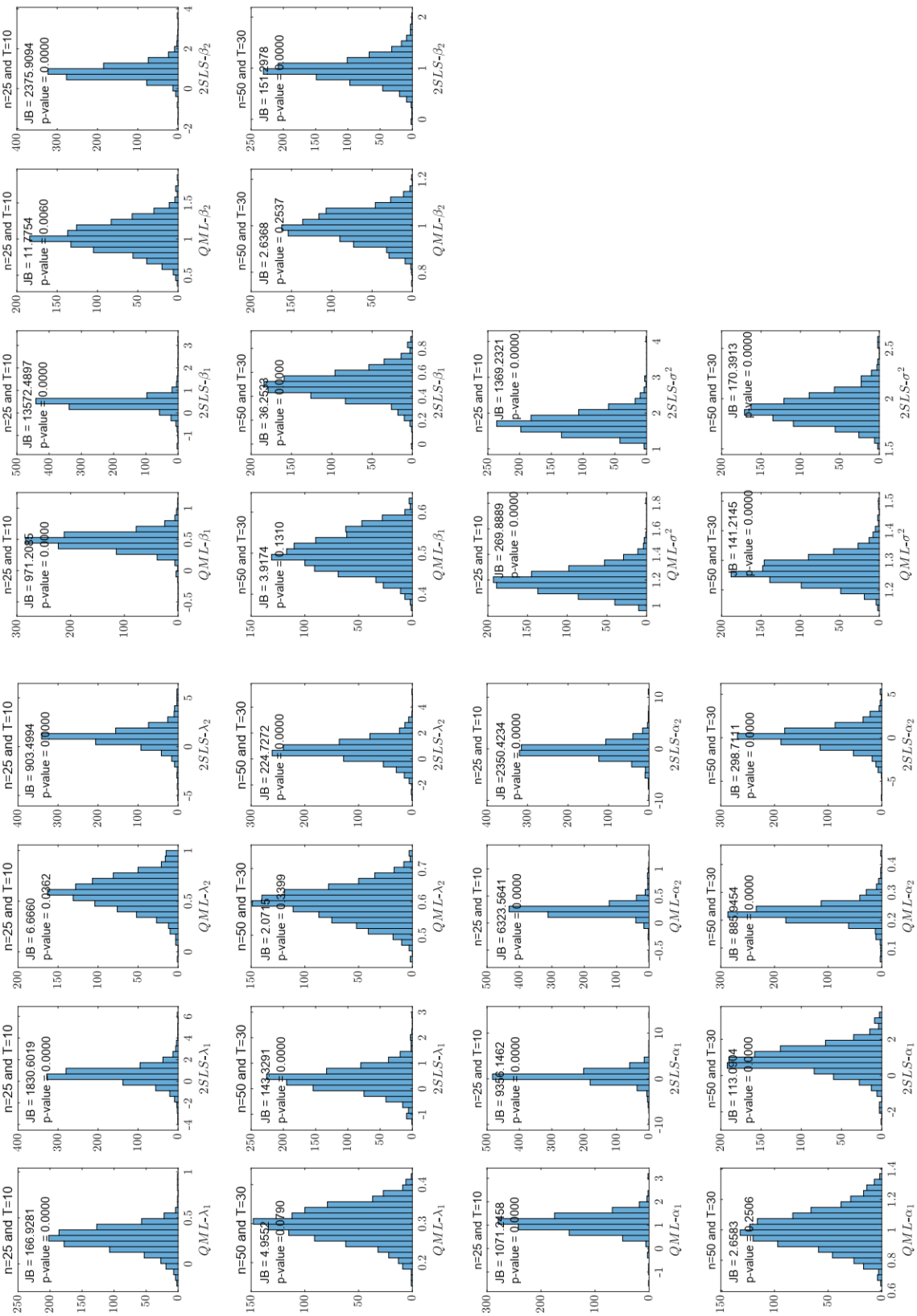

Figure 3.5.11. Histograms of the estimated non-threshold parameters for a two-regime PBTSD model, with $v_{i,t} \sim t(5)$, $X_{i,t} \sim \mathcal{N}(0,1)$, *and* $q_{i,t} \sim \mathcal{N}(0,1)$.

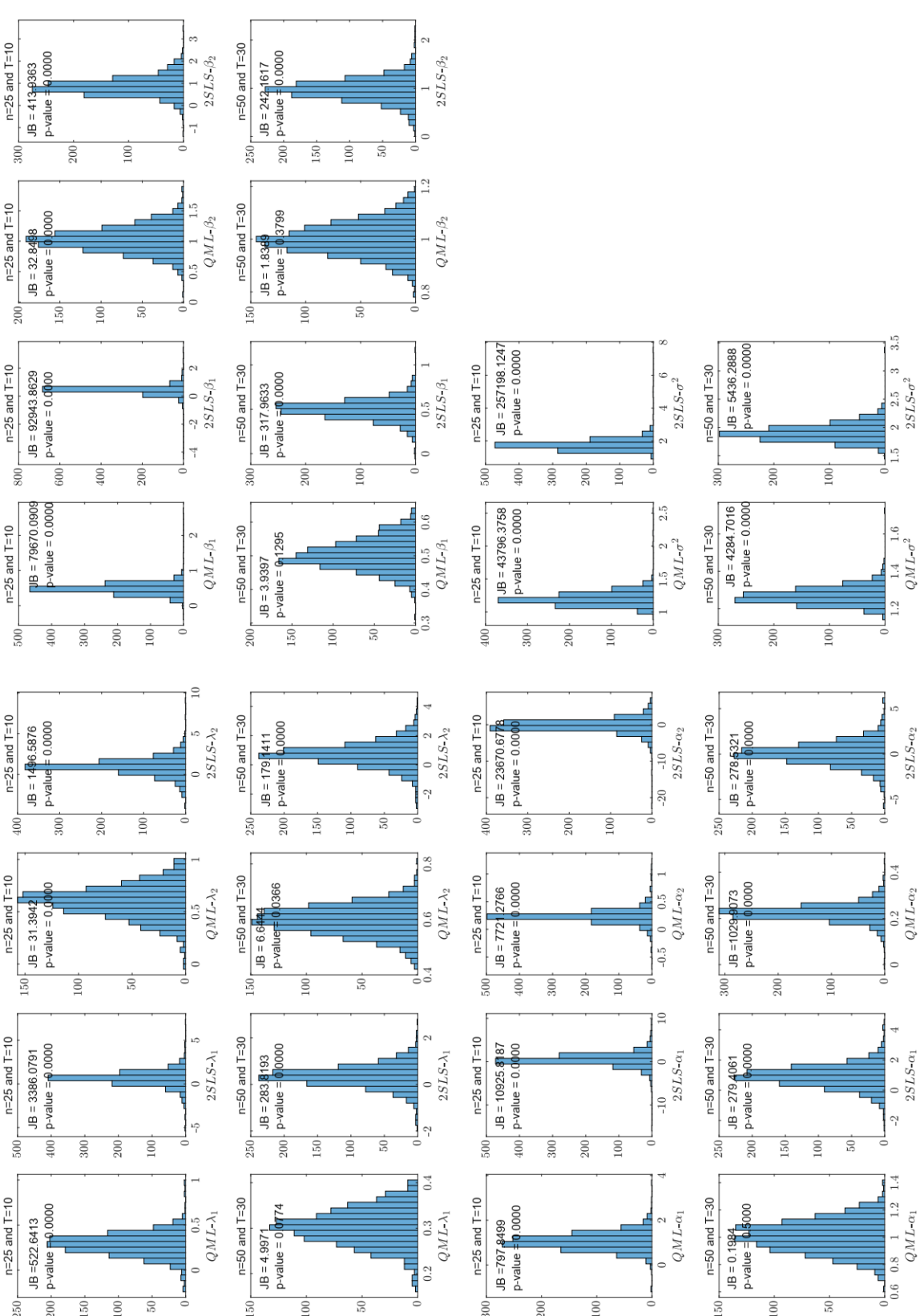

Figure 3.5.12. Histograms of the estimated non-threshold parameters for a two-regime PBTSD model, with $v_{i,t} \sim$ centered $\mathcal{E}(1)$, $X_{i,t} \sim \mathcal{N}(0,1)$, and $q_{i,t} \sim \mathcal{N}(0,1)$.

Chapter 4

Spatial Effects of R&D expenditure on Innovation

4.1 Introduction

The importance of innovation and R&D spending as drivers of economic growth is now widely acknowledged. Since the seminal contributions of Arrow (1962) and Romer (1990), and later Aghion and Howitt (1992) and Grossman and Helpman (1991), research has emphasized the critical role of human capital, technology, and innovation in sustaining long-term growth. This explains why policymakers increasingly prioritize education, research, and innovation to foster competitiveness and reduce regional disparities (Crescenzi and Jaax, 2017).

The classical Knowledge Production Function (KPF) framework established a positive link between R&D inputs and outputs such as innovation and growth. More recent approaches (Lee and Kim, 2020) extend this model by incorporating factors such as innovation stock and the number of researchers and engineers. Yet, despite extensive theoretical and empirical work, several aspects remain underexplored most notably the international diffusion of innovation. Cross-border knowledge transfer depends on education systems, public policies, trade, foreign direct investment, and scientific cooperation, all of which facilitate the circulation of ideas and technologies.

Innovation dynamics also reveal strong disparities depending on development levels. Rodríguez-Pose and Burlina (2021), for example, show that advanced cities benefit more from R&D spillovers and human capital than less-developed ones. Institutional quality and trade openness are also decisive in shaping countries' capacity to leverage technological transfers

(Polenske, 2007).

Empirical evidence broadly confirms a positive correlation between innovation and growth (Maradana et al., 2017; Mensah et al., 2019; Rahman & Malik, 2023), but findings remain heterogeneous across contexts. In some countries, innovation significantly contributes to growth (Haftu, 2019; Anakpo & Oyenubi, 2022), while in others its impact is weaker or insignificant (Szirmai & Verspagen, 2015; Sesay et al., 2018). In developing regions such as Africa, the lack of reliable innovation data often forces reliance on R&D intensity as a proxy (Olaoye et al., 2021).

In this chapter, we aim to capture these heterogeneous dynamics by employing the Panel Buffered Threshold Spatial Durbin (PBTSD) model. This framework allows us to simultaneously account for threshold effects linked to development levels, spatial spillovers across economies, and the non-linear relationship between R&D, innovation, and growth.

4.2 Data description

This study examines the effects of R&D expenditure (as a share of GDP), trade openness (trade as a share of GDP), and GDP per capita on patent applications, while accounting for regional characteristics and spatial dependencies. It uses different threshold variables (GDP per capita to capture a country's level of development, and rule of law to reflect institutional quality) in order to better address cross-country heterogeneity. The analysis is conducted using a Spatial Durbin Panel model for 32 countries over the period 2007–2020.

To capture heterogeneity across economies, we employ a buffered regime-switching specification, allowing us to investigate how the interaction between R&D intensity, trade openness, and income levels influences innovation outcomes. The list of countries included in the sample is provided in Table 4.2.1, while Table 4.2.2 presents the definitions of the variables used.

Table 4.2.1. Sample countries

Australia	Austria	Brazil	Canada	Chile	China	Czech Republique
Denmark	Egypt	Estonia	Finland	France	Germany	Greece
India	Italia	Japan	Latvia	Malaysia	Mexico	New zeland
Poland	Portugal	Romania	Singapore	Sweeden	Switzerland	Thailand
Tunisia	Turkey	United kingdom	United states			

Table 4.2.2. Description of the variables used

Variable	Description
Pat	Patent Application: A patent is an exclusive right granted for an invention, which is a product or a process that provides, in general, a new way of doing something, or offers a new technical solution to a problem. To get a patent, technical information about the invention must be disclosed to the public in a patent application.
LPat	Log (Pat)
R&D expenditure (%GDP)	Gross domestic expenditures on research and development (R&D), expressed as a percentage of GDP. They include both capital and current expenditures in the four main sectors: Business enterprise, Government, Higher education and Private non-profit. R&D covers basic research, applied research, and experimental development.
Trade(%GDP)	Trade is the sum of exports and imports of goods and services measured as a share of gross domestic product.
GDP percapita	GDP per capita is gross domestic product divided by midyear population. GDP is the sum of gross value added by all resident producers in the economy plus any product taxes and minus any subsidies not included in the value of the products. It is calculated without making deductions for depreciation of fabricated assets or for depletion and degradation of natural resources. Data are in current U.S. dollars
LGDP	Log(GDP)
Rule of law	Rule of law reflects the extent to which people trust and follow society's rules —especially contract enforcement, property rights, police and court effectiveness, and crime levels—with the score given on a scale of roughly 0 to 1.
Sources: WorldBank	

Our multidimensional approach seeks to reflect the complex interplay between economic, technological, and human factors in shaping regional innovation dynamics and economic growth. Spatial dependencies are modeled using three distinct spatial weight matrices, each capturing a different dimension of spatial interaction. The contiguity matrix reflects proximity between regions. The inverse distance matrix assigns higher weights to closer regions,

accounting for the effect of proximity on spatial dependence. The flux matrix measures interactions between regions through flows of people, goods, or information, capturing functional connectivity.

Table 4.2.3 reports the descriptive statistics for the dataset. The results indicate that patent applications remained relatively stable during 2007–2020, while R&D expenditure showed a modest increase (from 1.478% to 1.790% of GDP). By contrast, trade openness declined (from 87.18% to 81.79%), and GDP per capita displayed a slight upward trend (from 9.767 to 9.954 in log values).The Rule of Law index (RL) remained nearly constant over the period, with only a marginal decrease from 0.684 in 2007 to 0.680 in 2020, suggesting that institutional quality and governance stability have changed little during this timeframe.

Table 4.2.3. Descriptive statistics

	Mean		*Max*		*Min*		*Std*	
	2007	2020	2007	2020	2007	2020	2007	2020
LPat	8.599	8.682	13.030	14.219	4.143	3.135	2.141	2.353
R&D	1.478	1.790	3.337	3.4896	0.200	0.296	0.982	0.975
Trade	87.1757	81.7881	394.288	332.773	25.2926	23.383	66.387	55.623
LGDP	9.767	9.954	11.082	11.358	6.930	7.556	1.128	0.973
RL	0.684	0.680	0.899	0.904	0.380	0.370	0.171	0.161

To assess the spatial dependency of patent applications, we apply Moran's I test, a widely used measure of spatial autocorrelation, to determine whether patent activity exhibits spatial clustering when analyzed in conjunction with our spatial weight matrix. Moran's I evaluates the extent to which similar or dissimilar values are spatially distributed, thereby testing for the presence of spatial effects in patent applications across regions. Through Moran's I test, we aim to identify whether patent applications exhibit significant spatial clustering, indicating that innovation activities are influenced not only by local factors but also by spatial proximity, as captured by all chosen weight matrices.

The results of the Moran's I test (Table 4.2.4) indicate a significant spatial autocorrelation across the analyzed regions. Specifically, the calculated Moran's I values were positive and statistically significant for all matrices, suggesting that regions with similar levels of economic activity tend to cluster geographically. For geographic-based matrices (contiguity and inverse-distance), the autocorrelation was moderate, indicating that neighboring regions are

Table 4.2.4. Moran's I test

W matrix	*Contiguity* (Wc)		*Inverse − distance* (Wd)		*Flux* (Wf)	
Period	$Moran's\ I$	$P-value$	$Moran's\ I$	$P-value$	$Moran's\ I$	$P-value$
2007	0.2597	0.001	0.1399	0.01	0.2433	0.000
2008	0.2779	0	0.1513	0	0.2547	0.000
2009	0.2442	0.001	0.1415	0.02	0.2430	0.000
2010	0.2004	0.0014	0.1249	0.06	0.2248	0.000
2011	0.2441	0.001	0.1469	0.01	0.2491	0.000
2012	0.2492	0.001	0.1540	0.01	0.2568	0.000
2013	0.2613	0.001	0.1551	0.02	0.2590	0.000
2014	0.2664	0	0.1622	0	0.2635	0.000
2015	0.2663	0	0.1645	0.01	0.2646	0.000
2016	0.2584	0.001	0.1606	0.02	0.2600	0.000
2017	0.2593	0.001	0.1556	0.01	0.2584	0.000
2018	0.2656	0	0.1518	0.02	0.2594	0.000
2019	0.2711	0	0.1627	0.01	0.2639	0.000
2020	0.2542	0.001	0.2542	0.03	0.2568	0.000

somewhat similar in their characteristics. In contrast, economic connectivity matrices (flux) showed stronger positive spatial autocorrelation, reflecting that regions connected through flows or high-tech trade exhibit pronounced clustering. These findings highlight that spatial patterns are shaped not only by geographic proximity but also by functional and economic linkages.

4.3 Results and discussions

We examine two models to analyze the interactions among R&D, trade, LGDP, and their impact on LPat. The first model employs our proposed PBTSD formulation, while the second model uses the standard threshold spatial Durbin formulation by Wei et al. (2021). To deepen our investigation of these relationships, we carry out linearity tests across all proposed spatial weight matrices and for every potential threshold variable. This test is crucial for identifying whether a linear or non-linear model better captures the dynamics of these interactions, as it assesses the consistency of the relationship between the dependent variable (LPat) and the independent variables (R&D, trade, and LGDP) across different levels of these predictors.

Table 4.3.1. Linearity test results with GDP percapita as the threshold variable

Threshold variable	*LGDP*		
Spatial weight	Wc	Wd	Wf
F_1	265.098	439.610	201.601
P_value	0.09	0.01	0.07

The results of the linearity test was conducted for the threshold variable LGDP using three different spatial weight matrices (Wc, Wd, Wf). The results, presented in Table 4.3.1, indicate that linearity cannot be rejected for Wc ($F_1 = 265.098$, $p = 0.09$) and Wf ($F_1 = 201.601, p = 0.07$). In contrast, for Wd ($F_1 = 439.610, p = 0.01$), the null hypothesis of linearity is rejected, indicating a significant threshold effect and implying that a nonlinear specification is more appropriate. These findings highlight that the presence of a threshold effect depends on the spatial weight structure, with Wd capturing spatial interactions that introduce nonlinearity in the model.

Table 4.3.2. Linearity test results with rule of law as the threshold variable

Threshold variable	*Rule of Law*		
Spatial weight	Wc	Wd	Wf
F_1	$297,412$	$493,984$	$214,250$
P_value	0.15	0.03	0.07

The linearity test for the threshold variable Rule of Law was conducted using three different spatial weight matrices (Wc, Wd, Wf). The results, presented in Table 4.3.2, indicate that the null hypothesis of linearity cannot be rejected for matrices Wc ($F_1 = 297.412, p = 0.15$) and Wf ($F_1 = 214.250, p = 0.07$). In contrast, for Wd ($F_1 = 493.984, p = 0.03$), the null hypothesis of linearity is rejected, indicating a significant threshold effect and implying that a nonlinear specification is more appropriate. These results suggest that the presence of a threshold effect is sensitive to the spatial weight structure, with Wd capturing spatial interactions that introduce nonlinearity in the model.

Table 4.3.3. Estimated two-regime PBTSD model with GDP percapita as threshold variable

Endogenous variable	*Lpat*	
Threshold variable	*LGDP*	
	Lower	*Upper*
Boundary parameters	$9,661$	$9,765$
λ_k	$-0,132^{***}$	$0,245^{***}$
$\alpha_{k,1}$ $(R\&D)$	$0,591^{**}$	$0,025^{***}$
$\alpha_{k,2}$ $(Trade)$	$-0,001$	$0,001^{***}$
$\alpha_{k,3}$ $(LGDP)$	$0,434^{***}$	$0,087^{***}$
$\beta_{k,1}$ $(R\&D)$	$0,212^{***}$	$0,037^{***}$
$\beta_{k,2}$ $(Trade)$	$0,0008$	$-0,004^{**}$
$\beta_{k,3}$ $(LGDP)$	$0,00031$	$0,0801^{**}$

***Significant at the level 0.01 level, ** at the 0.05 level, and *at the 0.10 level.

Table 4.3.3 presents the estimation results with LGDP as the threshold variable and Wd as the spatial weight matrix. The spatial lag coefficient for the lower bound, recorded as $\lambda_1 = -0.132$, suggests that when LGDP per capita is less than the lower bound threshold, there is evidence of a weak negative spatial correlation. This indicates that neighboring countries are more likely to exhibit dissimilar patent values, meaning that a lower LGDP per capita in one country corresponds to lower patent activity in adjacent countries. This pattern points to a divergence in patent levels across neighboring regions. Conversely, for the upper zone, the spatial autocorrelation coefficient $\lambda_2 = 0.2345$ indicates a moderate positive spatial autocorrelation. This suggests a tendency for neighboring countries to exhibit similar patent values, implying that higher patent in one country is generally associated with higher patent in adjacent countries. This pattern reflects a clustering effect where similar patent levels are more likely to be observed among neighboring nations.

The direct effect of R&D expenditure on patenting is positive and significant in both regimes, but the magnitude is higher in the first regime (0.59) than in the second (0.025). This suggests that, within our sample, less developed countries experience a stronger impact of R&D expenditure on patent compared to more developed economies. The impact of trade varies across the two regimes. In the lower-bound regime, the estimated effect is not statistically significant, whereas in the second regime, it exhibits a weak but positive effect. Similar to R&D, GDP per capita exhibits a comparable pattern: it has a positive and significant impact in both regimes, with the effect in the lower-bound regime substantially stronger than in the upper-bound regime.

The spatially lagged independent variable, represented by R&D expenditure, exhibits a positive impact. Specifically, a one-unit increase in R&D expenditure in a neighboring country leads to a 0.212 increase in patent in the focal country. This result underscores the influence of R&D expenditure on regional innovation. In the second regime, while the spatially lagged coefficient continues to exert an impact on neighboring countries, it remains in the same positive direction, though with a smaller magnitude of 0.037. This indicates a reduced but consistent effect of regional R&D expenditure on patent outcomes across borders. The indirect effect of trade in the first regime is found to be non-significant. However, in the second regime, trade exhibits a negative impact, with an estimated coefficient of $\alpha_{2,1} = -0.004$. This suggests that while trade does not play a substantial indirect role in influencing patent in the first regime, it has a minor yet negative effect in the second regime.

Finally, the spatial lag of GDP per capita for the lower bound demonstrates a non-significant effect. In contrast, for the second regime, it exhibits a positive effect with an estimated coefficient of 0.0801. This indicates that while spatial interactions related to GDP per capita do not significantly influence patent activity in the lower bound, they contribute positively in the second regime, implying that regional economic output may enhance patent across neighboring areas in this context.

Table 4.3.4. Estimated two-regime PBTSD model with rule of law as the threshold variable

Endogenous variable	*Lpat*	
Threshold variable	*Rule of law*	
	Lower	*Upper*
Boundary parameters	0.454	0.486
λ_k	$-0,413^{***}$	$0,308^{***}$
$\alpha_{k,1}$ $(R\&D)$	1.546^{***}	$0,040^{***}$
$\alpha_{k,2}$ $(Trade)$	$0,017^{***}$	$0,000$
$\alpha_{k,3}$ $(LGDP)$	0.789^{***}	$0,025$
$\beta_{k,1}$ $(R\&D)$	-1.230^{***}	$0,165$
$\beta_{k,2}$ $(Trade)$	-0.003	$-0,003$
$\beta_{k,3}$ $(LGDP)$	$-0,072$	$0,021$

***Significant at the level 0.01 level, ** at the 0.05 level, and *at the 0.10 level.

Table 4.3.4 presents the estimated results of the two-regime PBSTD model, where patent is the endogenous variable and rule of law acts as the threshold variable. Two regimes are identified based on the value of rule of law, with the lower-bound regime defined for countries

where rule of law is below 0.4540 and the upper-bound regime for countries where rule of law exceeds 0.4862.

The spatial lag coefficient for the lower regime indicates a strong negative spatial autocorrelation when institutional quality is weak. In this context, neighboring countries tend to display dissimilar patenting behavior, suggesting that low levels of institutional quality hinder technological diffusion across borders. Conversely, in the upper regime, the spatial lag coefficient indicates positive spatial dependence, suggesting that when countries benefit from stronger institutional frameworks, patenting activity tends to converge across geographic space. In other words, higher patent in one country is associated with higher patenting levels in adjacent economies, reflecting a clustering effect among countries with better governance and higher rule of law levels.

Regarding the direct effects, R&D expenditure exhibits a positive and significant impact in both regimes. However, this effect is substantially stronger in the first regime, with an estimated coefficient of 1.5468, while it decreases sharply to 0.040 in the upper regime. This implies that for countries with weaker institutional environments, investments in R&D generate a more pronounced increase in patent outputs, suggesting that R&D expenditure compensates for institutional weaknesses. In contrast, in countries where rule of law is high, innovation systems are already established, and the marginal effect of additional R&D becomes smaller. Trade also exerts a positive and significant direct effect in the first regime, with a weak coefficient of 0.017. This suggests that in countries with weaker institutional quality, greater openness to trade stimulates patenting. However, in the upper regime, the effect of trade becomes extremely small and statistically insignificant, indicating that once institutions are strong enough, trade openness alone does not further enhance domestic innovation. As for GDP per capita, in the lower regime, LGDP has a strong and highly significant positive effect (0.7894), suggesting that economic capacity is a key driver of innovation where institutional frameworks are weak. However, in the upper regime, its effect becomes small and statistically insignificant (0.025), indicating that once countries reach higher institutional quality, improvements in income levels alone are no longer sufficient to explain cross-country differences in patenting.

Turning to the indirect spatial effects, the spatially lagged R&D coefficient is negative and significant at 10% in the first regime (-1.230). This result suggests a substitution effect:

higher R&D expenditure in neighboring countries reduces domestic patenting. In the upper regime, the spatial R&D effect becomes positive but statistically insignificant.

The indirect effects of trade and GDP per capita are not statistically significant in either regime, suggesting that spatial spillovers associated with market openness and income levels do not meaningfully influence patenting outcomes across borders.

4.4 Comparaison between Panel threshold spatial durbin model and panel buffered threshold spatial durbin model

For comparison purposes, we perform a similar analysis using the $PTSD$ model of Wei et al. (2021). Within the PTSD framework, linearity test results reveal significant non-linear relationships among R&D, trade, LGDP, and LPat (with $\hat{r} = 8.947, F = -2.0132 \times 10^5$ and $p-value = 0.06 < 10\%$) with GDP per capita as the threshold variable, (with $\hat{r} = 0.46, F = 154.564$ and $p - value = 0.04 < 5\%$) with rule of law as threshold variable.

Table 4.4.1 presents the estimation results, showing that the two estimated regimes (for GDP percapita as threshold variable) yield outcomes that differ significantly from $PBTSD$ modeling, particularly regarding the assignment of countries to the two regimes and the patent spillover effect. In fact, the estimated threshold value, $\hat{r} = 8.947$, lies below the lower limit of the buffer zone, $\hat{r}_L = 9.661$.

Table 4.4.1. Estimated two-regime PTSD model with GDP percapita as the threshold variable

Endogenous variable	*Lpat*	
Threshold variable	*LGDP*	
Threshold parameters	8.947	
	Lower	*Upper*
λ_k	$-0,997^{***}$	$0,349^{***}$
$\alpha_{k,1}$ $(R\&D)$	$0,166^{**}$	$0,060^{***}$
$\alpha_{k,2}$ $(Trade)$	$0,004$	$4,813$
$\alpha_{k,3}$ $(LGDP)$	$1,027^{**}$	$-0,138^{***}$
$\beta_{k,1}$ $(R\&D)$	$-0,488$	$0,332^{***}$
$\beta_{k,2}$ $(Trade)$	$-0,004$	$-0,002$
$\beta_{k,3}$ $(LGDP)$	$0,190^{***}$	$-0,022^{***}$

***Significant at the level 0.01 level, ** at the 0.05 level, and *at the0.10 level.

Furthermore, the patent spillover effect associated with countries in the lower regime is significantly negative, at the 1% significance level, with $\lambda_1 = -0.997$, indicating that neighboring countries in this regime tend to exert a strong negative influence on one another. Based on the $PTSD$ modeling results, a 1% increase in the LPat of neighboring countries leads to a 0.997% decrease in the LPat of adjacent countries. This rate is significantly higher than what was estimated by the $PBTSD$ modeling. In contrast, the upper regime exhibits a positive spatial autocorrelation and the patent spillover effect is similar to the one obtained from the $PBTSD$ modeling, with $\lambda_2 = 0.349$.

Table 4.4.2. Estimated two-regime PTSD model with rule of law as the threshold variable.

Endogenous variable	*Lpat*	
Threshold variable	*Rule of Law*	
Threshold parameters	0.46	
	Lower	*Upper*
λ_k	$-0,996^{***}$	$0,300^{***}$
$\alpha_{k,1}$ $(R\&D)$	$0,233^{**}$	$0,077^{***}$
$\alpha_{k,2}$ $(Trade)$	$0,005^{***}$	0.000
$\alpha_{k,3}$ $(LGDP)$	0.919^{**}	0.233^{***}
$\beta_{k,1}$ $(R\&D)$	$-0,117^{***}$	0.150^{***}
$\beta_{k,2}$ $(Trade)$	$-0,005$	-0.003^{***}
$\beta_{k,3}$ $(LGDP)$	$0,353^{***}$	$-0,149^{***}$

***Significant at the level 0.01 level, ** at the 0.05 level, and *at the0.10 level.

Table 4.4.2 reports the estimation results of the $PTSD$ model with rule of law as the threshold variable. The results of the PTSD model differ from those obtained under the $PBTSD$

specification. Specifically, the spatial spillover coefficient is strongly negative (-0.996) in the lower regime, while it becomes positive in the upper regime.

The behavior of the spatial lag is similar to that observed in the $PBTSD$ model, although the effect is stronger in the PTSD framework. Regarding the indirect spatial effects, most parameters are statistically significant (except for trade in the first regime), whereas in the PBTSD model they are not statistically significant.

We now aim to compare the regime state of each country over time based on the regime indicator ($R_{i,t}$) values derived from the estimated $PBTSD$ and $PTSD$ models for GDP percapita as threshold variable (see Figures 4.4.1 and 4.4.2) and rule of law as a threshold variable (see Figures 4.4.3 and 4.4.4).

For GDP per capita as threshold variable, the estimated models reveal that most countries (30 out of 32 for the PBTSD model and 29 out of 32 for the PTSD model) did not experience a switch in their patent application regimes during the study period. For many countries, classifications remain aligned between the $PBTSD$ and $PTSD$ models. Countries such as Australia, Austria, Canada, Denmark, Finland, France, Germany, and the United States are classified in the upper regime under both models across all years. Similarly, India, Egypt, Thailand, Tunisia, and China (before 2010) are consistently in the lower regime.

	2007	2008	2009	2010	2011	2012	2013	2014	2015	2016	2017	2018	2019	2020
Australia	2	2	2	2	2	2	2	2	2	2	2	2	2	2
Austria	2	2	2	2	2	2	2	2	2	2	2	2	2	2
Brazil	1	1	1	1	1	1	1	1	1	1	1	1	1	1
Canada	2	2	2	2	2	2	2	2	2	2	2	2	2	2
Chile	1	1	1	1	1	1	1	1	1	1	1	1	1	1
China	1	1	1	1	1	1	1	1	1	1	1	1	1	1
Czech Republic	2	2	2	2	2	2	2	2	2	2	2	2	2	2
Denmark	2	2	2	2	2	2	2	2	2	2	2	2	2	2
Egypt	1	1	1	1	1	1	1	1	1	1	1	1	1	1
Estonia	1	2	1	1	2	2	2	2	2	2	2	2	2	2
Finland	2	2	2	2	2	2	2	2	2	2	2	2	2	2
France	2	2	2	2	2	2	2	2	2	2	2	2	2	2
Germany	2	2	2	2	2	2	2	2	2	2	2	2	2	2
Greece	2	2	2	2	2	2	2	2	2	2	2	2	2	2
India	1	1	1	1	1	1	1	1	1	1	1	1	1	1
Italy	2	2	2	2	2	2	2	2	2	2	2	2	2	2
Japan	2	2	2	2	2	2	2	2	2	2	2	2	2	2
Latvia	1	1	1	1	1	1	1	1	1	1	1	2	2	2
Malaysia	1	1	1	1	1	1	1	1	1	1	1	1	1	1
Mexico	1	1	1	1	1	1	1	1	1	1	1	1	1	1
New Zealand	2	2	2	2	2	2	2	2	2	2	2	2	2	2
Poland	1	1	1	1	1	1	1	1	1	1	1	1	1	1
Portugal	2	2	2	2	2	2	2	2	2	2	2	2	2	2
Romania	1	1	1	1	1	1	1	1	1	1	1	1	1	1
Singapore	2	2	2	2	2	2	2	2	2	2	2	2	2	2
Sweden	2	2	2	2	2	2	2	2	2	2	2	2	2	2
Switzerland	2	2	2	2	2	2	2	2	2	2	2	2	2	2
Thailand	1	1	1	1	1	1	1	1	1	1	1	1	1	1
Tunisia	1	1	1	1	1	1	1	1	1	1	1	1	1	1
Turkey	1	1	1	1	1	1	1	1	1	1	1	1	1	1
United kingdom	2	2	2	2	2	2	2	2	2	2	2	2	2	2
United States	2	2	2	2	2	2	2	2	2	2	2	2	2	2

Figure 4.4.1. Regime indicator (Ri,t) values obtained from the estimated PBTSD model with GDP percapita as threshold variable.

	2007	2008	2009	2010	2011	2012	2013	2014	2015	2016	2017	2018	2019	2020
Australia	2	2	2	2	2	2	2	2	2	2	2	2	2	2
Austria	2	2	2	2	2	2	2	2	2	2	2	2	2	2
Brazil	1	2	2	2	2	2	2	2	2	2	2	2	2	1
Canada	2	2	2	2	2	2	2	2	2	2	2	2	2	2
Chile	2	2	2	2	2	2	2	2	2	2	2	2	2	2
China	1	1	1	1	1	1	1	1	2	2	2	2	2	2
Czech Republic	2	2	2	2	2	2	2	2	2	2	2	2	2	2
Denmark	2	2	2	2	2	2	2	2	2	2	2	2	2	2
Egypt	1	1	1	1	1	1	1	1	1	1	1	1	1	1
Estonia	2	2	2	2	2	2	2	2	2	2	2	2	2	2
Finland	2	2	2	2	2	2	2	2	2	2	2	2	2	2
France	2	2	2	2	2	2	2	2	2	2	2	2	2	2
Germany	2	2	2	2	2	2	2	2	2	2	2	2	2	2
Greece	2	2	2	2	2	2	2	2	2	2	2	2	2	2
India	1	1	1	1	1	1	1	1	1	1	1	1	1	1
Italy	2	2	2	2	2	2	2	2	2	2	2	2	2	2
Japan	2	2	2	2	2	2	2	2	2	2	2	2	2	2
Latvia	2	2	2	2	2	2	2	2	2	2	2	2	2	2
Malaysia	1	2	1	2	2	2	2	2	2	2	2	2	2	2
Mexico	2	2	2	2	2	2	2	2	2	2	2	2	2	2
New Zealand	2	2	2	2	2	2	2	2	2	2	2	2	2	2
Poland	2	2	2	2	2	2	2	2	2	2	2	2	2	2
Portugal	2	2	2	2	2	2	2	2	2	2	2	2	2	2
Romania	2	2	2	2	2	2	2	2	2	2	2	2	2	2
Singapore	2	2	2	2	2	2	2	2	2	2	2	2	2	2
Sweden	2	2	2	2	2	2	2	2	2	2	2	2	2	2
Switzerland	2	2	2	2	2	2	2	2	2	2	2	2	2	2
Thailand	1	1	1	1	1	1	1	1	1	1	1	1	1	1
Tunisia	1	1	1	1	1	1	1	1	1	1	1	1	1	1
Turkey	2	2	2	2	2	2	2	2	2	2	2	2	2	2
United kingdom	2	2	2	2	2	2	2	2	2	2	2	2	2	2
United States	2	2	2	2	2	2	2	2	2	2	2	2	2	2

Figure 4.4.2. Regime indicator (Ri,t) values obtained from the estimated PTSD model with GDP percapita as threshold variable.

Note that the $PTSD$ model indicates a regime switch for Brazil, transitioning from the lower regime in 2007 to the upper regime in 2008 and thereafter. In contrast, the $PBTSD$ model classifies Brazil in the lower regime throughout the period, reflecting a more stable categorization. For China, the $PTSD$ model shows a transition from the lower regime (2007–2010) to the upper regime from 2011 onward. However, the $PBTSD$ model retains China in the lower regime for all years, suggesting a delayed or mitigated shift. In the

case of Latvia, the $PBTSD$ model shows a transition from the lower regime (2007–2011) to the upper regime from 2012 onward. In contrast, the $PTSD$ model classifies Latvia in the upper regime throughout, indicating an earlier and abrupt switch. For Malaysia, the $PTSD$ model exhibits fluctuations between regimes: the lower regime in 2007, the upper regime in 2008, a return to the lower regime in 2009, and then the upper regime from 2010 onward. By contrast, the $PBTSD$ model keeps Malaysia in the lower regime throughout the study period, avoiding abrupt changes.

When using rule of law as the threshold variable, the estimated model shows that most countries (28 out of 32 under the PTSD specification), as previously observed, did not experience a regime shift in patent applications throughout the study period.

In the case of Brazil, both models indicate the presence of a regime change. However, under the $PBTSD$ model, the transition in 2009 occurs within a buffer zone, whereas in the $PTSD$ model the shift takes place immediately.

For Egypt, the timing and nature of the regime change also differ between the two specifications. Under the $PTSD$ model, Egypt moves from the first to the second regime in 2008, before returning to the first regime in 2011. In contrast, under the $PBTSD$ model, the year 2008 places Egypt in a buffer zone, delaying any confirmed regime transition for three years, until 2011 when it finally stabilizes again in the first regime.

These observations highlight that the $PBTSD$ model allows for smoother transitions through buffer zones, providing more stable classifications. It avoids frequent regime switches for countries near thresholds and better reflects gradual changes in dynamics.

Table 4.4.3. Linear estimation of spatial weight using Wf and Wc

Endogenous variable	*Lpat*	
Spatial weight	W_C	W_f
λ_k	-0.439^{***}	-0.360^{***}
α_1 $(R\&D)$	0.261^{***}	0.166
α_2 $(Trade)$	-0.004^{***}	-0.002^{***}
α_3 $(LGDP)$	-0.026^{***}	0.369^{***}
β_1 $(R\&D)$	1.716^{***}	0.743^{***}
β_2 $(Trade)$	-0.008	-0.005
β_3 $(LGDP)$	0.308^{***}	-0.005

***Significant at the level 0.01 level, ** at the 0.05 level, and *at the0.10 level.

As previously discussed, when considering both the contiguity-based spatial weight matrix (Wc) and the flux weight matrix (Wf), the models exhibit a linear specification (see Table 4.3.1 and 4.3.2). Therefore, we estimate the Spatial Durbin Model (SDM) as presented in Equation (1.5.1). The corresponding estimation results are reported in Table 4.4.3.

We observe that, for all countries selected in our sample, in both specifications, the spatial autoregressive parameter is negative and highly significant (-0.439 with Wc and -0.360 with Wf). This result indicates the presence of negative spatial dependence in innovation activity: an increase in patenting in neighboring or economically connected regions is associated with a reduction in local patenting. Such a pattern suggests competitive dynamics across regions, where innovative activity in one area may draw resources, skilled labor, or markets away from its neighbors.

Regarding the direct effects of the explanatory variables, R&D expenditure shows a positive and significant impact on local patent output when spatial dependence is defined through geographical contiguity (0.261), whereas the coefficient becomes smaller and statistically insignificant when economic flows are used. This finding implies that the contribution of domestic R&D to local innovation is stronger when knowledge diffusion is spatially bounded. Trade openness exhibits a weak negative and significant effect in both models (-0.004 with Wc and -0.002 with Wf), suggesting that exposure to external competition or the availability of imported technologies may reduce incentives for local patent creation. The level of economic development (LGDP) displays an asymmetric pattern: it has a negative and significant direct effect under contiguity (-0.026), but becomes strongly positive when connectivity is defined by flows (0.369). This contrast indicates that geographic proximity captures resource competition or structural substitution effects, while economic networks reinforce the innovation capacity of richer regions.

The indirect or spillover effects confirm the existence of spatial externalities. R&D in neighboring regions significantly enhance local patenting, with large and highly significant coefficients in both matrices (1.716 for Wc and 0.743 for Wf). These results demonstrate that knowledge investment generates substantial positive externalities, particularly when regions are geographically close. By contrast, the spillover effects of trade openness are statistically insignificant in both models, implying that cross-regional trade linkages do not transmit

innovation benefits. The spatial spillover of GDP percapita is positive and significant only under contiguity (0.308), while disappearing under the flux matrix (-0.005).

Overall, the findings highlight strong spatial interactions in innovation. Patent application is shaped not only by local R&D investment and economic conditions but also by the innovative environment of neighboring territories. The negative spatial dependence suggests competition between regions, while the positive spillovers from R&D indicate that regional innovation systems benefit from mutual knowledge exchange. These results underline the importance of coordinated regional innovation policies, particularly those supporting R&D cooperation and reducing competitive losses between geographically close areas.

	2007	2008	2009	2010	2011	2012	2013	2014	2015	2016	2017	2018	2019	2020
Australia	2	2	2	2	2	2	2	2	2	2	2	2	2	2
Austria	2	2	2	2	2	2	2	2	2	2	2	2	2	2
Brazil	1	1	1	2	2	2	2	2	2	2	1	1	1	1
Canada	2	2	2	2	2	2	2	2	2	2	2	2	2	2
Chile	2	2	2	2	2	2	2	2	2	2	2	2	2	2
China	1	1	1	1	1	1	1	1	1	1	1	1	1	1
Czech Republic	2	2	2	2	2	2	2	2	2	2	2	2	2	2
Denmark	2	2	2	2	2	2	2	2	2	2	2	2	2	2
Egypt	1	1	1	1	1	1	1	1	1	1	1	1	1	1
Estonia	2	2	2	2	2	2	2	2	2	2	2	2	2	2
Finland	2	2	2	2	2	2	2	2	2	2	2	2	2	2
France	2	2	2	2	2	2	2	2	2	2	2	2	2	2
Germany	2	2	2	2	2	2	2	2	2	2	2	2	2	2
Greece	2	2	2	2	2	2	2	2	2	2	2	2	2	2
India	2	2	2	2	2	2	2	2	2	2	2	2	2	2
Italy	2	2	2	2	2	2	2	2	2	2	2	2	2	2
Japan	2	2	2	2	2	2	2	2	2	2	2	2	2	2
Latvia	2	2	2	2	2	2	2	2	2	2	2	2	2	2
Malaysia	2	2	2	2	2	2	2	2	2	2	2	2	2	2
Mexico	1	1	1	1	1	1	1	1	1	1	1	1	1	1
New Zealand	2	2	2	2	2	2	2	2	2	2	2	2	2	2
Poland	2	2	2	2	2	2	2	2	2	2	2	2	2	2
Portugal	2	2	2	2	2	2	2	2	2	2	2	2	2	2
Romania	1	2	2	2	2	2	2	2	2	2	2	2	2	2
Singapore	2	2	2	2	2	2	2	2	2	2	2	2	2	2
Sweden	2	2	2	2	2	2	2	2	2	2	2	2	2	2
Switzerland	2	2	2	2	2	2	2	2	2	2	2	2	2	2
Thailand	1	1	1	1	1	1	1	1	1	2	2	2	2	2
Tunisia	2	2	2	2	2	2	2	2	2	2	2	2	2	2
Turkey	2	2	2	2	2	2	2	2	1	1	1	1	1	1
United kingdom	2	2	2	2	2	2	2	2	2	2	2	2	2	2
United States	2	2	2	2	2	2	2	2	2	2	2	2	2	2

Figure 4.4.3. Regime indicator (Ri,t) values obtained from the estimated PBTSD model with rule of law as threshold variable.

	2007	2008	2009	2010	2011	2012	2013	2014	2015	2016	2017	2018	2019	2020
Australia	2	2	2	2	2	2	2	2	2	2	2	2	2	2
Austria	2	2	2	2	2	2	2	2	2	2	2	2	2	2
Brazil	1	1	2	2	2	2	2	2	2	2	1	1	1	1
Canada	2	2	2	2	2	2	2	2	2	2	2	2	2	2
Chile	2	2	2	2	2	2	2	2	2	2	2	2	2	2
China	1	1	1	1	1	1	1	1	1	1	1	2	1	2
Czech Republic	2	2	2	2	2	2	2	2	2	2	2	2	2	2
Denmark	2	2	2	2	2	2	2	2	2	2	2	2	2	2
Egypt	1	2	2	2	1	1	1	1	1	1	1	1	1	1
Estonia	2	2	2	2	2	2	2	2	2	2	2	2	2	2
Finland	2	2	2	2	2	2	2	2	2	2	2	2	2	2
France	2	2	2	2	2	2	2	2	2	2	2	2	2	2
Germany	2	2	2	2	2	2	2	2	2	2	2	2	2	2
Greece	2	2	2	2	2	2	2	2	2	2	2	2	2	2
India	2	2	2	2	2	2	2	2	2	2	2	2	2	2
Italy	2	2	2	2	2	2	2	2	2	2	2	2	2	2
Japan	2	2	2	2	2	2	2	2	2	2	2	2	2	2
Latvia	2	2	2	2	2	2	2	2	2	2	2	2	2	2
Malaysia	2	2	2	2	2	2	2	2	2	2	2	2	2	2
Mexico	1	1	1	1	1	1	1	1	1	1	1	1	1	1
New Zealand	2	2	2	2	2	2	2	2	2	2	2	2	2	2
Poland	2	2	2	2	2	2	2	2	2	2	2	2	2	2
Portugal	2	2	2	2	2	2	2	2	2	2	2	2	2	2
Romania	2	2	2	2	2	2	2	2	2	2	2	2	2	2
Singapore	2	2	2	2	2	2	2	2	2	2	2	2	2	2
Sweden	2	2	2	2	2	2	2	2	2	2	2	2	2	2
Switzerland	2	2	2	2	2	2	2	2	2	2	2	2	2	2
Thailand	2	2	1	1	1	2	2	2	2	2	2	2	2	2
Tunisia	2	2	2	2	2	2	2	2	2	2	2	2	2	2
Turkey	2	2	2	2	2	2	2	2	1	1	1	1	1	1
United kingdom	2	2	2	2	2	2	2	2	2	2	2	2	2	2
United States	2	2	2	2	2	2	2	2	2	2	2	2	2	2

Figure 4.4.4. Regime indicator (Ri,t) values obtained from the estimated PTSD model with rule of law as threshold variable.

Chapter 5

Conclusion and perspectives

In this thesis, we have developed and analyzed a novel framework for spatial panel data models with threshold effects, namely the $PBTSD$ model. By extending the conventional $PTSD$ model and introducing a buffered regime-switching mechanism, we provided a more flexible approach that allows for smooth transitions between regimes, thereby avoiding the abrupt jumps typically observed in classical threshold models. This advancement not only improves the interpretability of the results but also enhances the empirical relevance of the model for capturing gradual structural changes across spatial units.

From a methodological perspective, we have explored and compared two estimation strategies, namely the 2SLS and the QML methods. Our simulation study confirmed the empirical consistency of both approaches and highlighted the superior performance of the QML estimator, particularly in terms of efficiency and asymptotic behavior for non-threshold parameters. Nevertheless, given the explicit nature of 2SLS estimators, we have shown that they can serve as convenient initial values for QML estimation, thereby strengthening the overall estimation procedure. An important insight of our study is the persistence of non-normality in the distribution of estimated boundary parameters, regardless of the estimation method or sample size, which raises interesting methodological challenges for further research.

On the empirical side, the application of the $PBTSD$ model to the relationship between GDP per capita, rule of law and patent applications in 32 countries over the period 2007–2020 revealed heterogeneous spillover effects. Specifically, we found negative effects in the lower

regime and positive effects in the upper regime, illustrating how economic development stages condition innovation dynamics. Compared to the traditional PTSD model, the PBTSD specification offers a more nuanced depiction of these relationships by incorporating buffer zones, which better reflect gradual structural changes in cross-country innovation patterns.

Looking ahead, several avenues for further research can be identified. The theoretical properties of the $PBTSD$ model could be investigated more deeply, particularly the asymptotic distribution of boundary parameters and the development of refined inference procedures. The model may also be extended to include dynamic features, capturing temporal as well as spatial threshold effects. From an empirical perspective, the model can be applied to other domains such as environmental economics, regional inequality, or public health, where both spatial dependence and threshold effects are crucial. Considering larger panels, multi-threshold extensions, and the integration of institutional or policy variables would further enrich the understanding of spatial dynamics. Finally, exploring the role of international cooperation, technology transfer, and institutional quality in shaping innovation spillovers represents a promising line of inquiry for future policy-oriented studies.

Bibliography

Aghion, P., & Howitt, P. (1992). A model of growth through creative destruction. Econometrica, 60(2), 323–351.

Anakpo, G., & Oyenubi, A. (2022). Innovation, human capital and economic growth in Africa. African Journal of Economic Review, 10(1), 59–81.

Anselin, L. (1988). Spatial Econometrics: Methods and Models. Kluwer Academic.

Anselin, L. (2002). Under the hood: Issues in specification and interpretation of spatial regression models. Agricultural Economics, 27(3), 247–267.*

Anselin, L., & Bera, A. (1998). Spatial dependence in linear regression models with an introduction to spatial econometrics. In Handbook of Applied Economic Statistics.

Anselin, L., & Rey, S. J. (2014). Modern Spatial Econometrics in Practice.

Anselin, L., Gallo, J. L., & Jayet, H. (2008). Spatial panel econometrics. In The Econometrics of Panel Data, 625–660.

Aquaro, M., Bailey, N., & Pesaran, M. H. (2015). Quasi maximum likelihood estimation of spatial models with heterogeneous coefficients. USC-INET Research Paper (15-17).

Arellano, M., & Bover, O. (1995). Another look at the instrumental variable estimation of error-components models. Journal of Econometrics, 68(1).

Arrow, K. (1962). The economic implications of learning by doing. Review of Economic Studies, 29(3), 155–173.*

Baltagi, B. (2013). Econometric Analysis of Panel Data. Wiley.

Baltagi, B. H., & Elhorst, J. P. (2015). Oxford Handbook of Panel Data Econometrics.

Baltagi, B. H., Fingleton, B., & Pirotte, A. (2014). Multilevel and spillover effects estimated for spatial panel data, with application to English house prices. Region et Développement, 40, 25–36.

Belarbi, Y., Hamdi, F., Khalfi, A., & Souam, S. (2021). Growth, institutions and oil dependence: A buffered threshold panel approach. Economic Modelling, 99, 105477.

Blundell, R., & Bond, S. (1998). Initial conditions and moment restrictions in dynamic panel data models. Journal of Econometrics, 87(1).

Chen, X., Gao, J., & Li, D. (2012). Estimation in semiparametric spatial dynamic panel data models with fixed effects. Journal of Econometrics, 167(1).

Cliff, A., & Ord, J. (1973). Spatial Autocorrelation. London: Pion.

Cliff, A., & Ord, J. (1981). Spatial Processes: Models & Applications. London: Pion.

Cressie, N. (1993). Statistics for Spatial Data. Wiley.

Davies, R. B. (1987). Hypothesis testing when a nuisance parameter is present only under the alternative. Biometrika, 74, 33–43.

Deng, Y. (2018). Estimation for the spatial autoregressive threshold model. Economics Letters, 171, 172–175.

Elhorst, J. P. (2003). Specification and estimation of spatial panel data models. International Regional Science Review, 26(3), 244–268.

Elhorst, J. P. (2010). Applied spatial econometrics: Raising the bar. Spatial Economic Analysis, 5(1).

Elhorst, J. P. (2014). Spatial Econometrics: From Cross-Sectional Data to Spatial Panels. Springer.

Elhorst, J. P. (2017). Spatial panel data models. In Handbook of Spatial Econometrics.

Ertur, C., & Koch, W. (2007). Growth, technological interdependence and spatial externalities: Theory and evidence. Journal of Applied Econometrics, 22(6).

Gonzalez, A., Terasvirta, T., & van Dijk, D. (2005). Panel Smooth Transition Regression Models. SSE/EFI Working Paper No. 604.

Grossman, G., & Helpman, E. (1991). Innovation and Growth in the Global Economy. MIT Press.

Haftu, G. (2019). Information communications technology and economic growth in Sub-Saharan Africa. Telecommunications Policy, 43(1).

Halleck Vega, S., & Elhorst, J. P. (2015). The SLX model. Journal of Regional Science, 55(3).

Hansen, B. E. (1999). Threshold effects in non-dynamic panels: Estimation, testing, and inference. Journal of Econometrics, 93(2), 345–368.

Hansen, B. E. (2000). Sample splitting and threshold estimation. Econometrica, 68(3), 575–603.

Hamdi, F., Souam, S., & Zouikri, M. (2025). The heterogeneous effect of economic complexity on growth and human development: New evidence using buffered panel threshold regression. The World Economy.

Holly, S., Pesaran, M. H., & Yamagata, T. (2010). A spatio-temporal model of house prices in the USA. Journal of Econometrics, 158, 160–173.

Horn, R. A., & Johnson, C. R. (1985). Matrix Analysis. Cambridge University Press.

Hsiao, C. (2014). Analysis of Panel Data. Cambridge University Press.

Hsiao, C., Pesaran, M. H., & Pick, A. (2007). Diagnostic tests of threshold effects in non-dynamic panels. The Econometrics Journal, 10(1).

Kelejian, H. H., & Prucha, I. R. (1998). A generalized spatial two-stage least squares procedure. Journal of Real Estate Finance and Economics, 17(1), 99–121.

Lee, L. F. (2004). Asymptotic distributions of quasi-maximum likelihood estimators for spatial autoregressive models. Econometrica, 72(6).

Lee, L. F., & Yu, J. (2010). Estimation of spatial autoregressive panel data models with fixed effects. Journal of Econometrics, 154(2), 165–185.

Lee, L.-F., & Yu, J. (2012). Spatial panels: Random components vs fixed effects. International Economic Review, 53(4).

Lee, L.-F. (2007). GMM and 2SLS estimation of mixed regressive–spatial autoregressive models. Journal of Econometrics, 137(2), 489–514.

LeSage, J., & Pace, R. K. (2009). Introduction to Spatial Econometrics. CRC Press.

Li, G., Guan, B., Li, W. K., & Yu, P. L. (2015). Hysteretic autoregressive time series models. Biometrika, 102, 717–723.

Maradana, R., Pradhan, R., Dash, S., et al. (2017). Does innovation promote economic growth? Empirical evidence from OECD countries. Economic Modelling, 64, 255–277.

Mensah, M., et al. (2019). Innovation and growth nexus in emerging economies. Journal of Economic Studies.

Meng, X., & Yang, Z. (2022). Threshold spatial panel data models with fixed effects. Preprint.

Moran, P. A. P. (1950). Notes on continuous stochastic phenomena. Biometrika, 37(1–2), 17–23.

Olaoye, O., et al. (2021). R&D intensity and growth in Africa. Technology in Society, 66.

Parent, O., & LeSage, J. P. (2010). A spatial dynamic panel model of trade flows. Journal of Geographical Systems, 12(2).

Polenske, K. (2007). The Economic Geography of Innovation. Cambridge University Press.

Rahman, M., & Malik, S. (2023). Innovation-led growth: Evidence from developing economies. Technological Forecasting & Social Change.

Rodríguez-Pose, A., & Burlina, C. (2021). Institutions and the uneven geography of COVID-19. Journal of Regional Science, 61(4).

Romer, P. (1990). Endogenous technological change. Journal of Political Economy, 98(5), S71–S102.

Sesay, M., et al. (2018). Innovation and Growth in West Africa. African Development Review.

Szirmai, A., & Verspagen, B. (2015). Manufacturing and economic growth in developing countries. UNU-MERIT Working Paper.

Tobler, W. (1970). A computer movie simulating urban growth in the Detroit region. Economic Geography, 46(Suppl. 1), 234–240.

Tong, H. (1983). Threshold Models in Non-Linear Time Series Analysis. Springer.

Wei, S., Deng, Y., & Li, X. (2021). Panel threshold spatial Durbin models. Regional Science and Urban Economics, 90, 103710.

Wei, L., Zhang, C., Su, J. J., & Yang, L. (2021). Panel threshold spatial Durbin models with individual fixed effects. Economics Letters, 201, 109778.

Yu, J., de Jong, R., & Lee, L. F. (2008). Quasi-maximum likelihood estimators for spatial dynamic panel data. Journal of Econometrics, 146(1).

Zheng, H., & Ye, A. (2023). Peer effects in green innovation. Environmental Science and Pollution Research, 30, 41028–41044.

Zhu, X., Deng, Y., & Li, X. (2020). Threshold spatial Durbin models. Papers in Regional Science, 99(6), 1685–1712.

Zhu, Y., Han, X., & Chen, Y. (2020). Bayesian estimation and model selection of threshold spatial Durbin model. Economics Letters, 188, 108956.